AL/OE-TR-1995-0134

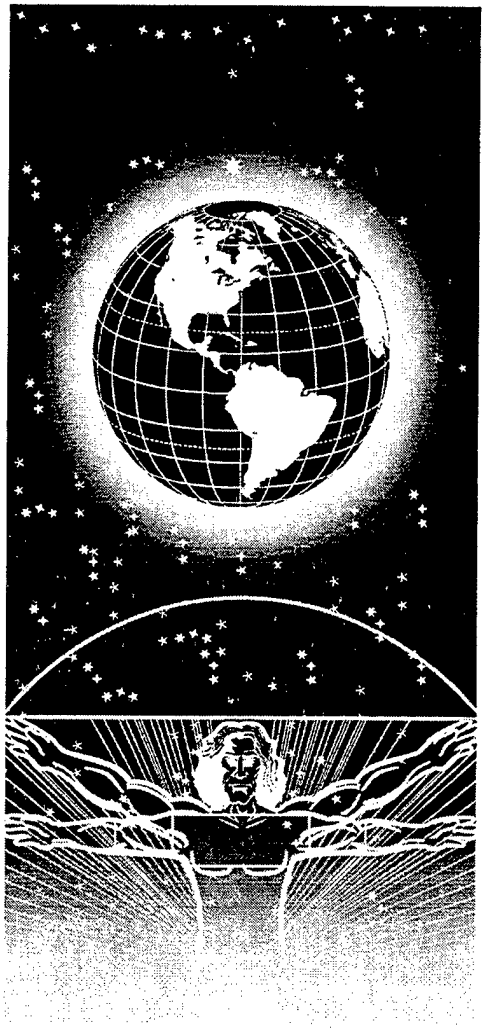

UNITED STATES AIR FORCE
ARMSTRONG LABORATORY

Estimation Of Dermal Permeability Coefficients For Dibromomethane And Bromochloromethane Pharmacokinetic Approach

G.W. Jepson

December 1995

Occupational and Environmental
Health Directorate
Toxicology Division
2856 G Street
Wright-Patterson AFB, OH 45433-7400

NOTICES

When US Government drawings, specifications or other data are used for any purpose other than a definitely related Government procurement operation, the Government thereby incurs no responsibility nor any obligation whatsoever, and the fact that the Government may have formulated, furnished, or in any way supplied the said drawings, specifications, or other data is not to be regarded by implication or otherwise, as in any manner licensing the holder or any other person or corporation, or conveying any rights or permission to manufacture, use, or sell any patented invention that may in any way be related thereto.

Please do not request copies of this report from the Armstrong Laboratory. Additional copies may be purchased from:

NATIONAL TECHNICAL INFORMATION SERVICE
5285 PORT ROYAL ROAD
SPRINGFIELD, VIRGINIA 22161

Federal Government agencies and their contractors registered with the Defense Technical Information Center should direct requests for copies of this report to:

DEFENSE TECHNICAL INFORMATION CENTER
8725 JOHN J. KINGMAN RD STE 0944
FT BELVOIR VA 22060-6218

DISCLAIMER

This Technical Report is published as received and has not been edited by the Technical Editing Staff of the Armstrong Laboratory.

TECHNICAL REVIEW AND APPROVAL

AL/OE-TR-1995-0134

The animals used in this study were handled in accordance with the principles stated in the *Guide for the Care and Use of Laboratory Animals* prepared by the Committee on Care and Use of Laboratory Animals of the Institute of Laboratory Animal Resources, National Research Council, National Academy Press, 1996, and the Animal Welfare Act of 1966, as amended.

This report has been reviewed by the Office of Public Affairs (PA) and is releasable to the National Technical Information Service (NTIS). At NTIS, it will be available to the general public, including foreign nations.

This technical report has been reviewed and is approved for publication.

FOR THE COMMANDER

TERRY A. CHILDRESS, Lt Col, USAF, BSC
Director, Toxicology Division
Armstrong Laboratory

REPORT DOCUMENTATION PAGE

Form Approved
OMB No. 0704-0188

1. AGENCY USE ONLY (Leave Blank)	2. REPORT DATE	3. REPORT TYPE AND DATES COVERED
	December 1995	Final - December 1992 - February 1995

4. TITLE AND SUBTITLE
Estimation of Dermal Permeability Coefficients for Dibromomethane and Bromochloromethane Using a Physiologically Based Pharmacokinetic Approach

5. FUNDING NUMBERS

PE	62202F
PR	6302
TA	630202
WU	63020218

6. AUTHOR(S)
G.W. Jepson

7. PERFORMING ORGANIZATION NAME(S) AND ADDRESS(ES)
Armstrong Laboratory, Occupational and Environmental Health Directorate
Toxicology Division, Human Systems Center
Air Force Materiel Command
Wright-Patterson AFB OH 45433-7400

8. PERFORMING ORGANIZATION REPORT NUMBER

9. SPONSORING/MONITORING AGENCY NAME(S) AND ADDRESS(ES)
Armstrong Laboratory, Occupational and Environmental Health Directorate
Toxicology Division, Human Systems Center
Air Force Materiel Command
Wright-Patterson AFB OH 45433-7400

10. SPONSORING/MONITORING AGENCY REPORT NUMBER
AL/OE-TR-1995-0134

11. SUPPLEMENTARY NOTES

12a. DISTRIBUTION/AVAILABILITY STATEMENT
Approved for public release; distribution is unlimited.

12b. DISTRIBUTION CODE

13. ABSTRACT (Maximum 200 words)

An understanding of dermal permeability of organic chemicals is important where occupational and environmental chemical exposures to humans are likely. It is equally important in the selection of therapeutic agents for and in the design of transdermal drug delivery systems. A great deal of *in vitro* work has been done to describe the involved transport processes, but very little research attention has been paid to systemic involvements and the overall pharmacokinetics of the relevant uptake and distribution processes. In this work, a physiologically based pharmacokinetic modeling approach is presented which describes chemical concentrations in rat blood following dermal exposures to two halogenated hydrocarbons, dibromomethane and bromochloromethane. These chemicals were dermally administered to live rats using and exposure cell with an area of 3.14cm^2. Each rat was surgically fitted with a jugular cannula and a dermal exposure cell 24 hours prior to the chemical exposure. Water, corn oil, and mineral oil were used a vehicles. Blood concentrations of the test substances were measured and physiologically based model was used to quantitatively describe their distribution, metabolism, and elimination. An experimentally good mass balance in conjunction with the model allowed permeability coefficients to be estimated for given chemical exposures. These were normalized to actual partitioning into the skin and used to calculate normalized permeability coefficients. The normalized permeability coefficients were then used within the model to predict chemical concentrations in blood that resulted from independent chemical exposures. The model was modified for use in an open dermal exposure and model simulations were generated to predict chemical blood concentrations for a range of exposures and physiological conditions. This work demonstrated the utility of a physiologically based model in applications where quantitative descriptions of dermally absorbed chemicals are important.

14. SUBJECT TERMS

Dermal permeability	*In Vitro*	Pharmacokinetics
Blood	Permeability Coefficients	Halogenated hydrocarbons

15. NUMBER OF PAGES
186

16. PRICE CODE

17. SECURITY CLASSIFICATION OF REPORT	18. SECURITY CLASSIFICATION OF THIS PAGE	19. SECURITY CLASSIFICATION OF ABSTRACT	20. LIMITATION OF ABSTRACT
UNCLASSIFIED	UNCLASSIFIED	UNCLASSIFIED	UL

THIS PAGE INTENTIONALLY LEFT BLANK

TABLE OF CONTENTS

LIST OF FIGURES

Figure | Page

LIST OF FIGURES (Cont'd)

LIST OF FIGURES (Cont'd)

LIST OF TABLES

I. INTRODUCTION

APPLICATION

Absorption of chemicals through the skin is a phenomenon of great interest and significance in the areas of occupational toxicology, pharmaceutical therapy and human health risk assessment (Banks, et al., 1990; Bucks, et al., 1985; Fisher et al., 1989; Kemppainen, et al., 1986; Surber, et al., 1990; Wester et al., 1990). Occupational settings can offer a variety of exposure scenarios where the dermal route of exposure is a primary route of chemical entry into the systemic circulation of the body. Such a situation might develop when respiratory protection is provided but the skin is allowed to come in contact with a chemical vapor. Alternately, liquid chemicals may directly contact skin in occupational operations where chemicals are used as part of industrial or processing applications (Woollen, et al., 1985). Once into the blood, an absorbed chemical or its metabolic products may interact with biological tissues or components to produce toxic effects which can even be lethal. The potential for dermal contact with occupational,

as well as environmental, chemicals has led researchers to explore predictive and descriptive techniques for percutaneous absorption of chemicals (Cooper and Berner, 1985; Genderen, et al., 1985; Leung and Paustenbach, 1994).

In contrast to the potentially adverse effects of dermal absorption of occupational chemicals, the absorption of therapeutic agents into and through the skin may provide effective, safe mechanisms for delivering drugs to the skin and systemic circulation (Black and Kamat, 1988; Groning, 1987). Routine use of transdermal drug delivery systems is common in the prophylactic treatment of motion sickness and therapeutic treatment of nicotine dependence. The transdermal delivery of drugs could be especially beneficial for the systemic delivery of drugs that are degraded or cause adverse effects in the gastrointestinal tract following oral administration (Chien, et al., 1988).

A final area where the dermal absorption of chemicals is an area of interest, debate and active research is human health risk assessment. This area crosses both occupational and environmental lines and is focused on establishing the health risk and appropriate regulatory standards associated with chemical exposure via the dermal route (Anderson, et al., 1993, Frederick and Chang-Mateu, 1990, McDougal and Clewell, 1990). Examples of dermal exposure scenarios that would be subject to risk assessment activities may range

from chemicals used in the workplace and home to chemicals that contact the body through contaminated water or soil sources (Shu, et al., 1988). In both occupational and environmental exposure scenarios the quantitative rather than the qualitative description of dermal absorption kinetics and mechanisms could improve the quality of regulatory standard setting activities. Following this reasoning, a reliable quantitative method for describing dermal absorption kinetics could support an approach where dermal exposure limits are related to existing inhalation exposure limits. The value of such a relationship between dermal and inhalation exposure has been suggested and could help regulators better decide on acceptable exposure standards for occupational chemicals (Fiserova-Bergerova, 1993). In general, the exposure standards are set to provide a socially acceptable balance between human safety, environmental welfare and economic concerns.

As demonstrated in the previous paragraphs, dermal absorption kinetics is an area of interest in a fairly wide range of applications. In order to produce experimental results that can be applied to issues surrounding dermal exposure of chemicals, a quantitative, systematic approach is required. Such an approach requires appropriate description of dermal absorption in structural and mechanistic terms.

SKIN STRUCTURE

The skin has several physiological roles, none more important than its chemical barrier function. This barrier function is in contrast to structures like the intestinal membranes and lung or blood capillaries which facilitate, or at least accommodate, absorption functions while performing their normal physiological functions. The dermal barrier function of the skin of greatest physiological relevance is minimization of loss of water from the body. A thin, compact layer of dead cells, the stratum corneum, provides this protection. Whether by evolutionary design or not, the stratum corneum is also highly impervious to other chemicals as well, but not to an extent where it provides absolute protection. One has to appreciate the structure of the skin to understand its barrier role.

Skin is structurally organized into several morphologically or physiologically distinct components or layers as shown in Figure 1. The layer that is in direct contact with the external environment and may be the primary determinant of dermal penetration for many chemicals is the stratum corneum (Emmett, 1986). The stratum corneum is composed of packed dead cells that are filled with the protein keratin (Jacob, et al., 1978).

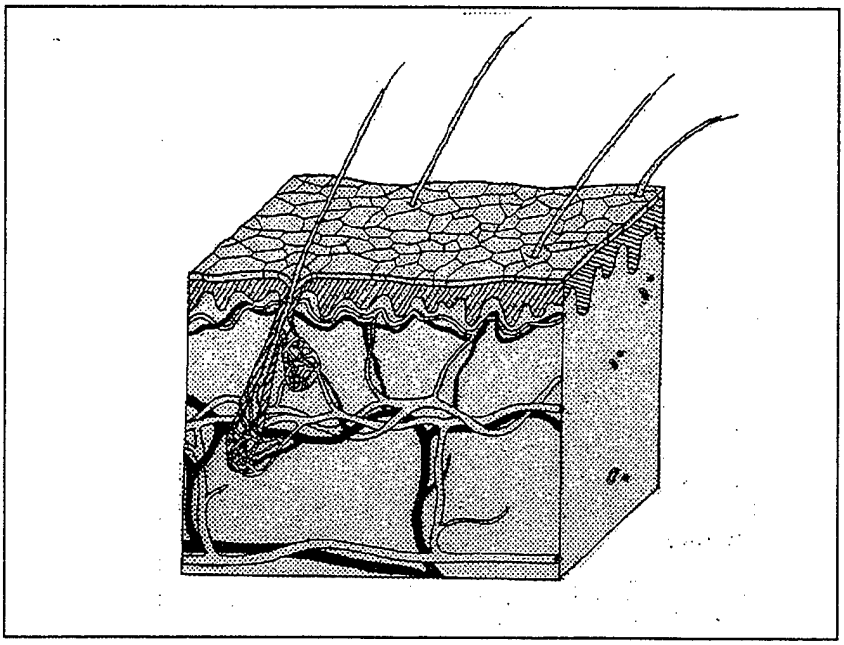

Figure 1. Skin Structure. Drawing Courtesy of Ms Marcia Freedman, 1994.

Intercellular lipids which exist in bilayer configuration act to cement the cells of the stratum corneum. There is little doubt that the intercellular lipids provide the non-polar character observed in the stratum corneum (Loth, 1989). The stratum corneum lipids are composed of ceramides, 50%, and fatty acids (palmitic, stearic, oleic, and arachidonic acid), 25%, cholesterol sulfate and other minor components. Very little or no phosphatidyl choline, phosphatidylethanolamine or sphingomyelin as seen in common bilayers are found in the stratum corneum (Curatolo, 1987). The ceramide and fatty acids in the stratum corneum are associated with cholesterol which accounts for about 20% of the total lipid weight. The

particular components and relative abundance of the components in the stratum corneum determine its fluidity and polarity as required for normal dermal barrier function. The thickness of the stratum corneum varies among species and by location on the body but, excepting for frictional surfaces, typical human stratum corneum measures about 10-50 um (Ritschel and Hussain, 1988).

The epidermis has several other well-defined layers. The layers represent differing states of cell differentiation as the cells migrate from the basement layer where they are formed toward the stratum corneum. The layer ordinarily found immediately underneath the stratum corneum is the stratum granulosum. This layer is only a few cells thick but, it is the region where keratin production is completed and the cell's substructures are recycled. As a result one observes the loss of cell nuclei and an increase in cell compactness. Underneath the stratum granulosum is the variable thickness stratum spinosum which is composed of cells with spinous projections drawn out of their points of desmosomal attachment. The next layer is the stratum germinativum. In humans it is here that all new cells are formed via mitosis which then make up the layers of epidermis. The part of the epidermis that includes the stratum germinativum up to but not including the stratum corneum is often referred to as the viable epidermis by

those who study skin permeation because there are no diffusionally distinct layers within this region of the skin. The viable epidermis contains the enzymes responsible for xenobiotic metabolism and, therefore, could influence the rate and impact of percutaneous absorption of chemicals (Storm, et al., 1990; Bronaugh, 1990).

The remainder of the true skin lying beneath the epidermis is the dermis. The dermis is roughly ten times thicker than the epidermis and is structurally acellular. It is a fibrous tissue, mostly collagen, fully 1-5 mm thick. It also contains the elastic fiber, elastin, which restores the shape of the structure as it stretches through body movements. Fibroblasts, macrophages and lymphocytes are to be found in the interstitial spores between the fibers that support the delicate vasculature of the skin. Additionally, the dermis is a residence for sensory and sensorimotor nerves that contribute to the physiological role of the skin. The epidermis and dermis are highly integrated anatomically as well as in physiological function. For example, hair follicles, sebaceous glands and sweat glands, epidermal structures all, penetrate deeply into the dermal layer of skin. At the base of the dermis, a subcutaneous layer of fat and connective tissue supports the dermis layer and provides for dermal attachment to underlying tissue.

Among other roles, this hypodermis is an important thermal insulator.

The physical structure of the skin is a starting place for preparing a description of chemical movement across the skin and into the systemic circulation. Researchers have described the various anatomical compartments of the skin and postulated the role of individual skin components in the overall process of skin permeability (Scheuplein and Blank, 1971). The task of describing the physical composition of skin in absolute terms is complicated by the variability in skin thickness and composition, even on a single individual.

If skin variability is combined with the possible interaction between skin components and dermally diffusing chemicals, the task of identifying critical kinetic skin components and quantitatively describing chemical movement across the skin is enormous. Several microscopic paths of chemical diffusion across skin have been postulated, namely transcellular, intercellular and appendageal paths, and a given chemical can diffuse in different proportions through these routes depending on exposure conditions and physiochemical considerations (Scheuplein and Blank, 1971, Guy and Hadgraft, 1988).

The appropriate level of complexity for the skin compartment in dermal penetration activities focused on human health assessment is still an area of active debate.

In one approach, the physicochemical concepts of dermal permeability have been considered in terms of function and applicability in order to establish appropriate skin permeation model complexity for risk assessment applications (Flynn, 1990).

To quantitatively describe the systemic appearance of chemicals following dermal exposure, a mechanistically sound pharmacokinetic model is needed. In any such quantitative description, the compartments should maintain physiological identity, but at the same time, they may be organized to each have distinct kinetic character. Such an organization allows focus on the kinetic and mechanistic data requirements and identification of parameters requiring definition or estimation. Once the data requirements are satisfied, the predictive capability of the quantitative description can be tested against reliable experimental data.

DERMAL ABSORPTION OF CHEMICALS

The absorption of chemicals through the skin and into systemic circulation can be approached quantitatively by considering the flux ($mg/hr/cm^2$) of chemical across the dermal barrier. Chemical flux across the skin is generally described in terms of Fickian behavior (see Equation 1).

$$FLUX = F = \frac{D \times P_{s/v} \times C}{L} \qquad \textbf{Eq 1}$$

In Equation 1, F is the flux per unit area, D is the diffusion coefficient (cm^2/hour), $P_{s/v}$ is the skin to vehicle partition coefficient, C is the concentration difference across the dermal barrier (mg/mL) and L is the diffusion pathlength (cm).

While the diffusion coefficient is one of the more fundamental descriptors of chemical movement across skin, the structure of skin is so organizationally and compositionally complex that it defies estimation of this operational parameter. Much the same can be said about the path length of diffusion and even the distribution coefficient attending the transport process. Because of such practical considerations, experimentally definable but diffusionally less fundamental permeability coefficients are often used.

The permeability coefficient, K_p (cm/hour), combines terms for diffusion, partitioning and pathlength. The description of unit area chemical flux in terms of the permeability coefficient is given in Equation 2.

$$F = K_P \times C \quad \left\{ Where \;\; K_P = \frac{D \times P_{s/v}}{L} \right\} \qquad \textbf{Eq 2}$$

Equation 2 indicates that the flux of chemical is proportional to the chemical driving force, C. The

permeability coefficient in Equation 2 can be isolated and defined as in Equation 3.

$$\frac{F}{C} = K_P \qquad \textbf{Eq 3}$$

With the permeability coefficient defined as in Equation 3, the experimental variables and thus data requirements for a model become relatively evident. Consider, for instance, that the permeability coefficient necessarily takes the form shown in Equation 4.

$$K_P = \frac{F}{C} = \frac{Amount\ Absorbed}{Area \times Time \times Concentration} \qquad \textbf{Eq 4}$$

The skin area exposed, the time of exposure and the chemical concentration in the exposure must be controlled as part of the experimental design and procedure. However, to assign a value to the term representing the amount of chemical absorbed, one must describe not just the absorption but also the distribution, metabolism and elimination processes that are part of an *in vivo* system.

The post dermal absorption behavior of the chemical must be quantitatively considered if meaningful descriptions of blood levels or health risk are to be derived from the experimental work. In order to keep track of chemical mass throughout the exposure period in a complex, *in vivo* system, a physiologically based pharmacokinetic (PBPK) model can be used (Andersen, 1981). A PBPK model appropriate for the

chemicals and the biological systems of interest can be developed by considering the physical characteristics of the chemicals of interest, the kinetically distinct compartments that make up the system and the physiologically important aspects of the system.

PHYSICAL CHARACTERISTICS OF TEST CHEMICALS

The chemicals used in this work are dibromomethane and bromochloromethane. Their structures are shown in Figure 2. Both chemicals are halogenated hydrocarbons with molecular weights of 173.85 and 129.39 for dibromomethane (DBM) and bromochloromethane (BCM), respectively. Selected physical characteristics of these chemicals are shown in Table 1.

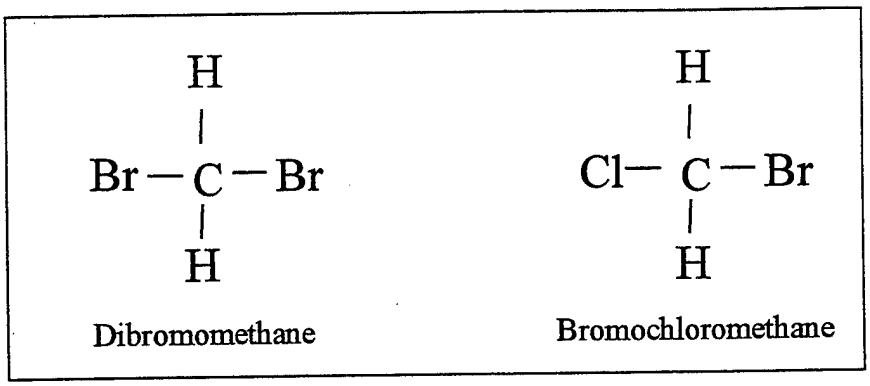

Figure 2. Chemical Structures of Test Chemicals

These chemicals, especially dibromomethane, provided the advantages of being well characterized from a metabolic

perspective and provide excellent sensitivity in analytical procedures.

*Table 1. Physical Characteristics of DBM and BCM**

	Dibromomethane	Bromochloromethane
Molecular Weight	173.83	129.39
Melting Point	-52°C	-87°C
Boiling Point	97.0°C	68.1°C
Density	2.497 g/mL @20°C	1.934 g/mL @20°C

** Values from CRC Handbook of Chemistry and Physics, 67th Edition, Weast RC (Editor),1987.*

Additionally, tissue:air partition coefficients shown in Table 2 have been published for both of these chemicals (Gargas, et al., 1989).

*Table 2. DBM and BCM Tissue:Air Partition Coefficients**

CHEMICAL	BLOOD	FAT	LIVER	MUSCLE
DBM	74.1(1.5)	792(14)	68.1(1.4)	40.5(2.0)
BCM	41.5(0.9)	325(3)	29.2(0.5)	11.1(1.8)

** Tissue:air partition coefficients for dibromomethane (DBM) and bromochloromethane (BCM). Values are means with standard error in parenthesis.*

PHYSIOLOGICALLY BASED PHARMACOKINETIC MODEL

The strategy for developing the PBPK model is to build a mathematical structure which is able to explain important facets of the experimental experience but which is also as elementary as possible. With this strategy in mind, tissue compartments with kinetically similar and inseparable properties are combined into one. The tissues that are kinetically distinct or have some property requiring explicit description are described separately.

The slowly and rapidly perfused compartments are examples of lumped compartments. The slowly perfused compartment is composed primarily of muscle tissue, whereas, the rapidly perfused compartment is composed primarily of gastrointestinal, kidney and brain tissue. The slowly perfused tissue can be described kinetically as shown in Figure 3 and Equations 5-8.

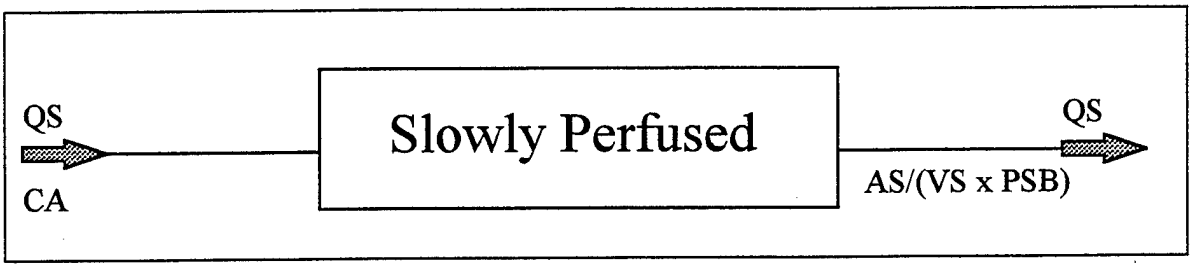

Figure 3. Slowly Perfused Compartment

$$VS \times \frac{dC_s}{dt} = \frac{dA_s}{dt} = QS \times \left(CA - \frac{AS}{VS \times PSB} \right) \qquad \text{Eq 5}$$

$$dAS = QS \times \left(CA - \frac{AS}{VS \times PSB} \right) dt \qquad \text{Eq 6}$$

$$\int_{A=0}^{A} dAS = \int_{t=0}^{t} [\ QS \times \left(CA - \frac{AS}{VS \times PSB} \right)]dt \qquad \text{Eq 7}$$

$$AS = \int_{t=0}^{t} [\ QS \times \left(CA - \frac{AS}{VS \times PSB} \right)]dt \qquad \text{Eq 8}$$

In Figure 3, VS is the volume (L) of the slowly perfused compartment, C_s is the chemical concentration (mg/L) in the slowly perfused compartment, AS is the amount (mg) of chemical in the slowly perfused compartment, QS is the blood flow (L/hour) to the slowly perfused compartment, CA is the arterial blood chemical concentration (mg/L), PSB in the slowly perfused tissue to blood partition coefficient and t is time (hours).

The other lumped compartment, the rapidly perfused compartment, as well as the fat compartment, are described identically in structure to the slowly perfused compartment. Of course, terms assigned to the flows, volumes and partition coefficients are compartment specific. While the fat compartment shares compartmental structure with the slowly perfused compartment, in this work it must be separated from the slowly perfused compartment because dibromomethane and bromochloromethane both have high

preferential lipid solubilities. It is on this basis that the fat compartment is distinguished from the musculature.

Unlike the slowly perfused, rapidly perfused and fat compartments, the liver compartment is a site of metabolism for both bromochloromethane and dibromomethane (Gargas and Andersen, 1982). The metabolic capability of the liver makes it a kinetically distinct compartment and requires it to be separated from the rapidly perfused compartment. The liver compartment can be described kinetically as shown in Figure 4 and Equations 9 and 10.

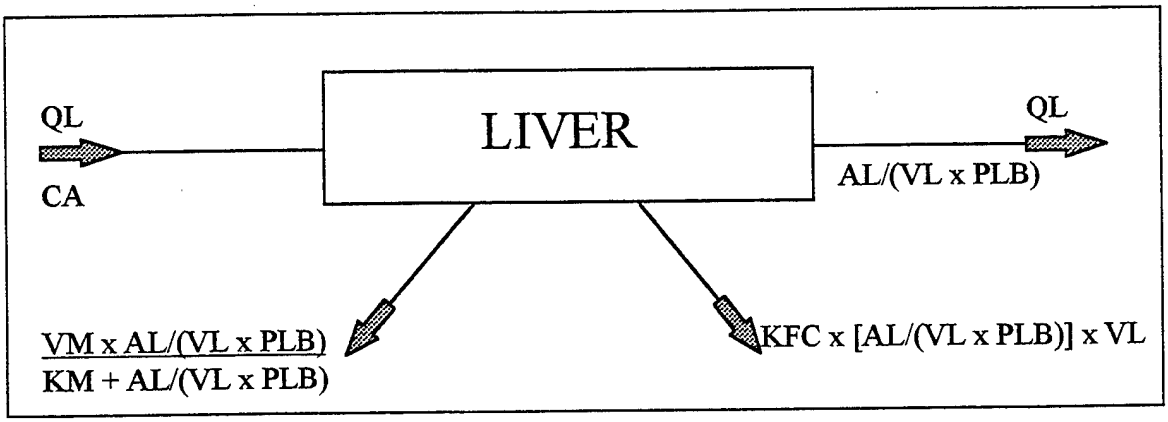

Figure 4. Liver Compartment

In Figure 4, QL is the liver blood flow (L/hour), AL is the amount (mg) of chemical in the liver, VL is the liver volume (L), PLB is the liver to blood partition coefficient, CA is the chemical concentration in arterial blood (mg/L), VM is the maximum velocity (mg/hour) of saturable metabolism, KM

is an affinity constant (mg/L) and KFC is a first order metabolism constant (1/hour).

$$\frac{dA_L}{dt} = QL \times \left(CA - \frac{AL}{VL \times PLB} \right) - \frac{VM \times AL/(VL \times PLB)}{KM + AL/(VL \times PLB)} - KFC \times VL \times AL/(VL \times PLB)$$

Eq 9

$$AL = \int_{t=0}^{t} \left[QL \times \left(CA - \frac{AL}{VL \times PLB} \right) - \frac{VM \times AL/(VL \times PLB)}{KM + AL/(VL \times PLB)} - KFC \times VL \times AL/(VL \times PLB) \right] dt$$

Eq 10

The metabolism of both dibromomethane and bromochloromethane occurs along the same saturable and pseudo-first order pathways used by other dihalomethanes. A simplified metabolic scheme for dibromomethane is shown in Figure 5.

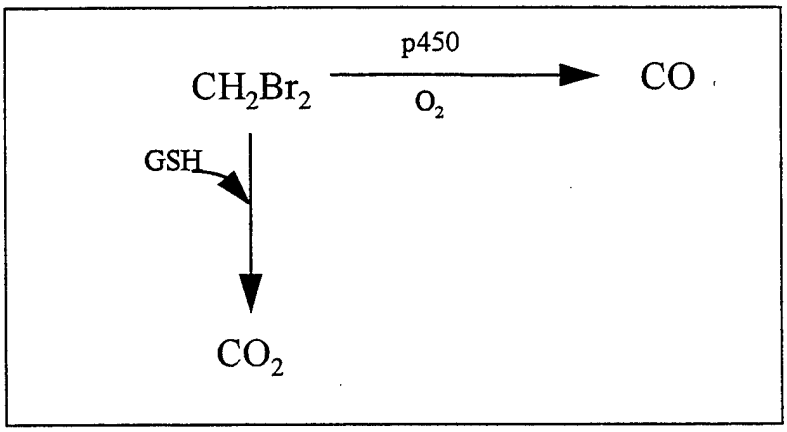

Figure 5. Metabololic Scheme of Dibromomethane.

An identical scheme to Figure 5 can be drawn for the saturable and first order metabolism of bromochloromethane

by simply replacing one of the bromine atoms with a chlorine.

The liver is not the only tissue group involved in clearance of dibromomethane or bromochloromethane from the biological system. These chemicals are also appreciably exhaled as a consequence of their high volatility (Lam, et al., 1993). This process does not involve metabolism or biotransformation as in the liver. The rate and extent of chemical exhalation is driven by the chemical's volatility and the blood to air partition coefficient. The kinetic structure of the lung compartment is shown in Figure 6 with description of the chemical exhalation process shown in Equations 11 and 12.

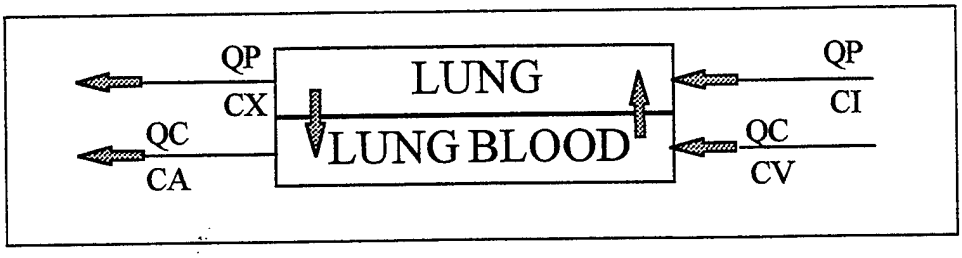

Figure 6. Lung Compartment

$$\frac{dAX}{dt} = QP \times CX = QP \times \frac{CA}{PB} \qquad \text{Eq 11}$$

$$AX = \int_{t=0}^{t} \left(QP \times \frac{CA}{PB} \right) dt \qquad \text{Eq 12}$$

In Figure 6, QP is the ventilation rate (L/hour), CX is the exhaled chemical concentration (mg/L), CI is the inhaled chemical concentration (mg/L), QC is the cardiac output (L/hour), CV is the venous blood chemical concentration (mg/L), PB is the blood to air partition coefficient for the chemical and CA is the arterial blood concentration (mg/L). Using the assumption of rapid equilibration of chemical between alveolar air and blood, the arterial blood concentration can be calculated using a steady-state approach as shown in Equations 13 and 14. The arterial blood concentration, CA, is the input chemical concentration for the other tissue groups.

$$(QC \times CV) + (QP \times CI) = (QC \times CA) + \left(QP \times \frac{CA}{PB}\right) \qquad \textbf{Eq 13}$$

$$\frac{\left[(QC \times CV) + (QP \times CI)\right]}{QC + \frac{QP}{PB}} = CA \qquad \textbf{Eq 14}$$

The one remaining tissue compartment required to describe the dermal absorption of organic chemicals is the skin compartment. The skin compartment is similar to the other compartments described in that it has a volume, blood flow and the other physiological characteristics of biological organs. However, the skin is given special treatment in dermal permeability applications since it represents the route of exposure for the chemicals of

interest. The structure of a simple skin compartment is shown in Figure 7.

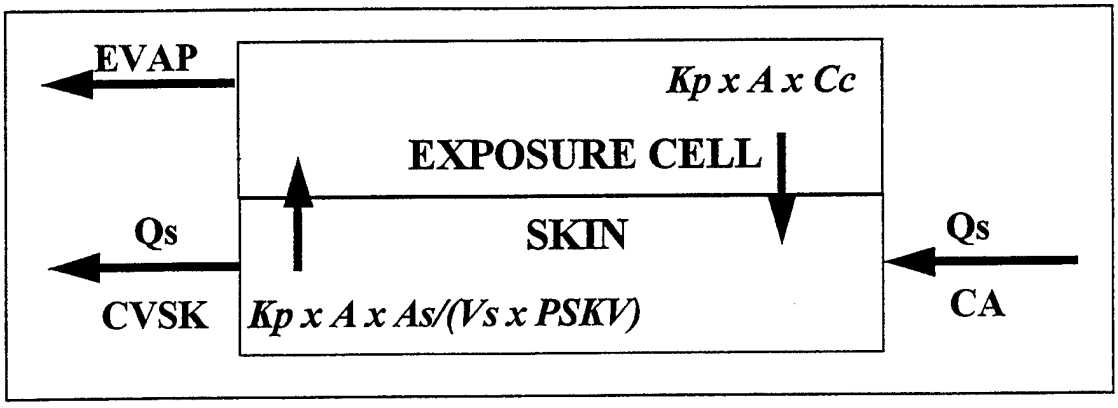

Figure 7. Skin Compartment.

$$\frac{dA_S}{dt} = Kp \times A\left(C_C - \frac{A_S}{(V_S \times PSKV)}\right) + Q_S\left(CA - \frac{A_S}{(V_S \times PSKB)}\right) - EVAP \qquad \text{Eq 15}$$

In Figure 7, Kp is the permeability coefficient (cm/hour), A is the exposure area (cm^2), Vs is the volume of skin (mL), PSKV is the skin to vehicle partition coefficient, Qs is the blood flow to the skin (mL/hour), As is the amount of chemical in the skin (mg/mL), PSKB is the skin to blood partition coefficient, Cc is the chemical concentration in the exposure cell (mg/mL), CVSK in the concentration of chemical in venous blood leaving the skin (mg/mL), EVAP is the chemical evaporation rate (mg/hr) and CA is the chemical concentration (mg/mL) is arterial blood. In the context of

dermal absorption, the term vehicle is defined as the diluent for the test chemical in the dermal exposure.

The lung, fat, slowly perfused, rapidly perfused, liver and skin tissue compartments described above can be organized into a model for tracking chemical mass taken up by a biological system during the course of a dermal exposure. As mentioned earlier, the ability to account for chemical mass is essential for estimation of the total amount of chemical absorbed during the dermal exposure. In turn, the amount of chemical absorbed per unit time per exposure area represents the flux of chemical across the skin and provides a means for estimating the permeability coefficient, Kp, as discussed earlier (See Equation 4).

In theory, a relationship might exist between permeability and one or more of the parameters that describe a chemical's movement in, or interactions with, the skin. Such a relationship can be developed between the solubility or partitioning of the chemical in skin and the permeability coefficient. If Equations 2 and 3 are combined to illustrate the relationship between flux and the permeability coefficient the result is Equation 16.

$$\frac{F}{C} = Kp = \frac{D \times PSKV}{L} \qquad \textbf{Eq 16}$$

In Equation 16, F is flux, C is chemical concentration gradient across skin, D is the diffusion coefficient, PSKV

is the skin to vehicle partition coefficient and L is the pathlength of diffusion. If for a given chemical, the diffusion coefficient and pathlength of diffusion are constant, then the permeability coefficient is related to the skin:vehicle partition coefficient by the constant, D/L, as shown in Equation 17.

$$Kp = \left(\frac{D}{L}\right) \times PSKV \qquad \textbf{Eq 17}$$

If both sides of Equation 17 are divided by PSKV in order to normalize for chemical partitioning in the skin, Equation 18 results.

$$\frac{Kp}{PSKV} = \frac{D}{L} = CONSTANT \qquad \textbf{Eq 18}$$

Based on Equation 18, it should be possible to use the relationship between the permeability coefficient (Kp) and the skin to vehicle partition coefficient (PSKV) in order to predict the dermal permeability coefficient of the chemical from various vehicles. This approach uses a normalized permeability concept where the normalized permeability coefficient, $K_{p,n}$, is defined as shown in Equation 19.

$$\frac{K_p}{PSKV} = \frac{D}{L} = K_{p,n} \qquad \textbf{Eq 19}$$

The normalized permeability coefficient and the skin to vehicle partition coefficient can then in principle be used to predict the permeability coefficient for the chemical applied in another vehicle system, as shown in Equation 20..

$$K_p = K_{p,n} \times PSKV \qquad \textbf{Eq 20}$$

The importance of the skin to vehicle partition coefficient in predicting the permeability coefficient is readily apparent from Equation 20. The partition coefficient is often defined as the ratio of the chemical concentration in two interfacing phases where the chemical has come to equilibrium between the phases. The importance of the partition coefficient in pharmacokinetic applications has prompted investigators to pursue methods for determining partition coefficients in various biological tissues (Gallo, et al., 1987; Lin, et al., 1982; Paterson and Mackay, 1989; Sultatos, et al., 1990). Others have correlated partition coefficients with percutaneous absorption of organic chemicals (Bronaugh and Congdon, 1984; [b]Mattie, et al., 1994). However, it may be meaningful to view the partition coefficient in more fundamental terms. For a nonionized chemical z, that has equilibrated between phases A and B at constant pressure and temperature, the chemical potential, U_z, in each phase is as follows.

$$U_z = U_z^0 + RT \ln C_z \qquad \textbf{Eq 21}$$

In Equation 21, U_z^0 (cal/mole) is the standard state chemical potential for chemical z, T is temperature (°K), R is the gas constant (cal/(mole x T)) and C_z is the chemical concentration (activity) of chemical z.

At equilibrium the chemical potential for chemical z is the same in phases A and B and therefore the difference between $U_{z,A}$ and $U_{z,B}$ is zero as shown in Equation 22. The description of the partition coefficient is further developed in Equations 23-25.

$$U^0_{z,A} - U^0_{z,B} + RT\ln C_{z,A} - RT\ln C_{z,B} = 0 \qquad \text{Eq 22}$$

$$U^0_{z,A} - U^0_{z,B} = RT\ln\left(\frac{C_{z,A}}{C_{z,B}}\right) \qquad \text{Eq 23}$$

$$\frac{\left(U^0_{z,A} - U^0_{z,B}\right)}{RT} = \ln\left(\frac{C_{z,A}}{C_{z,B}}\right) \qquad \text{Eq 24}$$

$$e^{\left(\frac{\left(U^0_{z,A} - U^0_{z,B}\right)}{RT}\right)} = \frac{C_{z,A}}{C_{z,B}} = P \qquad \text{Eq 25}$$

In Equation 25, P is the partition coefficient for chemical z in equilibrium between phases A and B.

IN VITRO ESTIMATION OF DIFFUSION COEFFICIENTS

The movement of a chemical across the dermal barrier is often described in terms of a permeability coefficient, especially in situations involving the complexity of *in vivo* systems. The use of the permeability coefficient is practical in complex systems, but it can be resource intensive in terms of animals, time, analytical methods and chemicals. It would be useful to be able to estimate the

permeability coefficient using an *in vitro* approach that offers less system complexity. As discussed earlier, the permeability coefficient is composed of terms for diffusion, partitioning and diffusion path length. Unlike, the *in vivo* situation, the *in vitro* situation may lend itself to enhanced system definition and experimental control of the more fundamental parameters that make up the permeability coefficient.

Recently investigators pioneered the use of physical chemistry methodology in dermal absorption kinetics by applying thermal gravimetric analysis techniques to evaluate the diffusion coefficient of water vapor in porcine stratum corneum (Liron, et al., 1994). The concepts applied in water vapor diffusion studies should have application to organic vapors even though many organic vapors would be expected to diffuse through skin much more rapidly than water. It is possible, however, that the water content in skin may influence the absorption of organic chemicals (Chang and Riviera, 1991). Liron et al., 1994 reported diffusion coefficients in the 10^{-11} to 10^{-10} cm^2/second range for water in porcine stratum corneum. It is likely that halogenated hydrocarbons could possess diffusion coefficients an order of magnitude or more higher than the diffusion coefficients in water. Another significant difference between the water diffusion and halogenated

hydrocarbon diffusion in stratum corneum is the interaction of water with the stratum corneum. Water exists in different forms in the stratum corneum with differing degrees of binding between water and the cell membranes. Functionally this results in a variety of phases in water diffusion across the stratum corneum, and, kinetically the absorption and desorption processes differ. Halogenated hydrocarbons should be much less thermodynamically complex than water with absorption and desorption phases being kinetically similar in the stratum corneum. However, the challenge to adapting this method to organic vapors would be to develop an appropriate exposure interface with a thermal gravimetric analysis system. The exposure system used by investigators to study water diffusion in the stratum corneum will not work for halogenated hydrocarbons. The rapid diffusion of these organic chemicals requires a system that can deliver chemical vapor to the stratum corneum fast enough so that diffusion, not chemical delivery, is rate limiting.

The combination of *in vivo* and *in vitro* techniques offer flexibility in the estimation of dermal permeability coefficients. In a scenario where a relative ranking of dermal permeability is desired or where *in vivo* data generation is not possible, an *in vitro* system may be appropriate. However, if extrapolation or the impact of

dermal absorption of chemicals on physiological processes is desired, then perhaps a more comprehensive description of the system and its behavior is appropriate. Both *in vivo* and *in vitro* elements of dermal permeability are included in this research project.

The overall objective of this work is to develop a predictive approach for estimating permeability coefficients for a pair of halogenated hydrocarbons in vehicles ranging from polar to nonpolar. In order to accomplish the overall objective the development of several components are required. One component is a physiologically based mathematical framework for describing the dermal absorption and subsequent systemic distribution, metabolism and elimination of the chemicals of interest. Only by describing the "whole system" interaction between the absorbed chemicals and the intact living systems can useful therapeutic or health risk assessment applications be made from dermal absorption studies.

Another component of this work is the generation of the *in vivo* data required to develop, validate and exercise the predictive potential of the physiologically based description of dermal absorption. The blood levels of chemical and the iterative relationship between these levels and the physiologically based model are essential for

refinement of the normalized permeability coefficient concept.

A third component of value is the *in vitro* estimation of permeability coefficients. By isolation of the skin structure, the impact of particular skin layers or features may be described in terms of observed permeability or species variability. The availability of a relatively quick and flexible *in vitro* method for estimating the dermal permeability coefficient of a chemical may provide mechanistic information for incorporation into the physiologically based approach. The result may be a more complete and flexible tool for the evaluation of chemical interactions with the skin and biological systems.

II. MATERIALS AND METHODS

LABORATORY ANIMALS

Male Fischer-344 rats weighing 200-250 grams were used to investigate the absorption of dibromomethane and bromochloromethane from dermal exposures where the chemicals were in solution with mineral oil, corn oil and water vehicles. The rats were purchased from Charles Rivers Breeders and provided free access to food (Purina Rat Chow) and water while being maintained in a 12 hour light/dark cycle (6:00 a.m. to 6:00 p.m. lights were on). Rats were individually housed in plastic 24 cm x 45 cm x 20 cm cages with a 1.5 cm thick layer of cedar bedding.

The animals used in these studies were handled in accordance with the principles in the Guide for the Care and Use of Laboratory Animals, prepared by the Committee on Care and Use of Laboratory Animals, Institute of Health, Publication #86-23,1985, and the Animal Welfare Act of 1966, as amended.

CANNULATION PROCEDURE

A day prior to its chemical exposure, each rat was surgically implanted with a jugular cannula to facilitate blood sample drawing during the exposure period. Animals

were weighed and then anesthetized with a 1 mL per Kg body weight i.p. injection of a solution containing 70 mg/mL Ketamine (Ketaset, Ketamine Hydrochloride injection, Parke-Davis, Morris Plains, NJ) and 6 mg/mL Xylazine (Rompun injectable, Miles Laboratories, Shawnee Mission, KS). When the animals were under anesthesia, the fur on the back of each rat's back was closely clipped with a #40 blade in order to accommodate the dermal exposure cells. Additionally, the fur was clipped on the ventral and dorsal sides of each rat's neck to facilitate surgical incision and cannula routing. After the fur was clipped, opthalmalic ointment was applied to each animal's eyes to prevent drying during surgery and Betadine (10% Povidone Iodine, Purdue Frederick Co., Norwalk CT) was applied to the areas where skin incisions were planned. Areas treated with Betadine were wiped with alcohol swabs prior to surgical activities.

Following the animal preparation, each rat was surgically fitted with a jugular cannula. The cannulas were made of silastic medical grade tubing (Dow Corning, Midland, MI, Cat. No. 602-135) with an internal diameter of 0.02 inches. The cannulas were 10.5 inches long with silastic (Silicone Medical Adhesive, Dow Corning, Midland, MI, Cat. No. 890) bulbs placed appropriately for attachment of the cannula to the animal in order to ensure stability and patency of the jugular cannula. A 2.5 cm surgical incision

was made over the right ventral portion of the rat's neck. Lipid and connective tissue were cleared in order to isolate the right external jugular vein and curved hemostats were placed underneath the vein to further isolate the area selected for cannula insertion. After vein isolation, a 20 gauge hypodermic needle was inserted into the jugular vein. As the hypodermic needle was slowly removed the silastic cannula was inserted through the hole prepared by the hypodermic needle. The cannula was inserted approximately 25 mm and the vein posterior to the insertion area was tied around the cannula with 3.0 silk suture. The cannula was further secured by attaching the cannula to the structural tissue with another 3.0 silk suture. This second attachment was approximately 7 mm anterior to the first attachment. After insertion and attachment of the cannula, a 5 mm incision was made in the area behind the neck which was closely clipped and treated with Betadine as part of the surgical preparation activities. The cannula was then routed just below the skin and exteriorized through the incision. The cannula was filled with a 25% heparin (Heparin Sodium Injection, SoloPak Laboratories, Franklin Park, IL) in normal saline solution and then capped. A 30 cm length of 5 cm wide Vetrap (Vetrap Bandaging tape, 3M Animal Care Products, St. Paul, MN, No. 1410BO) was placed around the animal just behind the front legs. The Vetrap

provided for storage and protection of the cannula while the animals recovered from surgery and awaited exposure. The animals were housed individually and had free access to food and water during the recovery period. Animals regained consciousness approximately 30 minutes after the initial dose of Ketamine/Xylazine was administered.

PARTITION COEFFICIENTS

Partition Coefficients for dibromomethane and bromochloromethane in the corn oil, mineral oil, peanut oil and water vehicles were determined using the vial equilibration method published by Gargas et al., 1989, as modified from Sato and Nakajima, 1979. Briefly, 0.1 mL of oil vehicle or 2.0 mL of water vehicle were placed into a 24.65 mL, septum cap sealed scintillation vial. Reference vials of the same volume and type were sealed with no vehicle added to them. Vials were heated to 32 °C and vented to release pressure. In order to avoid a pressure increase when chemical vapors were added, 0.5 mL of headspace were withdrawn from reference and sample vials. Bromochloromethane or dibromomethane vapor (0.5 mL) was added to the sample and reference vials and equilibrated for 3 hours at 32 °C. Following the incubation, 0.5 mL headspace samples from each vial were analyzed using a HP

5880 gas chromatograph equipped with a flame ionization detector. Nitrogen carrier gas (15 mL/min) and a 10′ long, 1/8″ diameter SE-30 column were used to separate bromochloromethane and dibromomethane under isothermal (80 °C) conditions. The injector and detector temperatures were 125 °C and 250 °C, respectively. The resulting analysis of the headspace in the reference and sample vials were used to calculate the vehicle to air partition coefficients (PC) as shown in Equation 26.

$$PC = \frac{\left(A_{h,r} \times V_{h,r} - A_{h,s}\left(V_{h,r} - V_s\right)\right)}{A_{h,s} \times V_s} \qquad \text{Eq 26}$$

In Equation 26, $A_{h,r}$ is the area count in the headspace of the reference vial, $V_{h,r}$ is the volume of the headspace in the reference vial, V_s is the volume of sample, and $A_{h,s}$ is the area count in the headspace of the sample vial.

The partition coefficients for dibromomethane and bromochloromethane in skin were determined using a thermal gravimetric analysis approach. Stratum Corneum was separated from rat skin as described in the stratum corneum separation section. Four stratum corneum samples (approximately 5 mg) were placed in a titanium sample pan in the sample cell of a thermal gravimetric analyzer. An air flow of 50 ml/min was introduced into the sample cell holding the skin and the flow was maintained until the mass

of the skin sample was constant. The furnace temperature was maintained at 32 °C throughout the procedure. After the mass of the skin was constant, the air flow was increased in one step to 1.1 L/min and maintained until the temperature and mass stabilized. When the mass was again constant, the air flow was turned off as the chemical flow (1.1 L/min) was simultaneously turned on. The change in mass as the chemical was absorbed into the skin was monitored and recorded. At the point where chemical equilibrium occurred between the vapor and skin phases, the partition coefficient was calculated. Details of the thermal gravimetric analysis and partition coefficient calculation are given in the thermal gravimetric analysis section.

The partition coefficients for the neat (undiluted) dibromomethane and bromochloromethane liquid to skin were determined by incubating skin samples in the liquid and extracting the absorbed chemical in an organic solvent. Skin samples were obtained by euthanizing rats via CO_2 and shaving the fur on the back of the rat. A 2 cm x 2 cm area of skin was excised and cleaned of fat and connective tissue. Skin was punched with a small skin punch and placed into pre-weighed vials (approximately 20 mg skin wt). One mL of neat dibromomethane or bromochloromethane was added to the skin sample and incubated at 32 °C for 2 hours. After incubation, the skin sample was removed, dried with a gauze

pad and placed into a vial containing 4.0 mL of n-hexane. The skin sample was extracted into the n-hexane by shaking on a vortex evaporator for 1 hour. The extraction efficiency was 97.5%. The n-hexane layer was analyzed for dibromomethane or bromochloromethane using gas chromatography as described in the chromatographic analysis section. The neat liquid to skin partition coefficient was taken as the ratio of the chemical concentration in the neat liquid to the chemical concentration in the skin.

IN VIVO CHEMICAL/VEHICLE EXPOSURES

Rats were surgically fitted with jugular cannulas as described in the jugular cannulation portion of the Materials and Methods section. After the cannulation process was complete but before the animals began to recover from the anesthesia, a 3.14 cm^2 glass dermal exposure cell was attached to the area of the back where the fur was closely clipped. The cell was fitted with a Teflon septum and sealed with a crimp top cap prior to dermal attachment. The dermal exposure cell was attached mid-back with cyanoacrylate adhesive (Pacer Technology, Rancho Cucamonga, CA, PT-01) approximately 100 mm from a line drawn between the rat's ears.

The day following the surgery and dermal exposure cell attachment, a group of 20-25 animals was separated into

three or four groups which received different concentrations of a test chemical in a specific vehicle. The group of 20-25 rats would therefore constitute the exposure group for one chemical in one vehicle. The process was repeated until all of the chemical and vehicle combinations of interest were complete. The chemical/vehicle combinations selected for this work were dibromomethane (Aldrich Chemical Co., Milwaukee, WI, Cat. No. D4168-6, 99%) or bromochloromethane (Aldrich Chemical Co., Milwaukee, WI, Cat. No. 13526-7, 99%) in corn oil (Mazola Corn Oil, Best Foods, Englewood Cliffs, NJ), mineral oil (Heavy Mineral Oil, Meijer Inc., Grand Rapids, MI) or water. The dibromomethane and bromochloromethane concentrations (wt/vol) in both mineral oil and corn oil were 25%, 50% and 75%. The dibromomethane and bromochloromethane concentrations in water were 25% saturated, 50% saturated, 75% saturated and saturated at 25 °C. These saturation levels corresponded to dibromomethane concentrations of 2.42, 6.14, 7.55 and 9.36 mg/mL respectively. Similarly the stated saturation levels in water corresponded to bromochloromethane levels of 3.61, 6.60, 9.30 and 12.77 mg/mL, respectively.

The exposure was initiated by adding 3.0 mL of the chemical/vehicle mixture to the dermal exposure cell. The solution was injected into the exposure cell by penetrating the exposure cell septum with a 20 gauge needle attached to

a glass tuberculin syringe. A 23 gauge needle was inserted through the septum prior to and during addition of the chemical/vehicle solution in order to vent pressure build up. The 3.0 mL volume was chosen to ensure complete coverage of the skin during the exposure period. The total capacity of the cell was approximately 3.5-4.0 mL.

Blood samples were drawn immediately prior to addition of chemical to the dermal exposure cell and at 0.5, 1, 2, 4, 8, 12 and 24 hours after addition of the chemical or chemical/vehicle solution. Each blood sample had a volume of 0.1 mL and was collected through the cannula into a 0.25 mL glass tuberculin syringe (Yale Glass Luer Tip, Becton Dickinson, Franklin Lakes, NJ, Cat. No. 2001). A 25 gauge stainless steel needle was attached to the glass syringe and the blood was injected into a 2.0 mL septum sealed vial (National Scientific, Lawrenceville, GA, #C4010-17AW) containing 1.0 mL of n-hexane (Baxter, Burdick and Jackson, Muskegon, MI, Cat. No. GC60393-4, GC Quality 99.9+%). The cannula was filled with a 25% heparin in normal saline solution after each blood drawing. Immediately prior to each blood drawing the heparin solution in the cannula was removed and discarded. The dibromomethane or bromochloro-methane was extracted from the blood into the n-hexane by shaking the samples vigorously on a vortex evaporator (Haake-Buchler, Labconco Corp, Kansas City, MO, Model

4322000) for 15 minutes. After shaking, 500 uL of the n-hexane was removed and placed into a 2.0 mL autosampler vial (National Scientific, Lawrenceville, GA, # HC4011-2) and sealed with a Teflon crimp cap (Kimble, Owens, IL, # 73825B-11). The sample was analyzed using gas chromatography on a Hewlett-Packard 5890 series II gas chromatograph equipped with a ^{63}Ni electron capture detector.

FINITE DOSE *IN VIVO* EXPOSURES

Following surgical implantation of a jugular cannula as described above, a 3.8 cm^2 stainless steel dermal exposure cell was attached with cyanoacrylate adhesive. The attachment procedure and animal preparation was as described earlier except that the dermal cell was open to the atmosphere and an "Elizabethan" collar was placed around the animals neck. The collar was applied while the animal was under anesthesia for jugular cannula insertion.

The day following surgery, an air line supplying 150 mL of fresh breathing air was attached to the top of the "Elizabethan" collar. This was intended to further reduce the potential for any inhalation of evaporated chemical. The exposure was initiated by adding 250 uL of neat dibromomethane or bromochloromethane into the dermal exposure cell. Blood samples were drawn immediately prior

to the addition of chemical to the dermal exposure and at 2, 5, 10, 13, 16, 19, 25, 30, 35, 40, 45 and 60 minutes after addition of chemical. Blood sample volumes were 0.05 mL and as before, the cannula was flushed with a 25% heparin solution. Blood extraction was accomplished in n-hexane as previously described and subjected to chromatographic analysis as described in the chromatographic analysis section.

CANNULA EFFECT ON MEASURED BLOOD CONCENTRATIONS

A male rat was exposed to neat dibromomethane for 3 hours at which time it was euthanized via carbon dioxide inhalation and 6 mL of blood was collected from the abdominal vena cava into a heparinized 10 mL glass syringe. The blood sample was placed into a 20 mL glass vial fitted with a Teflon septum and a crimp top cap. A 12 gauge needle was placed through the Teflon septum to allow access to the blood via the cannula. The cannula was routed through the orifice of the needle into the blood and 0.1 mL of blood was drawn into a 0.25 glass tuberculin syringe. The sample was then transferred to a sealed vial containing 1.0 mL of n-hexane, was extracted and analyzed (see chromatographic analysis section) for its chemical content as previously described. This procedure was identical in components and

process to the blood drawing from exposed animals. As a comparison, a 0.25 mL glass tuberculin syringe fitted with a stainless steel needle was used to go directly through the septum and draw a 0.1 mL blood sample. The sample was extracted using the same procedure as with the cannula drawn blood sample. The order of drawing alternated between cannula drawn and stainless steel needle drawn blood. Ten pairs of samples were drawn (20 blood samples)and the blood levels of dibromomethane were compared between the cannula and stainless steel derived blood samples. The entire process was repeated except that bromochloromethane was used in place of dibromomethane.

CHROMATOGRAPHIC ANALYSIS

The blood samples drawn during all of the *in vivo* exposures were analyzed for dibromomethane or bromochloromethane using gas chromatography. Once the samples were extracted and prepared as described above, 1 uL of sample was introduced via autoinjector into a Hewlett-Packard 5890 series II gas chromatograph equipped with an electron capture detector. The samples were introduced into a 30 meter long, 530 micron diameter, DB-1 wide bore gas chromatography column with a film thickness of 3.0 micron. The carrier gas was an ultrapure blend in the ratio of 95%

argon to 5% methane. Standard curves were done with DBM or BCM in n-hexane and treated as samples drawn from the laboratory animals. Analytical linearity was achieved at chemical concentrations of 0.05 ug/mL and greater. The conditions specific for dibromomethane were a column carrier flow of 6.85 mL/min with an isothermal oven temperature of 80 °C. The resulting column retention time was 3.1 minutes. The injector and detector temperatures were 125 and 300 °C, respectively. The conditions specific for bromochloromethane were a column flow of 7.15 mL/min with an isothermal oven temperature of 60 °C. The resulting column retention time was 2.9 minutes. All other gas chromatography conditions were the same as described above.

STRATUM CORNEUM SEPARATION

Stratum corneum was separated from whole skin for use in the thermal gravimetric analysis cell using the technique described in the evaluation of water vapor diffusion in porcine stratum corneum (Liron, et al., 1994). This proven technique was selected based on relevant applications from the several methods described in the literature (Willsteed, et al., 1991). The whole skin samples were obtained from male Fischer-344 rats, 200-250 grams. A 55 mm x 95 mm skin patch was removed from the mid backs of rats that had been

euthanized via CO_2 inhalation. The skin was removed using scissors. Immediately after removal, the skin was blotted with gauze to remove blood and debris. The edges of the skin were cut square with a razor blade in order to facilitate dermatoming. The skin samples were dermatomed to a thickness of 0.025 mm. The resulting 0.025 mm thick skin sections were cut with a razor blade into 25 mm x 25 mm squares and placed onto filter paper saturated with 0.5% trypsin (Type II, 1130 units/mg solid, Sigma Chemical Co., St. Louis, MO). The filter paper resided in a petri dish and the trypsin was made up in 0.05 M phosphate buffered saline at pH 7.4. The petri dish containing the skin sample and trypsin were placed into a CO_2 free incubator at 37 °C for 2 hours. After two hours of incubation, the skin samples were removed and placed into a beaker containing 100 mL of 0.005% trypsin inhibitor (Type II-S, Sigma Chemical Co, St. Louis, MO). The trypsin inhibitor was made up in 0.05 M phosphate buffered saline at pH 7.4. After 10 minutes of incubation in the trypsin inhibitor, the stratum corneum was carefully removed from the dermis using forceps. The stratum corneum was then floated on distilled water for 30 minutes. Following the 30 minutes in water chamber, the stratum corneum was removed from the water using stainless steel screen. The screen was placed under the floating samples and as the screen was lifted, the stratum corneum

attached to the screen. The screen containing the stratum corneum was placed on gauze and allowed to air dry. After the skin was dry it was placed into a desiccator jar until needed. Stratum corneum separation was verified using light microscopy and prior to use the stratum corneum pieces were cut into circles weighing approximately 1.25 mg each.

THERMAL GRAVIMETRIC ANALYSIS

Skin samples for use in the thermal gravimetric analyzer were prepared as described in the stratum corneum separation section. The chemical exposure apparatus that supplied the sample cell of the thermal gravimetric analyzer (TGA51 Thermal Gravimetric Analyzer with a Thermal Analyst 2200 data acquisition module, TA Instruments, Inc., New Castle, DE) contained two Plexiglas chemical containment boxes for housing of the chemical sample bags. The Plexiglas was 9.0 mm thick and was constructed in the dimensions of 75.6 cm x 75.6 cm x 35.2 cm. Ports (3/8 inches diameter) were drilled in opposite sides of each containment box. One port was used to route the cord for a hot plate that was placed inside the containment box and the other port was used to connect the chemical sample bag to the TGA system. The lids of the containment boxes had a 9.0 mm wide rubber gasket attached to the rim of the lid. The

gasket was used to create a gas tight seal between the lid and the sides of the box. Additionally, the lid had three ports attached for use in sample flow and chamber atmosphere control. Clamps were attached to both the lid and sides of the boxes to make as tight a seal as possible.

Three sample bags (Tedlar gas sample bags, 40 liter, Dupont, Wilmington, DE) were prepared for use the chemical containment boxes. One of the bags contained only air and was identified as the equilibrium bag. The second bag contained air and the chemical of interest and was identified as the sample bag. A third bag identified as the pre-equilibrium bag contained only air with the desired humidity level and it was placed in a second containment chamber. The pre-equilibrium bag was used to condition the skin with the proper humidity level prior to introduction of the equilibrium flow. Exposures where other than dry air is desired can be accommodated in this system and the water concentration, $C_{H_2O,air}$, in each bag could be as calculated as shown in Equation 27.

$$C_{H_2O,air} = \frac{VP_{H_2O,21^oC}}{VP_{ATM}} \times 10^6 ppm \times \frac{mg/m^3}{ppm} \times \frac{m^3}{10^3 L} \times RH = \frac{mgH_2O}{L_{air}} \qquad \text{Eq 27}$$

In Equation 27, VP is the vapor pressure in mmHg, atm is atmospheric pressure and RH is relative humidity.

For the exposures conducted in this work, the sample bag had either liquid dibromomethane or bromochloromethane added. The volume of DBM or BCM added to the sample bag was calculated using Equation 28. Both of these chemicals were rapidly vaporized using a hot air gun following addition to the Tedlar bag.

$$V_{LB} = V_T(L) \times \frac{MW(g/mole)}{24.45(L/mole)} \times \frac{1}{D(g/mL)} \times \frac{PPM_T}{10^6} \qquad \text{Eq 28}$$

In Equation 28, V_{LB} is the volume (mL) of liquid dibromomethane or bromochloromethane to be added to the Tedlar sample bag, V_T is the total volume in sample bag, MW is the molecular weight, D is the liquid density, PPM_T is the target chemical concentration in parts per million in the sample bag. Units for each of the terms are shown in parenthesis in equation 28. The chemical containment chambers that housed the pre-equilibrium, equilibrium and sample bags were prepared so that the atmosphere surrounding the bags was similar to the atmosphere inside the bags. This was done in order to reduce mass changes due to water vapor transfer between the bags in the containment chambers and the atmosphere surrounding them. All monitoring of temperature and humidity was accomplished using a LCD digital hydrometer (Model 3309-30, Cole-Parmer Instrument Co., Chicago, IL).

Once the chemical containment chambers and the pre-equilibrium, equilibration and sample bags were prepared, a flow of 50 mL/min from the pre-equilibrium bag was established through the thermal gravimetric analysis cell. The flow from the pre-equilibration bag was maintained until the mass of the sample became constant (water vapor was in equilibrium between the stratum corneum and the air stream above the sample). At that point the flow from the pre-equilibrium bag was terminated and 50 mL/min flow from the equilibrium bag was initiated. At the start of the equilibrium period, the thermal gravimetric analysis cell temperature was set at 32 °C and maintained at that temperature throughout the exposure. The mass was monitored continuously via the data acquisition module attached to the thermal gravimetric analysis cell. After the mass was constant, the equilibrium flow was adjusted to the higher flow of 1.1 L/min. This increase in flow had a slight effect on temperature which took about five minutes for the thermal gravimetric analysis cell to correct. At the point where temperature and mass were constant, the equilibration bag flow was turned off as the sample bag flow was simultaneously turned on. The flow and water content of the sample bag was the same as in the equilibration bag. Therefore, no re-equilibration of water vapor or temperature change resulted from the switch to the sample bag. The mass

was monitored and recorded until the mass of the sample was constant. The time point were mass became constant was the point where the dibromomethane or bromochloromethane vapor was in equilibrium between the stratum corneum and the air stream above it. The stratum corneum to air partition coefficient (PSC) for dibromomethane or bromochloromethane was calculated from the equilibrium phase of the vapor exposure as shown in Equation 29.

$$PSC = \frac{C_{SC}}{C_A} = \frac{A_{SC} / V_{SC}}{C_A} \qquad \text{Eq 29}$$

In Equation 29, C_{SC} is the chemical concentration in the stratum corneum, C_A is the chemical concentration in the air above the stratum corneum sample, A_{SC} is the amount of chemical in the stratum corneum and V_{SC} is the volume of stratum corneum.

The diffusion coefficient was estimated using a solution to a non-steady state diffusion equation describing diffusion through a plane sheet (Crank, 1975; Quinn, 1994,). The mathematical equations and computer code used to evaluate mass vs. time data derived from the thermal gravimetric analysis experiments are shown in appendix C. The solution to the diffusion equation described above is shown in Equation 30.

$$\frac{M_t}{M_\infty} = \left(1 - e^{-bt}\right) - \sum_{n=0}^{\infty} \frac{16}{\pi^2(2n+1)^2} \times \frac{2L^2 b}{D(2n+1)^2\pi^2 - 4bL^2} \times \left[e^{-bt} - e^{-D(2n+1)^2\pi^2 T/4L^2}\right]$$

Eq 30

In Equation 30, M_t is the mass at time t, M_∞ is mass at time infinity, b is the constant for exponential rise of the chemical vapor concentration in the thermal gravimetric analysis cell, t is time (seconds), L is half thickness of the stratum corneum (cm) and D is the diffusion coefficient (cm^2/second).

A schematic of the thermal gravimetric analysis system used to generate the diffusion coefficient and partition coefficient information is provided in Figure 8.

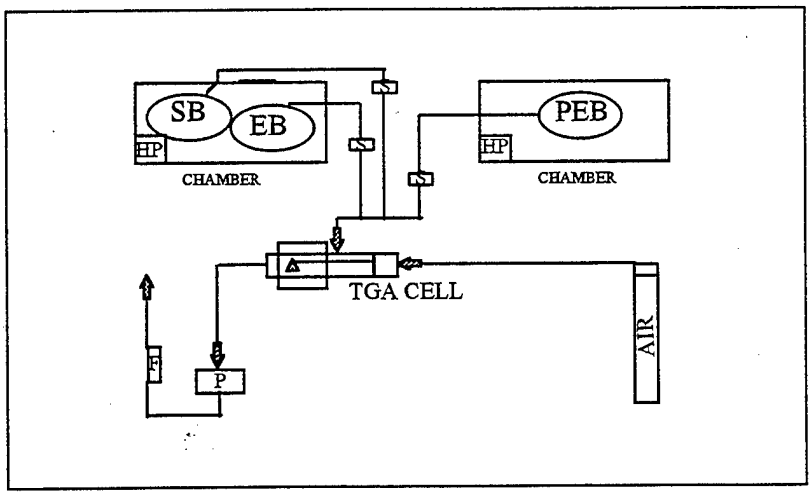

Figure 8. Schematic of Thermal Gravimetric Analysis System. **PEB is the pre-equilibrium bag, EB is the equilibrium bag, SB is the sample bag, S is an open/close switch, HP is a hot plate, F is a flow meter, P is a reciprocating stainless steel pump and the triangle in the TGA cell is a titanium sample pan that holds the stratum corneum.**

PHYSIOLOGICALLY BASED PHARMACOKINETIC MODEL

The physiological based model used in this work was composed of six physiological compartments. The rationale for selecting each of the compartments as well as their basic form was provided in the introduction section. The code for the physiologically based pharmacokinetic (PBPK) model as well as the data files are in included in Appendices A and B, respectively. A schematic of the PBPK model is provided in Figure 9.

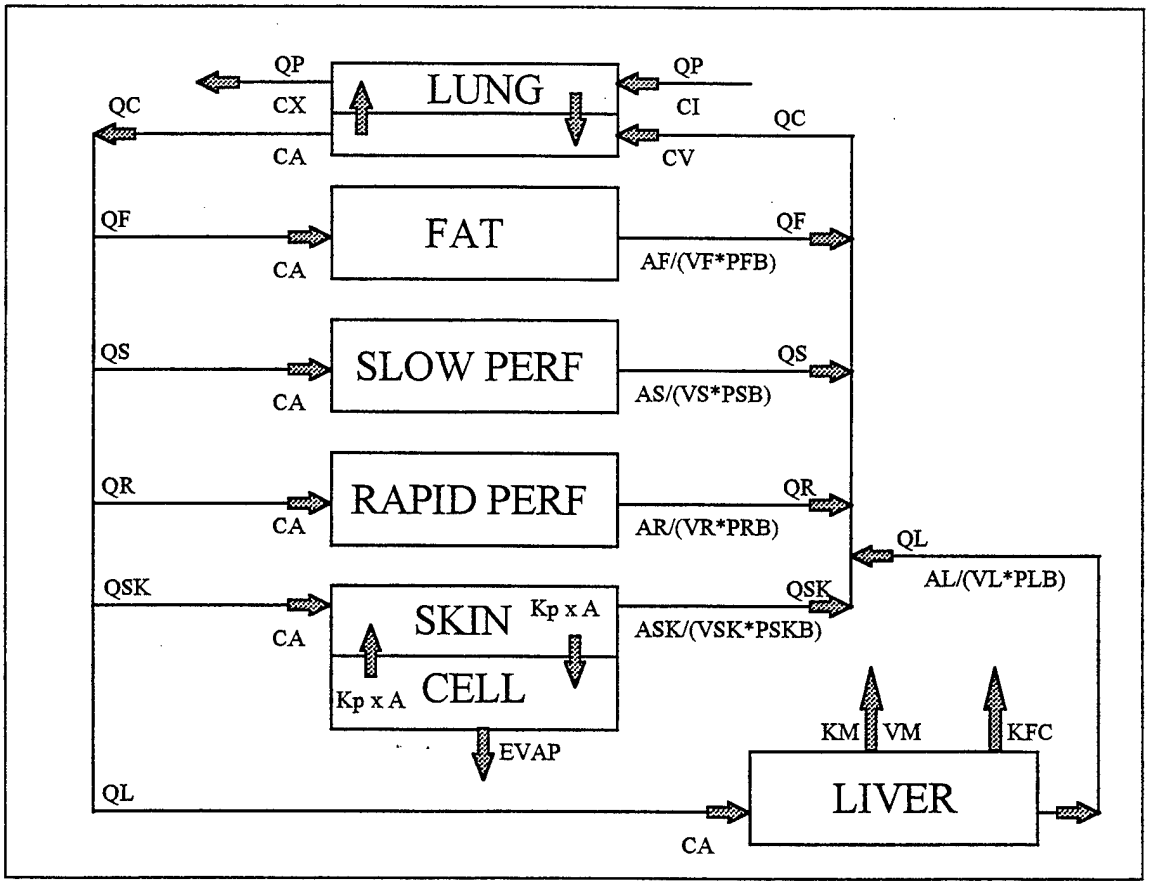

Figure 9. Schematic of the Physiologically Based Pharmacokinetic Model

In Figure 9, QF, QS, QR, QSK and QL represent the blood flow (L/hour) to the fat, slowly perfused, rapidly perfused, skin and liver compartments, respectively. QC is the cardiac output (L/hour) and QP is the pulmonary ventilation rate (L/hour). CA and CV are the arterial and venous blood concentrations (mg/L) of dibromomethane or bromochloromethane respectively. Kp is the permeability coefficient (cm/hour), A is the area across which diffusion occurs (cm^2), EVAP is the chemical evaporation rate from the skin surface (mg/hour), KM is the metabolic affinity constant (mg/L), VM is the maximum rate of saturable chemical metabolism (mg/hour), KFC is the first order rate constant for metabolism (1/hour), CX is the chemical concentration in expired air (mg/L) and CI is the chemical concentration in inspired air (mg/L). AF, AS, AR, ASK, AL, VF, VS, VR, VSK and VL are the amounts (mg) of chemical in the fat, slowly perfused, rapidly perfused, skin and liver compartments and the volumes (L) of the tissue compartments, respectively. PFB, PSB, PRB, PSKB and PLB are the fat, slowly perfused tissue, rapidly perfused tissue, skin and liver to blood partition coefficients, respectively.

The values for physiological parameters relating to organ volumes, blood flows, ventilation rate and cardiac output are specific for the biological species of interest. The physiological values used in the case of the Fischer-344

rat have previously been reported and since used in quantitative descriptions of biological systems (Ramsey and Andersen, 1984). A summary of the biological system specific, chemical independent values used in the PBPK model diagrammed above are provided in Table 3. The tissue to blood partition coefficient and metabolism values extracted from the literature and used in the PBPK model are shown in Table 4 (Gargas, et al., 1986, Gargas, et al., 1989). The remaining parameters are defined in the PBPK programming code in Appendix A and their values as used in the PBPK model are provided in the data file shown in Appendix B. The model code shown in Appendices A, B and C is written in Advanced Continuous Simulation Language (ACSL, Mitchell and Gauthier Associates, Inc., Concord, MA) which is imbedded in an optimization software package marketed as Simusolv (The Dow Chemical Company, Midland, MI). ACSL is a Fortran based simulation language designed for use in modeling systems described by time dependent, non-linear differential equations.

Features of ACSL include free form input, independent error control on the integrator and integration operators that transform a set of differential equations into a form that can be solved directly by integration. The Simusolv software package adds a dimension of usefulness to the ACSL software by adding an optimization capability. The Simusolv

optimization is accomplished using the statistical method of maximum likelihood.

Table 3. PBPK Model Values for Biological Parameters

PHYSIOLOGICAL PARAMETER	VALUE AND UNITS
QPC PULMONARY VENTILATION	15 LITER/KG/HOUR
QL LIVER BLOOD FLOW	25% CARDIAC OUTPUT
QF FAT BLOOD FLOW	7% CARDIAC OUTPUT
QSK SKIN BLOOD FLOW	5% CARDIAC OUTPUT
QS SLOWLY PERF BLOOD FLOW	24% CARDIAC OUTPUT-QF-QSK
QR RAPID PERF BLOOD FLOW	76% CARDIAC OUTPUT-QL
QCC CARDIAC OUTPUT	15 LITER/KG/HOUR
VF VOLUME FAT	7% BODY WEIGHT
VL VOLUME LIVER	4% BODY WEIGHT
VSK VOLUME SKIN	10% BODY WEIGHT
VS VOLUME SLOWLY PERF	82% BODY WEIGHT-VF-VSK
VR VOLUME RAPID PERF	9% BODY WEIGHT-VL

Table 4. Partition and Metabolism PBPK Values

PARAMETER	UNITS	DBM VALUES	BCM VALUES
LIVER:BLOOD PC	UNITLESS	0.918	0.70
FAT:BLOOD PC	UNITLESS	10.8	7.8
SLOW PERF:BLOOD PC	UNITLESS	0.55	0.27
RAPID PERF:BLOOD PC	UNITLESS	0.918	0.70
VMAXC	MG/KG/HOUR	12.5	7.0
KM	MG/L	0.36	0.40
KFC	1/KG/HOUR	0.557	0.70

III. RESULTS

PARTITION COEFFICIENTS

The stratum Corneum to air partition coefficients as determined using a thermal gravimetric analysis technique were 36.4 ± 3.1 and 120.4 ± 3.4 (mean ± standard deviation) for bromochloromethane and dibromomethane, respectively. Vehicle (Water, Corn Oil, Mineral Oil and Peanut Oil) to air partition coefficients for bromochloromethane and dibromomethane as measured using a standard vial equilibration method (Gargas, et al., 1989) ranged from 8.65 to 1023 and are included in Appendix B. The skin to neat (undiluted) chemical partition coefficients were 0.10 ± 0.02 and 0.08 ± 0.01 for bromochloromethane and dibromomethane, respectively.

CANNULA EFFECTS ON MEASURED BLOOD CONCENTRATIONS

The silastic material used in cannula preparation did not significantly affect the measured chemical concentration of dibromomethane or bromochloromethane in blood. The ratio of chemical concentration determined from blood drawn through the silastic cannula and blood drawn through a stainless steel needle was 1.006 ± 0.090 for dibromomethane

and 0.927 ± 0.049 for bromochloromethane. The ratios for the individual pairs are shown in Figures 10 and 11.

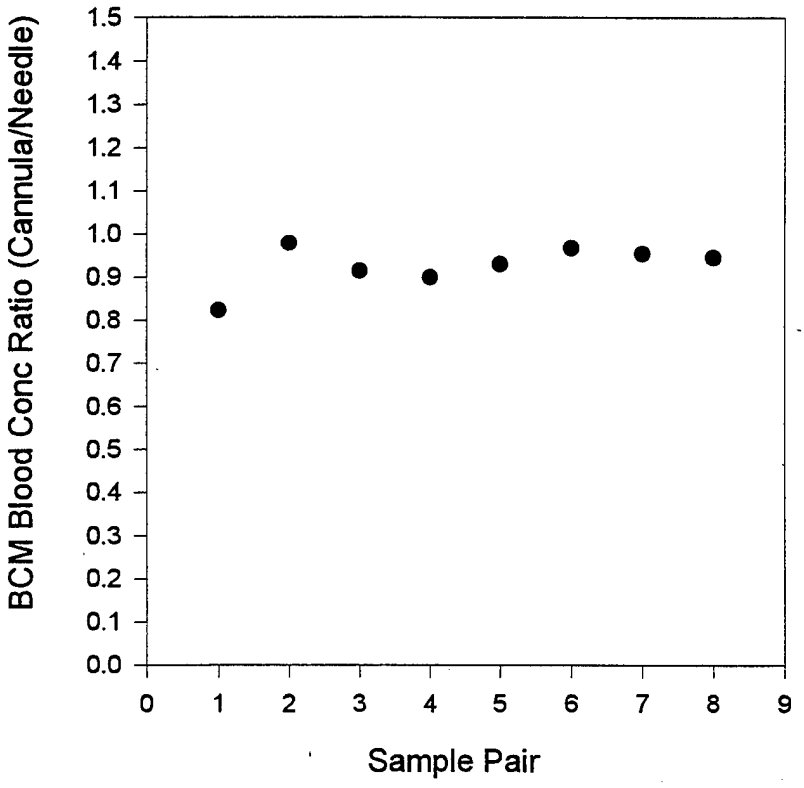

Figure 10. Cannula Effect on Measured Bromochloromethane (BCM) Concentration in Blood. Ratio of measured blood concentrations (Conc) of bromochloromethane as derived through a silastic cannula or stainless steel needle.

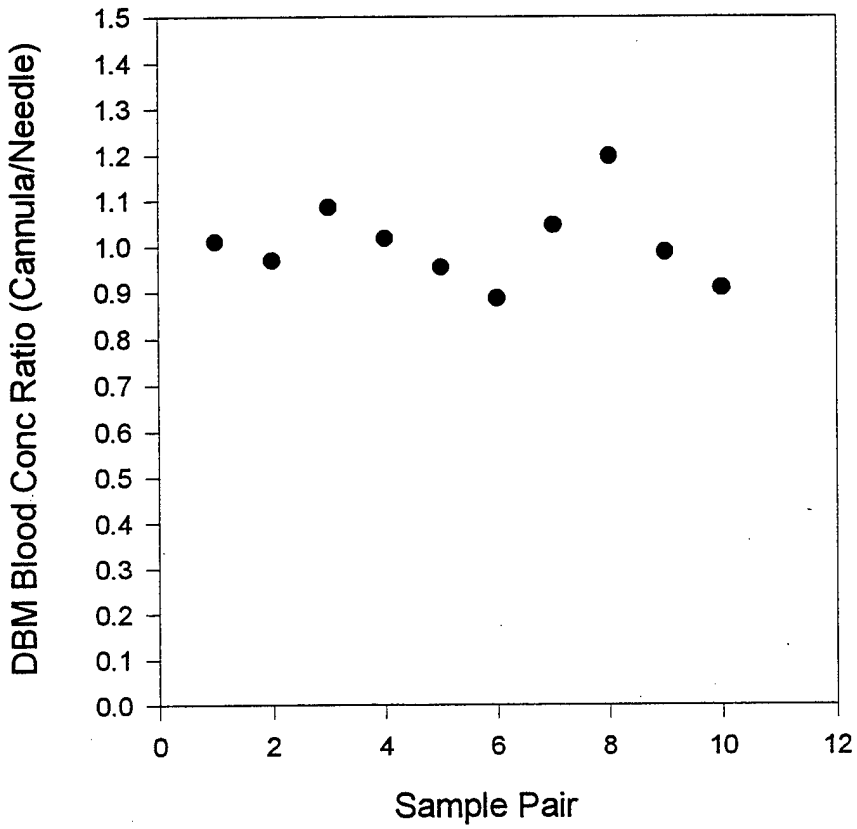

Figure 11. Cannula Effect on Measured Dibromomethane (DBM) Concentration in Blood. Ratio of measured blood concentrations (Conc) of dibromomethane as derived through a silastic cannula or stainless steel needle.

IN VIVO CLOSED DERMAL CELL EXPOSURES

Peak bromochloromethane concentrations in blood during a 24 hour, water vehicle, closed dermal cell exposure ranged from 0.82 ug/mL (6.34×10^{-6} M) in the 25% solution to 8.94 ug/mL (6.91×10^{-5} M) in the saturated solution. The blood concentrations resulting from the bromochloromethane in water exposures are shown in Figure 12. The blood concentrations peaked at about 2 hours and then declined to near zero as a result of a change in the exposure chemical concentration. The relatively low achievable exposure chemical concentration as compared to the oil vehicles was due to the low solubility of bromochloromethane in water. The loss of bromochloromethane from the dermal exposure cell as the bromochloromethane was absorbed into the animal served to deplete the exposure cell of bromochloromethane.

Peak bromochloromethane concentrations in blood during a 24 hour, corn oil vehicle, closed dermal cell exposure ranged from 27.99 ug/mL (2.16×10^{-4} M) in the 25% solution to 87.65 ug/mL (6.78×10^{-4} M) in the 75% solution. The blood concentrations resulting from the bromochloromethane in corn oil exposures are shown in Figure 13.

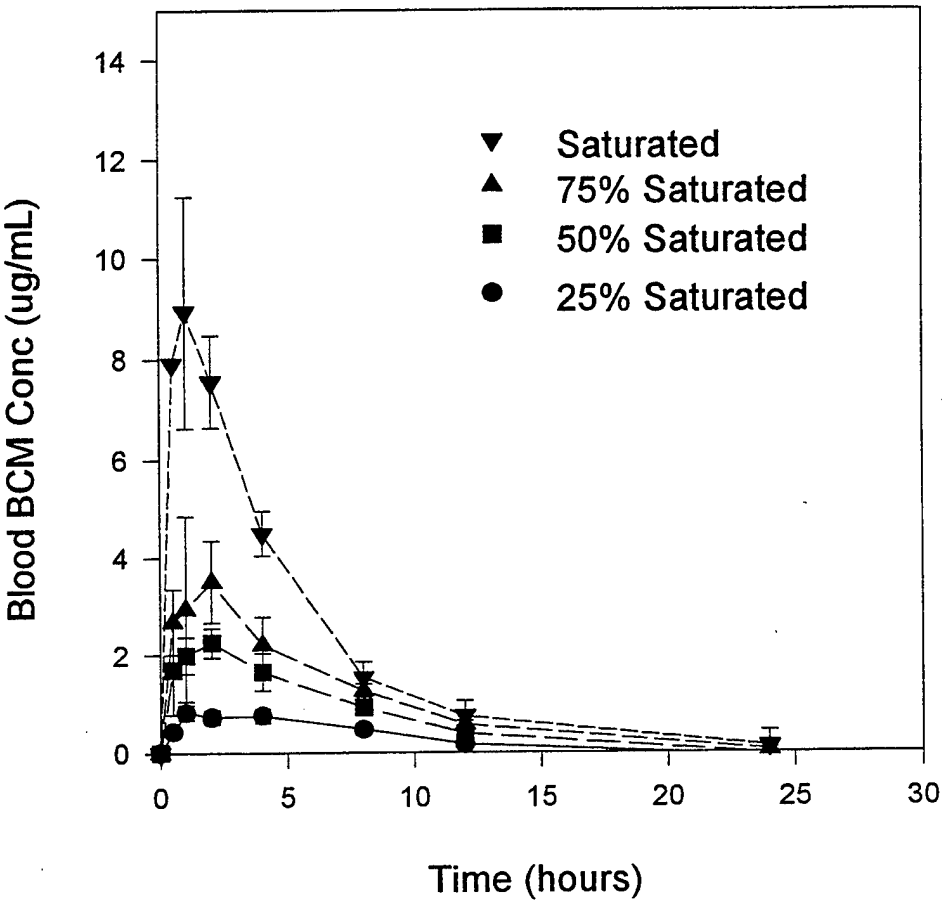

Figure 12. Bromochloromethane (BCM) Concentrations in Blood Following Dermal Doses of BCM in Water. Blood concentrations (Conc) are given as the mean with error bars representing the standard deviation. Each point on the graph represents blood samples taken from 5-10 animals. Bromochloromethane concentrations in water were 3.6 mg/mL, 6.6 mg/mL, 9.3 mg/mL and 12.8 ug/mL for the 25%, 50%, 75% and saturated solutions, respectively.

The blood concentration peaked at about five hours and remained relatively constant throughout the exposure. Unlike the water vehicle, corn oil was completely miscible with bromochloromethane and, because of the huge amount present, the amount of chemical absorbed did not significantly alter the exposure concentration of bromochloromethane.

Peak bromochloromethane concentrations in blood during a 24 hour, mineral oil vehicle, closed dermal cell exposure ranged from 45.53 ug/mL (3.52×10^{-4} M) in the 25% solution to 130.83 ug/mL (1.01×10^{-3} M) in the 75% solution. The blood concentrations resulting from the bromochloromethane in mineral oil exposures are shown in Figure 14. The peak blood concentration was achieved between 4 and 8 hours and then declined. With respect to the oil vehicles, a significant decline in chemical concentrations in the blood following attainment of the peak concentration was observed only in the bromochloromethane exposures.

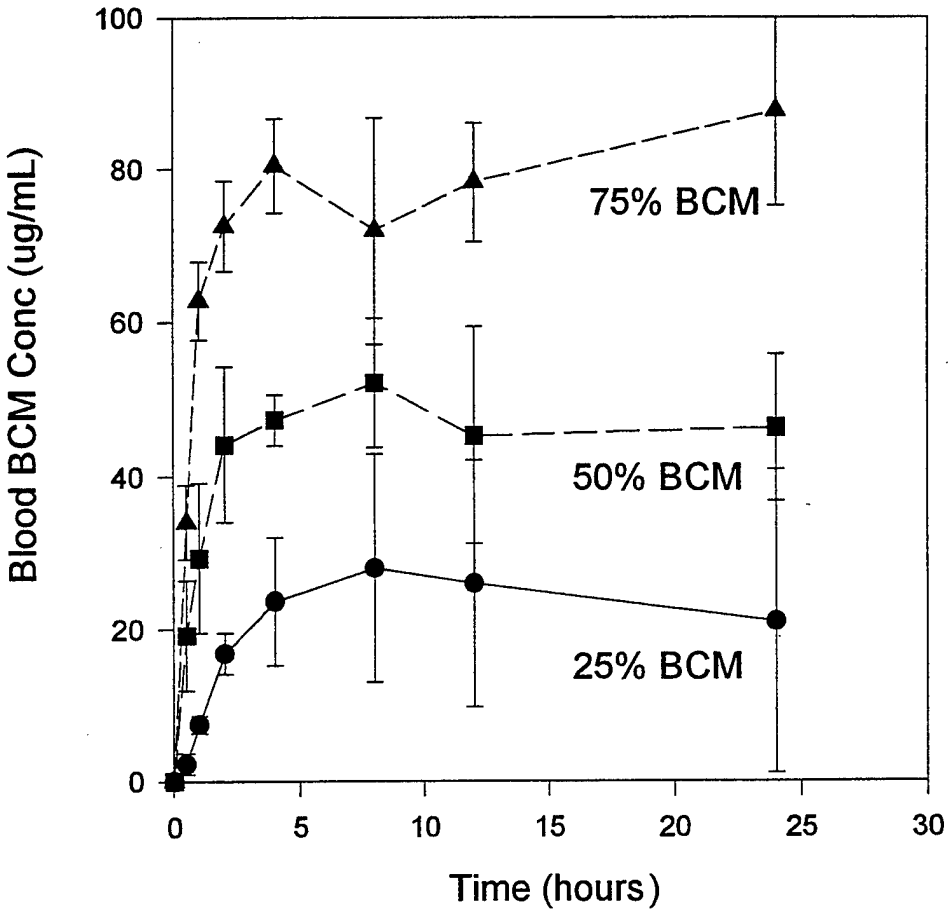

Figure 13. Bromochloromethane (BCM) Concentrations in Blood Following Dermal Doses of BCM in Corn Oil. Blood concentrations are given as the mean with error bars representing the standard deviation. Each point on the graph represents blood samples taken from 5-10 animals. Bromochloromethane concentrations in corn oil were 497.7 mg/mL, 995.3 mg/mL, and 1493 mg/mL for the 25%, 50%, and 75% solutions, respectively.

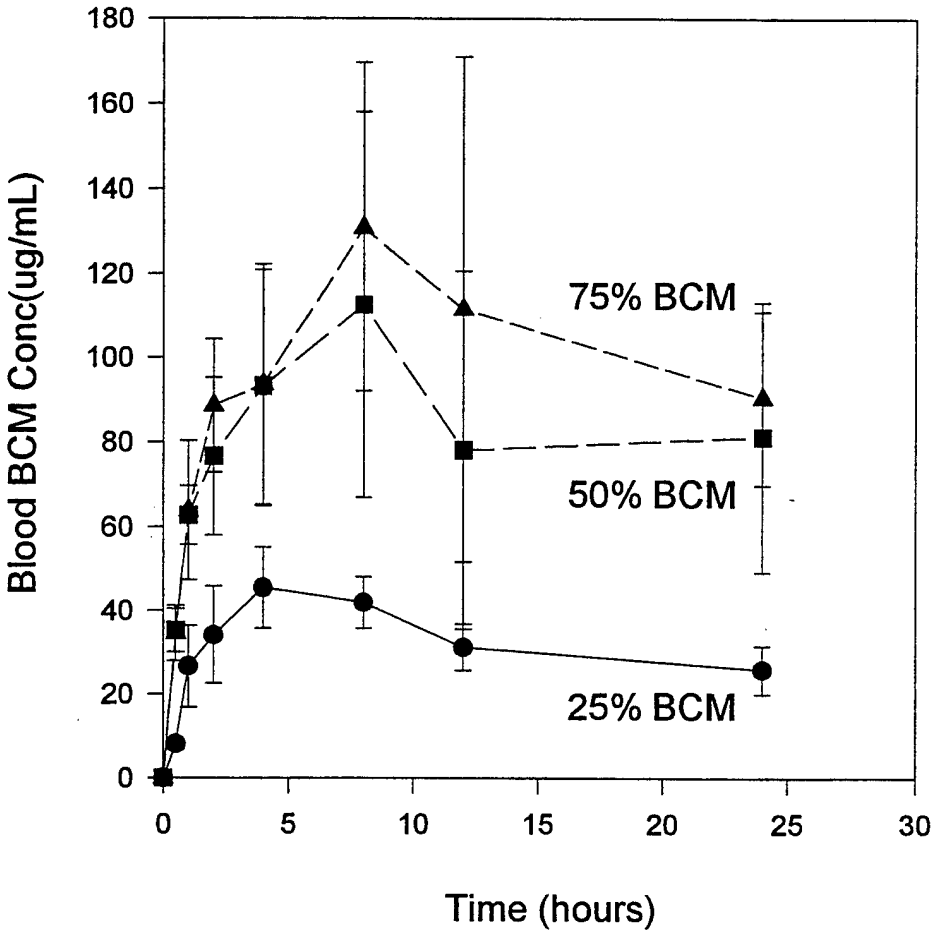

Figure 14. Bromochloromethane (BCM) Concentrations in Blood Following Dermal Doses of BCM in Mineral Oil. Blood concentrations are given as the mean with error bars representing the standard deviation. Each point on the graph represents blood samples taken from 5-10 animals. Bromochloromethane concentrations in mineral oil were 497.7 mg/mL, 995.3 mg/mL, and 1493 mg/mL for the 25%, 50%, and 75% solutions, respectively.

Peak dibromomethane concentrations in blood during a 24 hour, water vehicle, closed dermal cell exposure ranged from 1.00 ug/mL (5.75×10^{-6} M) in the 25% saturated solution to 5.86 ug/mL (3.37×10^{-5} M) in the saturated solution. The blood concentrations resulting from the dibromomethane in water exposures are shown in Figure 15. The peak concentrations of dibromomethane in blood occurred at approximately 2 hours and then declined toward baseline dibromomethane levels. The declining blood levels of dibromomethane in the water vehicle exposures reflected a decline of the dibromomethane exposure concentration as the chemical was absorbed. As with bromochloromethane, the dibromomethane has low water solubility and therefore has a limited achievable concentration range in water.

Peak dibromomethane concentrations in blood during a 24 hour, corn oil vehicle, closed dermal cell exposure ranged from 18.13 ug/mL (1.04 x 10-4 M) in the 25% solution to 128.77 mg/mL (7.40 x 10-4 M) in the 75% solution. The blood concentrations resulting from the dibromomethane in corn oil exposures are shown in Figure 16. The peak blood concentrations occurred at approximately 8 hours and remained relatively constant throughout the rest of the exposure.

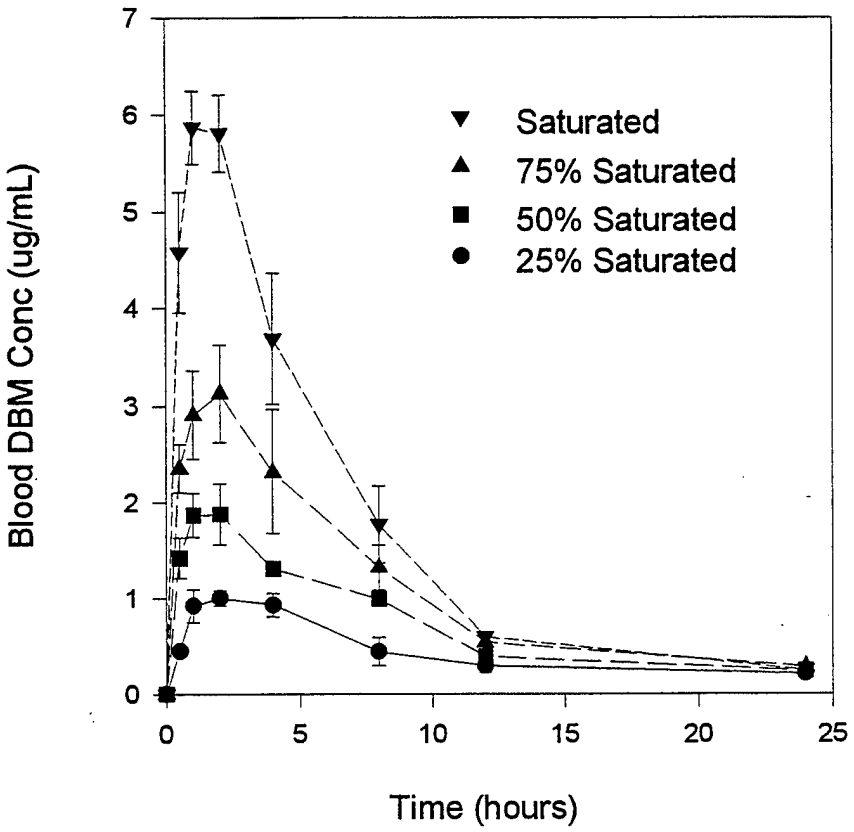

Figure 15. Dibromomethane (DBM) Concentrations in Blood Following Dermal Doses of DBM in Water. Blood concentrations are given as the mean with error bars representing the standard deviation. Each point on the graph represents blood samples taken from 5-10 animals. Dibromomethane concentrations in water were 2.42 mg/mL, 6.14 mg/mL, 7.55 mg/mL and 9.36 mg/mL for the 25%, 50%, 75% and saturated solutions, respectively.

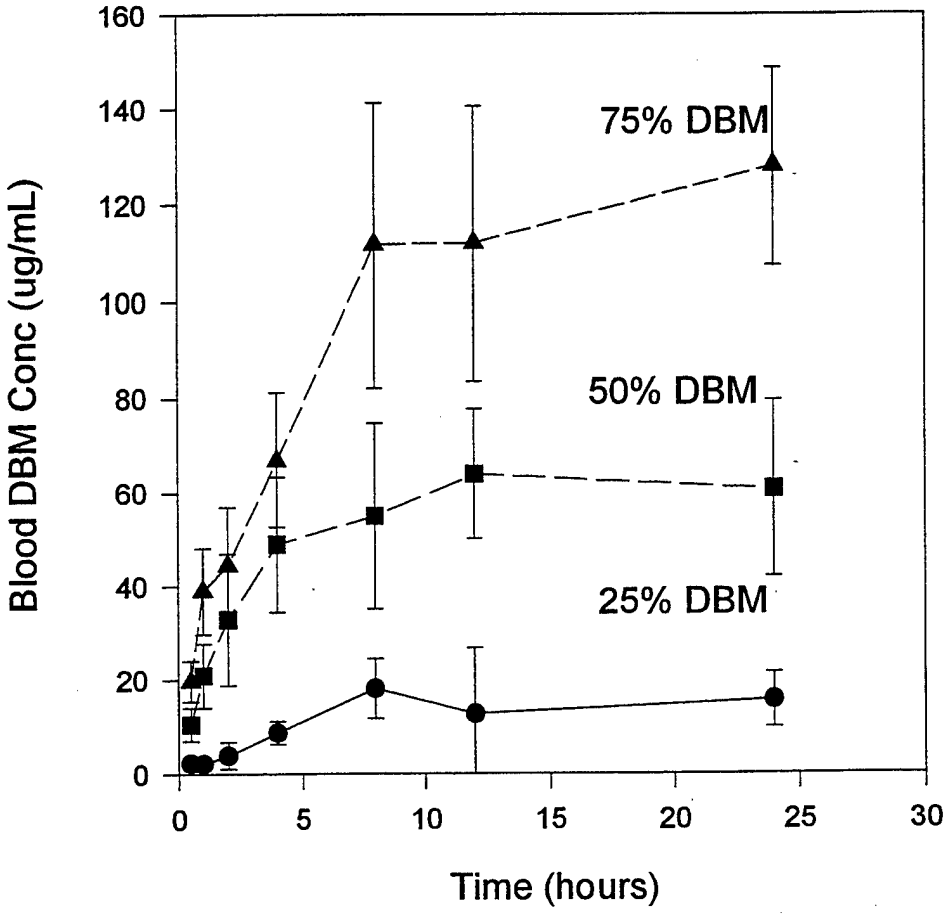

Figure 16. Dibromomethane (DBM) Concentrations in Blood Following Dermal Doses of DBM in Corn Oil. Blood concentrations are given as the mean with error bars representing the standard deviation. Each point on the graph represents blood samples taken from 5-10 animals. Dibromomethane concentrations in corn oil were 619.5 mg/mL, 1239.0 mg/mL and 1858.5 mg/mL for the 25%, 50% and 75% solutions, respectively.

Peak dibromomethane concentrations in blood during a 24 hour, mineral oil vehicle, closed dermal cell exposure ranged from 48.54 mg/mL (2.79×10^{-4} M) in the 25% solution to 162.41 mg/mL (9.34×10^{-4} M) in the 75% solution. Blood concentrations resulting from the dibromomethane in mineral oil exposures are shown in Figure 17. The maximum blood levels were achieved at approximately 8 hours in the 25% exposure and 12 hours or more in the 50% and 75% exposures. As with bromochloromethane in mineral oil, the dibromomethane in mineral oil produced data with greater variability than data generated from other vehicles. The decline in chemical concentration in blood observed in the bromochloromethane exposure was not observed in the dibromomethane exposure.

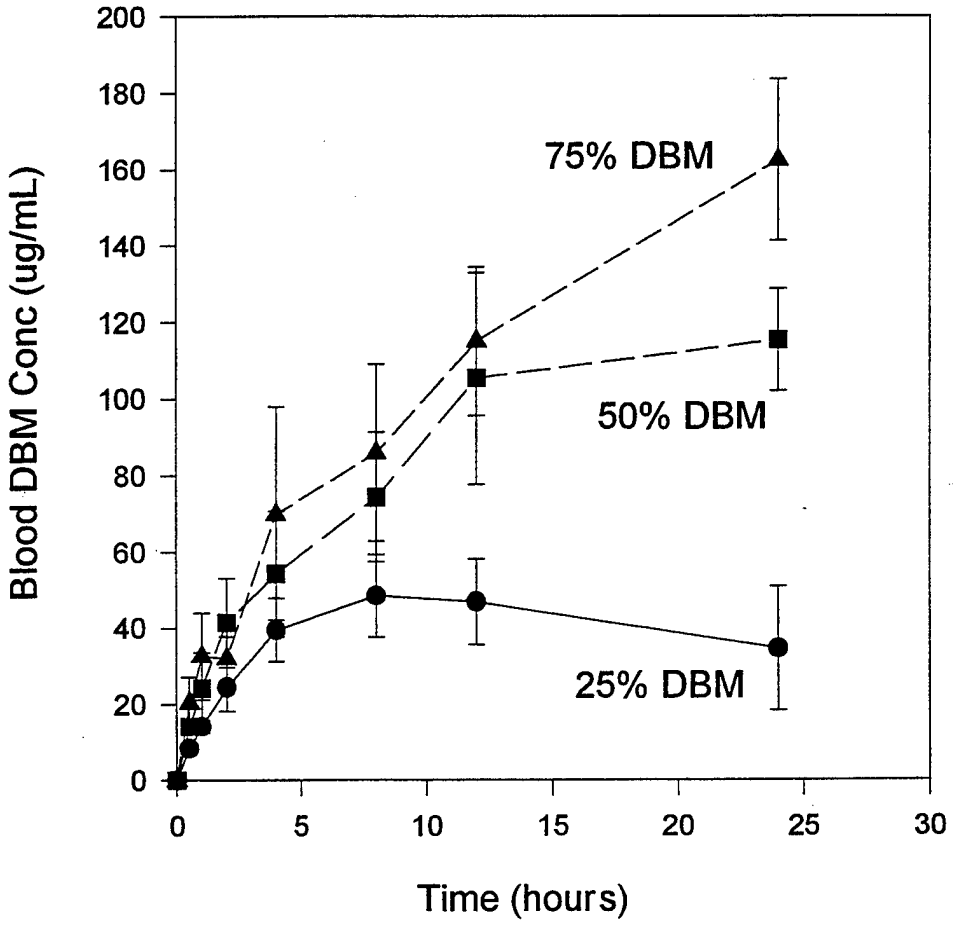

Figure 17. Dibromomethane (DBM) Concentrations in Blood Following Dermal Doses of DBM in Mineral Oil. Blood concentrations are given as the mean with error bars representing the standard deviation. Each point on the graph represents blood samples taken from 5-10 animals. Dibromomethane concentrations in mineral oil were 619.5 mg/mL, 1239.0 mg/mL and 1858.5 mg/mL for the 25%, 50% and 75% solutions, respectively.

OPTIMIZATION OF Kp FOR *IN VIVO* EXPOSURES

Computer simulations of dibromomethane and bromochloromethane blood levels following 24 hour dermal exposures to DBM or BCM in various vehicles were prepared using the physiologically based pharmacokinetic model presented earlier. The simulations were compared to experimentally derived DBM and BCM blood levels. While permeability coefficient values were adjusted in the model until an optimum fit to the experimental data was achieved, the metabolic constants, permeability coefficients, and all physiological parameter values that were measured or substantiated in independent published work were not altered as part of the optimization process. In all cases, the heteroscedasticity parameter was set to treat the error as relative to the mean.

The optimized permeability coefficient, Kp, was determined for each of the chemical/vehicle combinations. The visual or computer optimized permeability coefficient that best described the data near the steady-state level was selected as the best fit. In cases where blood levels dropped off after reaching their maximum value, the visual best fit and the computer best fit differed. In cases where chemical concentrations in blood remained relatively constant following attainment of a maximum value, the visual best fit and the computer statistical best fit were in

agreement. The agreement between the visual best fit and the computer best fit was good in the bromochloromethane in corn oil exposures as is evidence by the similarity between the resulting Log Likelihood Function values. The Log Likelihood Function with the largest value represents the parameter selection producing the best statistical fit within the error and distribution assumptions made in the computer optimization routine. A summary of the optimization values for bromochloromethane in corn oil is shown in Table 5.

The Kp selected for the 25% bromochloromethane in corn oil was 0.0040 cm/hr. This was a result of the visually optimized fit rather than the statistically optimized fit of Kp=0.0035 cm/hr. As was shown in Figures 13 and 18, there was a slight drop off in bromochloromethane concentrations in blood at the 12 and 24 hour time periods.

Table 5. Kp Optimization for BCM in Corn Oil**

Bromochloromethane in Corn Oil			
	25% BCM	50% BCM	75% BCM
Vehicle:air PC	367.85	378.26	389.28
Kp Visual	0.0040	0.0032	0.0030
Kp Computer	0.0035	0.0031	0.0030
LLF Visual	-23.87	-16.21	-23.84
LLF Computer	-22.58	-15.26	-23.83
Selected Kp	0.0040	0.0031	0.0030

*** Where vehicle is the composite of the bromochloromethane and the corn oil Kp is the permeability coefficient (cm/hour) and LLF is the Log Likelihood Function.*

This was due in part to a slight change in exposure chemical concentration due to absorption and was described by the model. The computer simulation of BCM concentration in blood using the optimized Kp value plotted against the experimentally generated data is shown in Figure 18.

The Kp values selected for the 50% and 75% bromochloromethane in corn oil exposures were 0.0031 and 0.0030 cm/hr, respectively. In both the 50% and 75% bromochloromethane in corn oil exposures, the visually optimized fit and the statistically optimized fit were nearly the same as shown in Table 5.

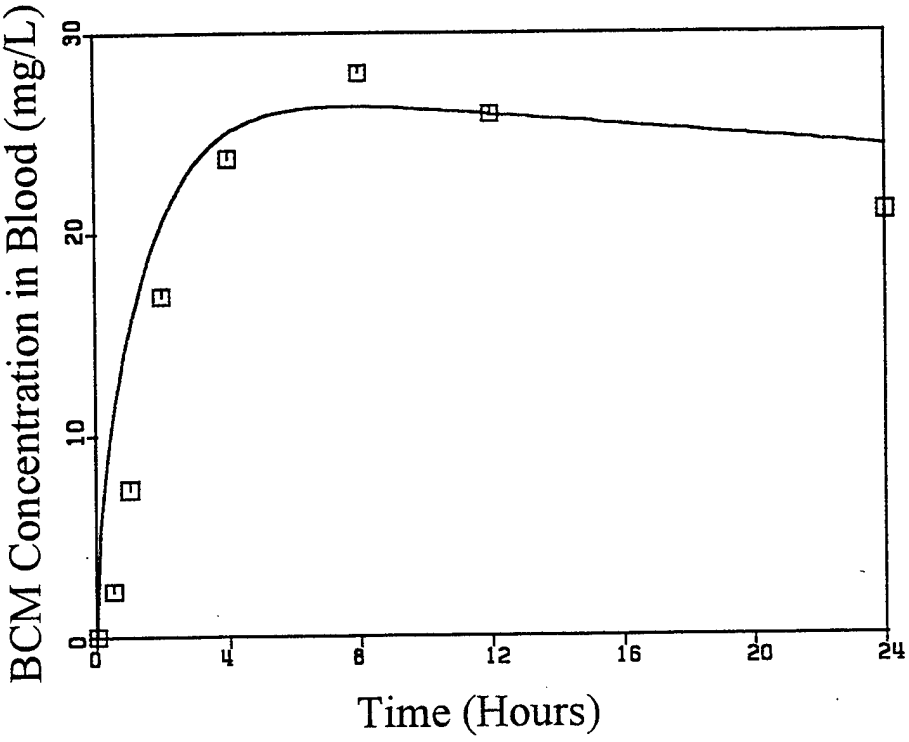

Figure 18. Simulation vs. Measured Blood Concentrations of Bromochloromethane (BCM) Following a Dermal Dose of 25% BCM in Corn Oil. Mean blood concentrations are shown as squares with the simulation shown as a line. The bromochloromethane concentration in corn oil was 497.7 mg/mL (25% solution).

The computer simulation of BCM concentration in blood using the optimized Kp value plotted against the experimentally generated data is shown in Figure 19 for the 50% BCM solution and in Figure 20 for the 75% BCM solution.

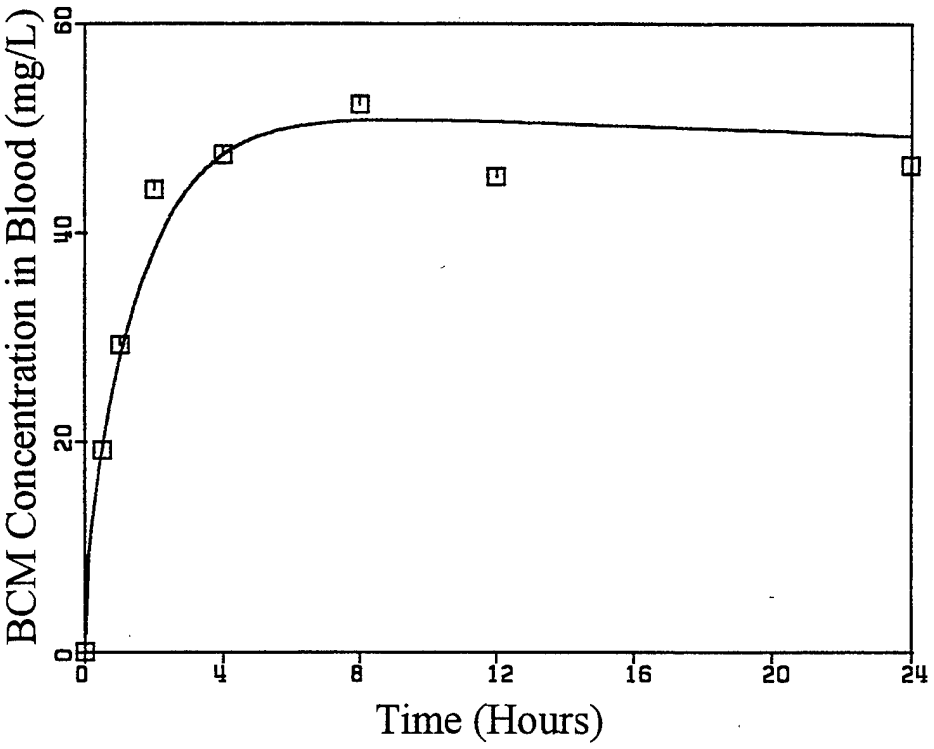

Figure 19. Simulation vs. Measured Blood Concentrations of Bromochloromethane (BCM) Following a Dermal Dose of 50% BCM in Corn Oil. Mean blood concentrations are shown as squares with the simulation shown as a line. The bromochloromethane concentration in corn oil was 995.3 mg/mL (50% solution).

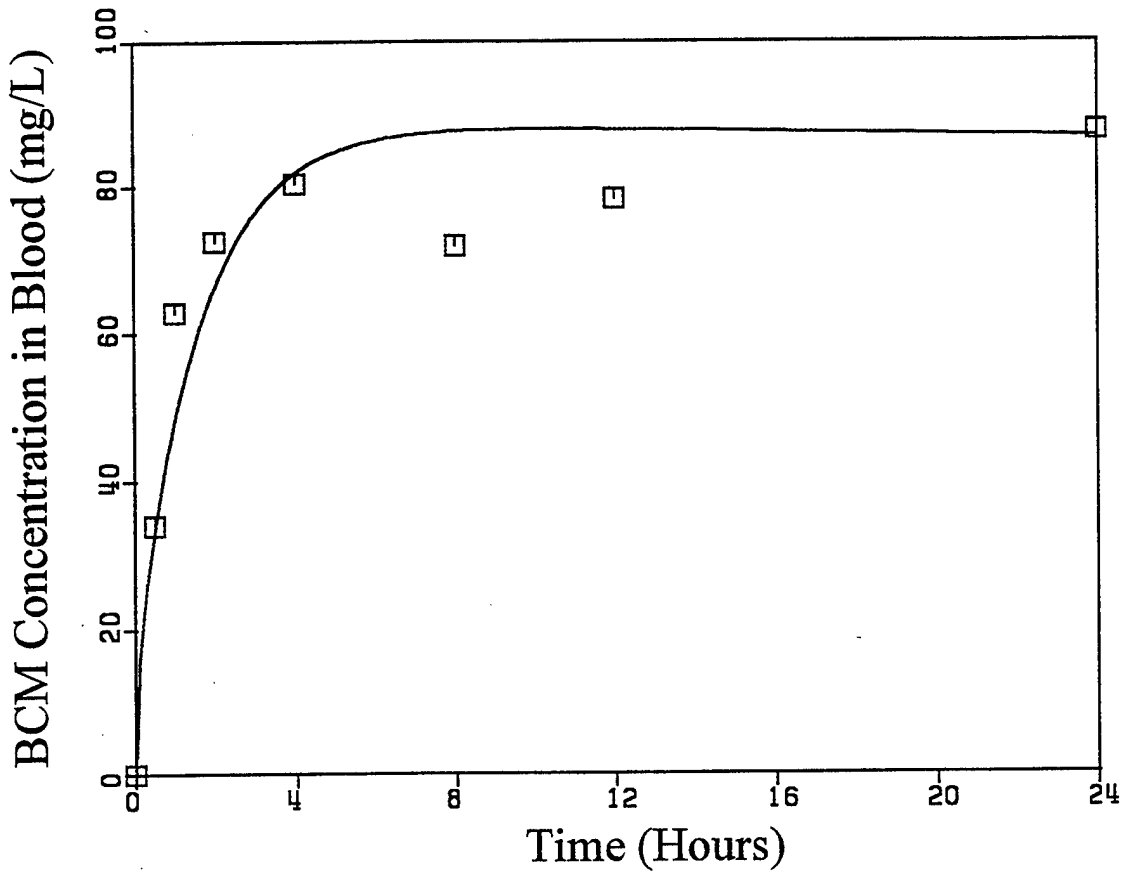

Figure 20. Simulation vs. Measured Blood Concentrations of Bromochloromethane (BCM) Following a Dermal Dose of 75% BCM in Corn Oil. Mean blood concentrations are shown as squares with the simulation shown as a line. The bromochloromethane concentration in corn oil was 1493 mg/mL (75% solution).

A summary of the optimization values for bromochloromethane in mineral oil is shown in Table 6. There was poor agreement between the visual and statistical optimizations as the statistical optimizations produced values that underestimated the steady-state blood levels of BCM.

*Table 6. Kp Optimization for BCM in Mineral Oil***

Bromochloromethane in Mineral Oil			
	25% BCM	50% BCM	75% BCM
Vehicle:air PC	167.18	207.46	273.30
Kp Visual	0.0052	0.0050	0.0038
Kp Computer	0.0044	0.0046	0.0035
LLF Visual	-25.35	-25.53	-28.13
LLF Computer	-23.71	-24.04	-25.00
Selected Kp	0.0052	0.0050	0.0038

*** Where vehicle partition coefficient is the composite of the bromochloromethane and the mineral oil Kp is the permeability coefficient (cm/hour) and LLF is the Log Likelihood Function.*

The Kp selected for the 25% bromochloromethane in mineral oil exposure was the visually optimized value of 0.0052 cm/hr. This contrasted with the statistically optimized value of 0.0044 cm/hr. As shown previously in Figure 14, the bromochloromethane blood levels declined dramatically after reaching a maximum value. This decline accounts for the difference between the visual and computer best fit estimates of Kp. The computer simulation of BCM concentration in blood using the optimized Kp against the experimentally generated data is shown in Figure 21.

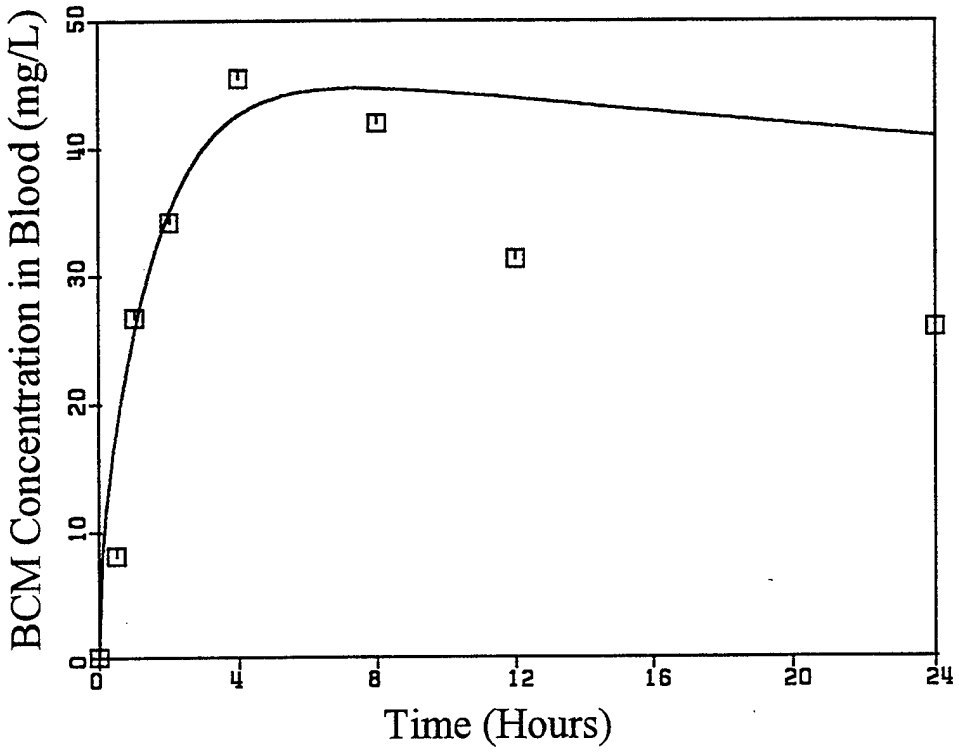

Figure 21. Simulation vs. Measured Blood Concentrations of Bromochloromethane (BCM) Following a Dermal Dose of 25% BCM in Mineral Oil. **Mean blood concentrations are shown as squares with the simulation shown as a line. The bromochloromethane concentration in mineral oil was 497.7 mg/mL (25% solution).**

The Kp selected for the 50% bromochloromethane in mineral oil exposure was the visually optimized value of 0.0050 cm/hr. The reason for the difference between the visual and computer (statistical) best fit is the decline in bromochloromethane concentration in blood observed in the 25% bromochloromethane exposure. The statistically optimized value was 0.0046 cm/hr. The computer simulation of BCM concentration in blood using the optimized value

plotted against the experimentally generated data is shown in Figure 22.

The Kp selected for the 75% bromochloromethane in mineral oil exposure was the visually optimized value of 0.0038 cm/hr. The statistically optimized value was 0.0035 cm/hr. The computer simulation of bromochloromethane concentration in blood using the optimized Kp value plotted against the experimentally generated data is shown in Figure 23.

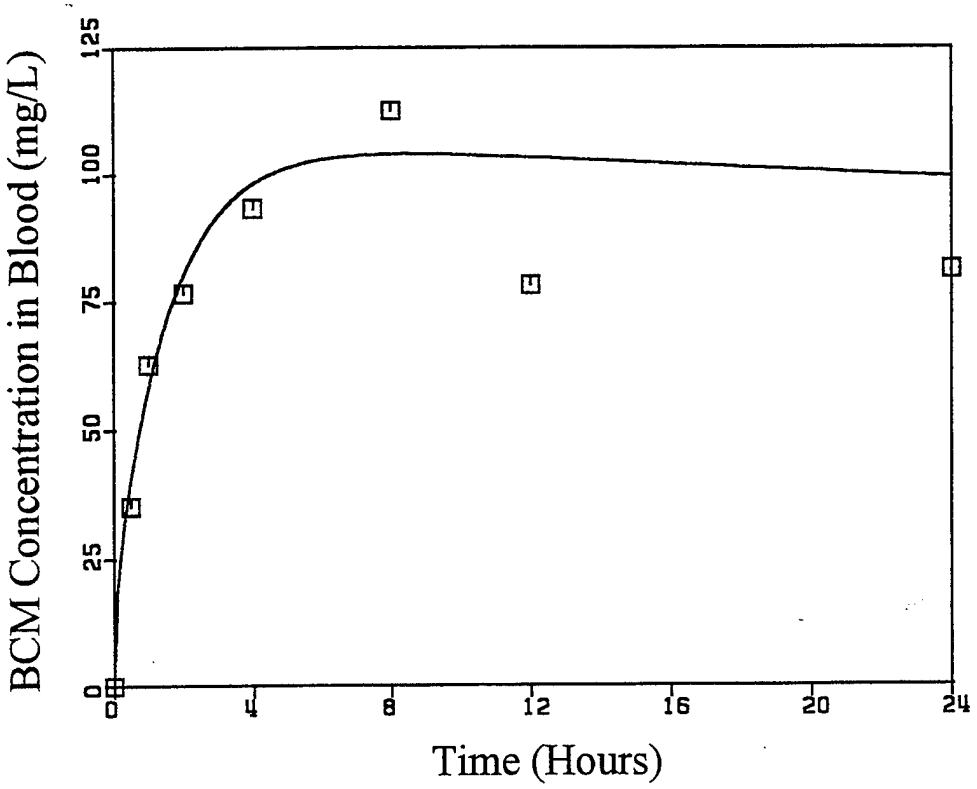

Figure 22. Simulation vs. Measured Blood Concentration of Bromochloromethane (BCM) Following a Dermal Dose of 50% BCM in Mineral Oil. Mean blood concentrations are shown as squares with the simulation shown as a line. The bromochloromethane concentration in mineral oil was 995.3 mg/mL (50% solution).

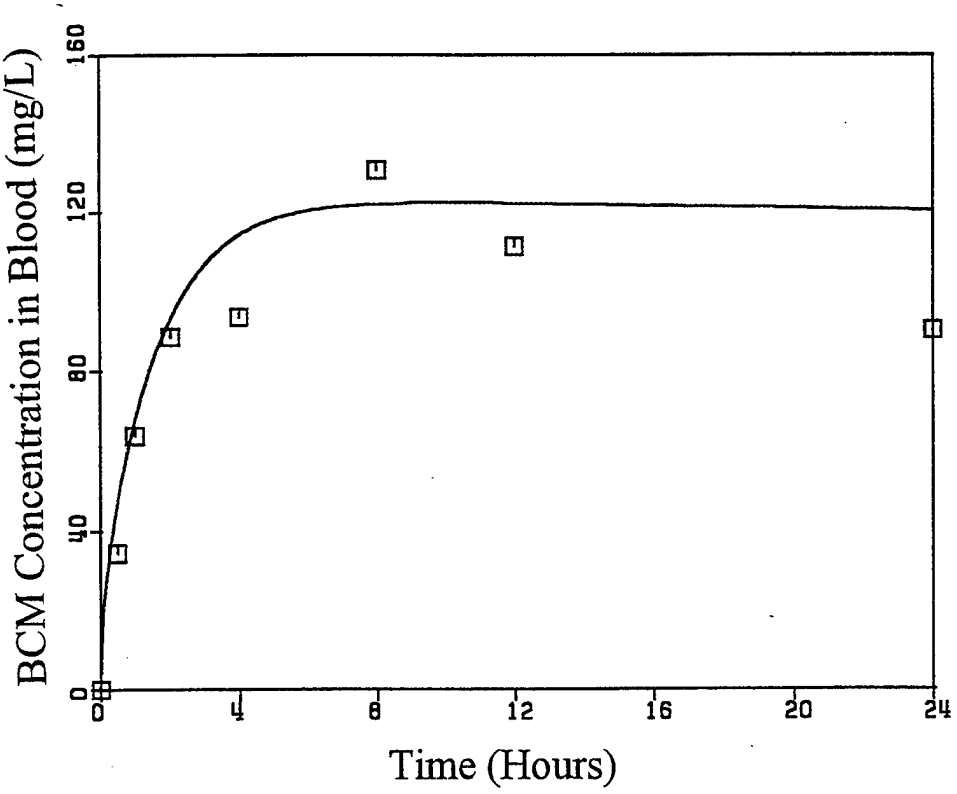

Figure 23. Simulation vs. Measured Blood Concentration of Bromochloromethane (BCM) Following a Dermal Dose of 75% BCM in Mineral Oil. **Mean blood concentrations are shown as squares with the simulation shown as a line. The bromochloromethane concentration in mineral oil was 1493 mg/mL (75% solution).**

The Kp selected for the bromochloromethane in water exposures was the visually optimized value of 0.1200 cm/hr. The bromochloromethane composed only a small fraction (0.006) of the total volume of bromochloromethane/water solution and therefore did not cause a partition coefficient change that required separate treatment as in the cases of the oil vehicles. The computer simulation of the BCM

concentration using the optimized Kp value plotted against the experimentally generated data is shown in Figure 24.

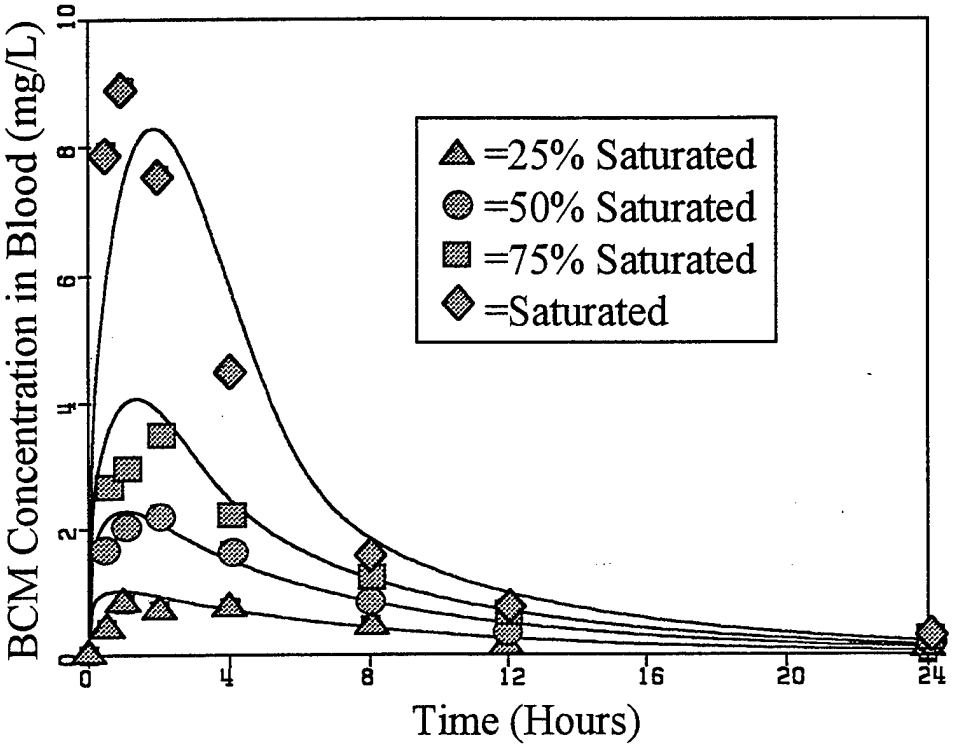

Figure 24. Simulation vs. Measured Bromochloromethane (BCM) Concentrations in Blood Following Dermal Doses of BCM in Water. Mean blood concentrations are shown as squares with the simulation shown as a line. The bromochloromethane concentration in water was 3.6 mg/mL, 6.6 mg/mL, 9.3 mg/mL and 12.8 mg/mL for the 25% saturated, 50% saturated, 75% saturated and saturated solutions, respectively.

A summary of the optimization values for dibromomethane in corn oil is shown in Table 7. There was good agreement

between the visually optimized Kp values and those produced by the statistical (computer) optimization.

*Table 7. Kp Optimization for DBM in Corn Oil***

Dibromomethane in Corn Oil			
	25% DBM	50% DBM	75% DBM
Vehicle:air PC	1110.31	1215.14	1340.32
Kp Visual	0.0037	0.0033	0.0030
Kp Computer	0.0034	0.0033	0.0030
LLF Visual	-20.03	-17.91	-22.13
LLF Computer	-19.38	-17.90	-22.12
Selected Kp	0.0037	0.0033	0.0030

***** Where vehicle partition coefficient (PC) is the composite of the dibromomethane and the corn oil Kp is the permeability coefficient (cm/hour) and LLF is the Log Likelihood Function.***

The Kp selected for the 25% dibromomethane in corn oil exposure was the visually optimized value of 0.0037 cm/hr. The statistically optimized Kp value was 0.0034 cm/hr. The DBM concentration in blood using the optimized Kp value plotted against the experimentally generated data is shown in Figure 25.

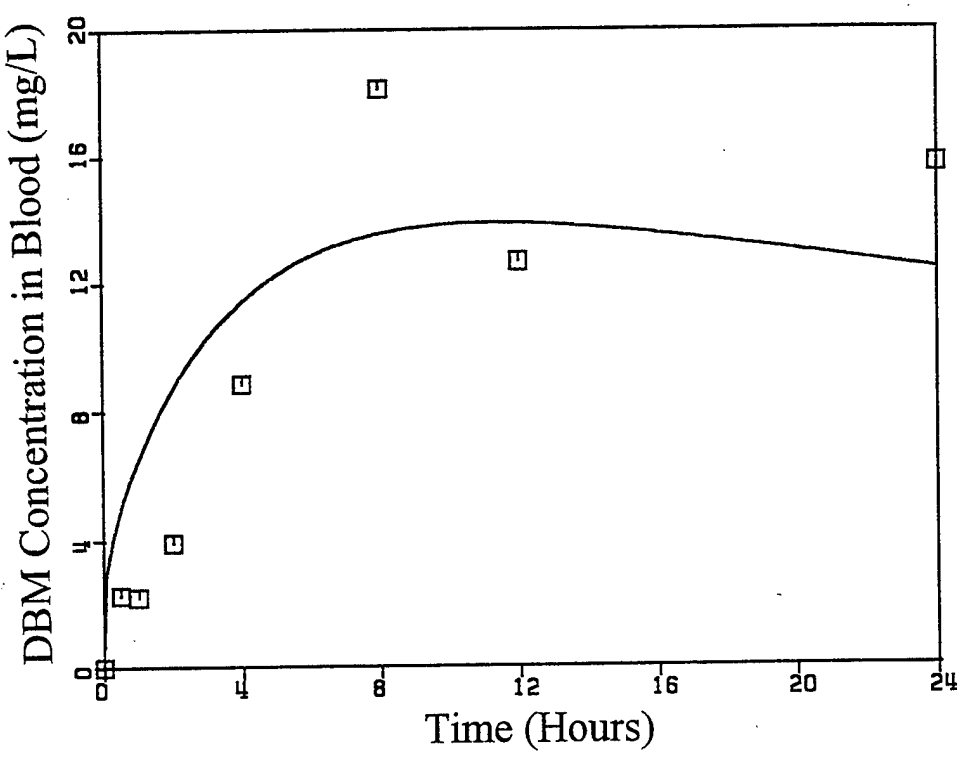

Figure 25. Simulation vs. Measured Blood Concentration of Dibromomethane (DBM) Following a Dermal Dose of 25% DBM in Corn Oil. Mean blood concentrations are shown as squares with the simulation shown as a line. The dibromomethane concentration in corn oil was 619.5 mg/mL (25% solution).

The selected Kp value for the 50% dibromomethane in corn oil exposure was 0.0033 and was the same for both visually and statistically optimized systems. The computer simulation of the DBM concentration in blood using the optimized Kp value against experimentally generated data is shown in Figure 26.

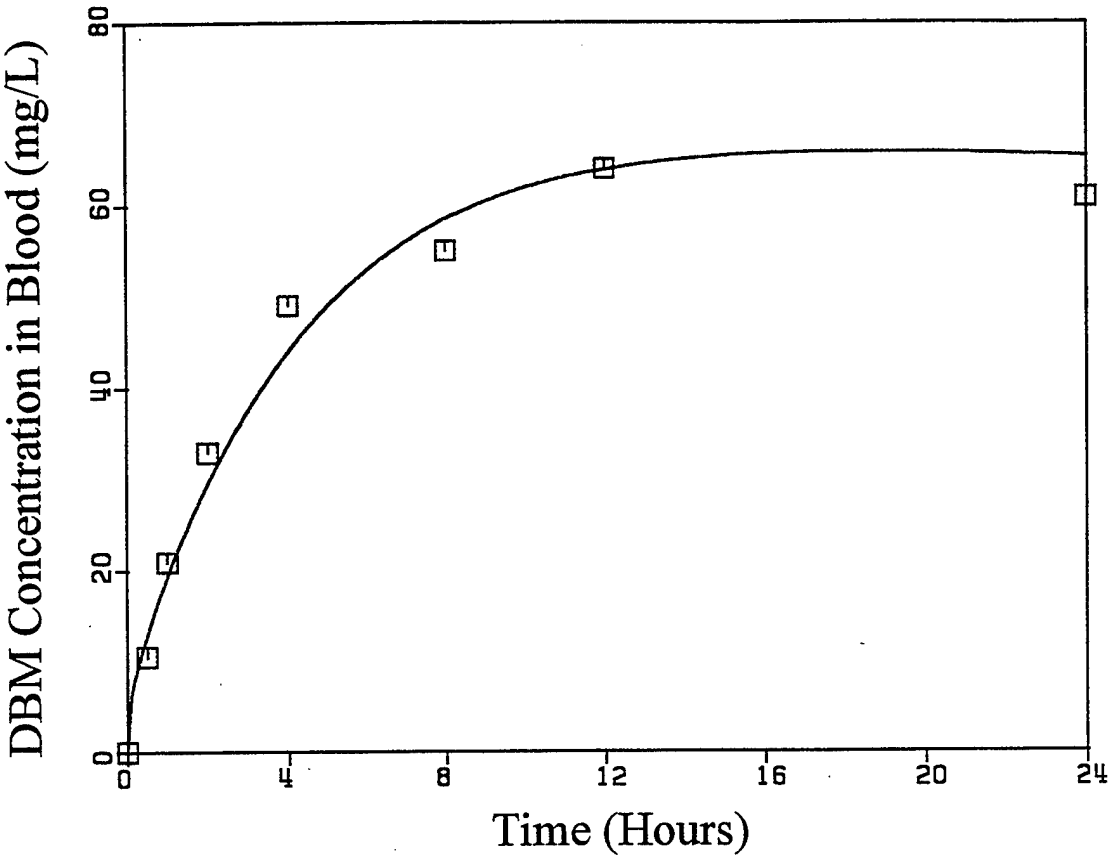

Figure 26. Simulation vs. Measured Blood Concentration of Dibromomethane (DBM) Following a Dermal Dose of 50% DBM in Corn Oil. Mean blood concentrations are shown as squares with the simulation shown as a line. The dibromomethane concentration in corn oil was 1239.0 mg/mL (50% solution).

The selected Kp value for the 75% dibromomethane in corn oil exposures was 0.0030 cm/hr and was also the same for both visually and statistically optimized systems. The computer simulation of the DBM concentration in blood using the optimized Kp value against experimentally generated data is shown in Figure 27.

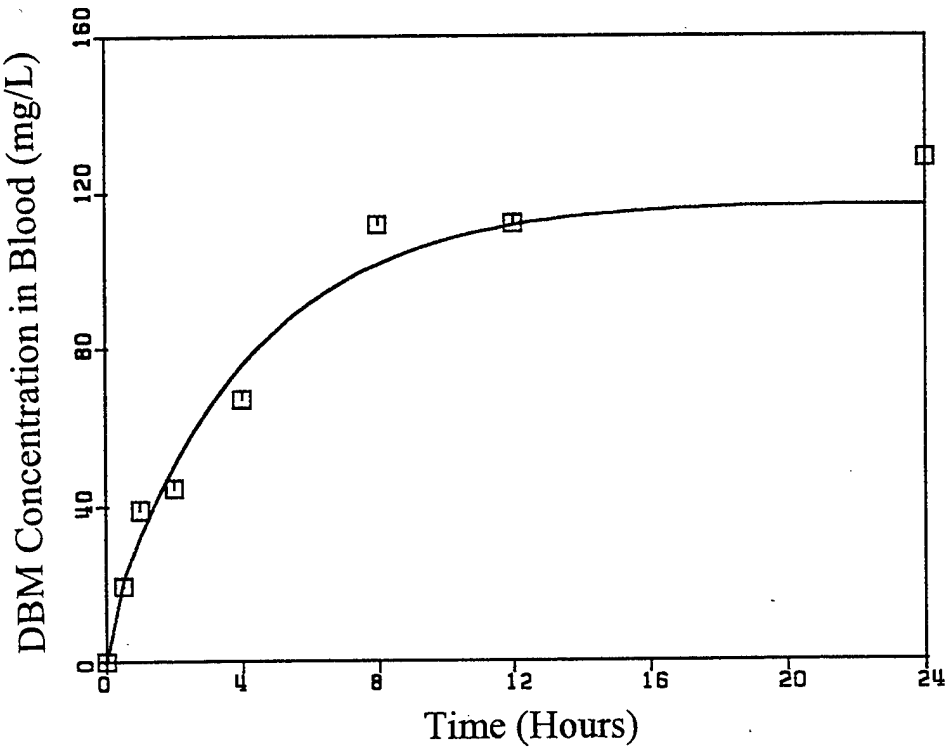

Figure 27. Simulation vs. Measured Blood Concentrations of Dibromomethane (DBM) Following a Dermal Dose of 75% DBM in Corn Oil. Mean blood concentrations are shown as squares with the simulation shown as a line. The dibromomethane concentration in corn oil was 1858.5 mg/mL (75% solution).

A summary of the optimization values for the dibromomethane in mineral oil exposures is shown in Table 8. There was fairly good agreement between the visually and statistically optimized Kp values. However, as illustrated earlier, the statistically optimized values tended to underestimate the experimentally generated data where chemical concentrations in blood declined after reaching a maximum value.

*Table 8. Kp Optimization for DBM in Mineral Oil***

Dibromomethane in Mineral Oil			
	25% DBM	50% DBM	75% DBM
Vehicle:air PC	485.19	626.57	883.56
Kp Visual	0.0049	0.0036	0.0028
Kp Computer	0.0049	0.0033	0.0025
LLF Visual	-17.74	-25.26	-28.62
LLF Computer	-17.74	-22.92	-26.35
Selected Kp	0.0049	0.0036	0.0025

** *Where vehicle partition coefficient (PC) is the composite of the dibromomethane and the mineral oil Kp is the permeability coefficient (cm/hour) and LLF is the Log Likelihood Function.*

The selected Kp value for the 25% dibromomethane in mineral oil was 0.0049 cm/hr and was the result of both visual and statistical (computer) optimizations. The computer simulation of DBM concentration in blood using the optimized Kp against experimentally generated data is shown in Figure 28.

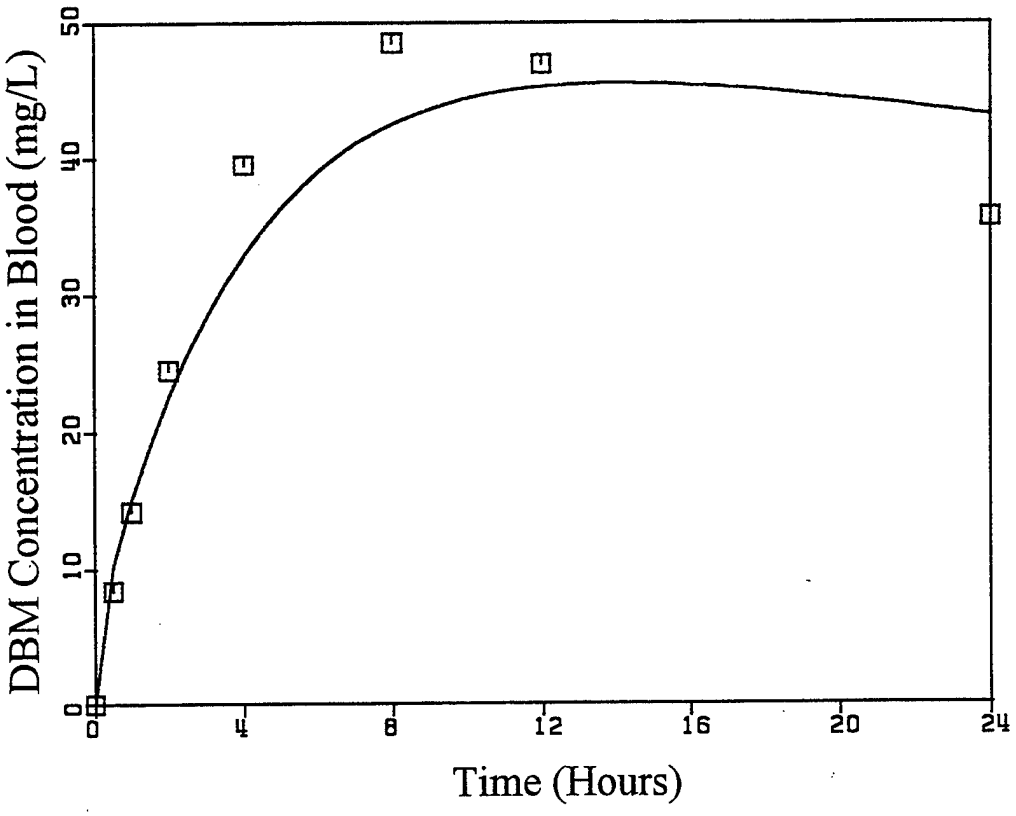

Figure 28. Simulation vs. Measured Blood Concentration of Dibromomethane (DBM) Following a Dermal Dose of 25% DBM in Mineral Oil. Mean blood concentrations are shown as squares with the simulation shown as a line. The dibromomethane concentration in mineral oil was 619.5 mg/mL (25% solution).

The selected Kp value for the 50% dibromomethane in mineral oil exposure was the visually optimized value of 0.0036 cm/hr which contrasted slightly (< 10% difference) with the statistically optimized value of 0.0033 cm/hr. The computer simulation of the DBM concentration in blood using the optimized Kp plotted against the experimentally generated data is shown in Figure 29.

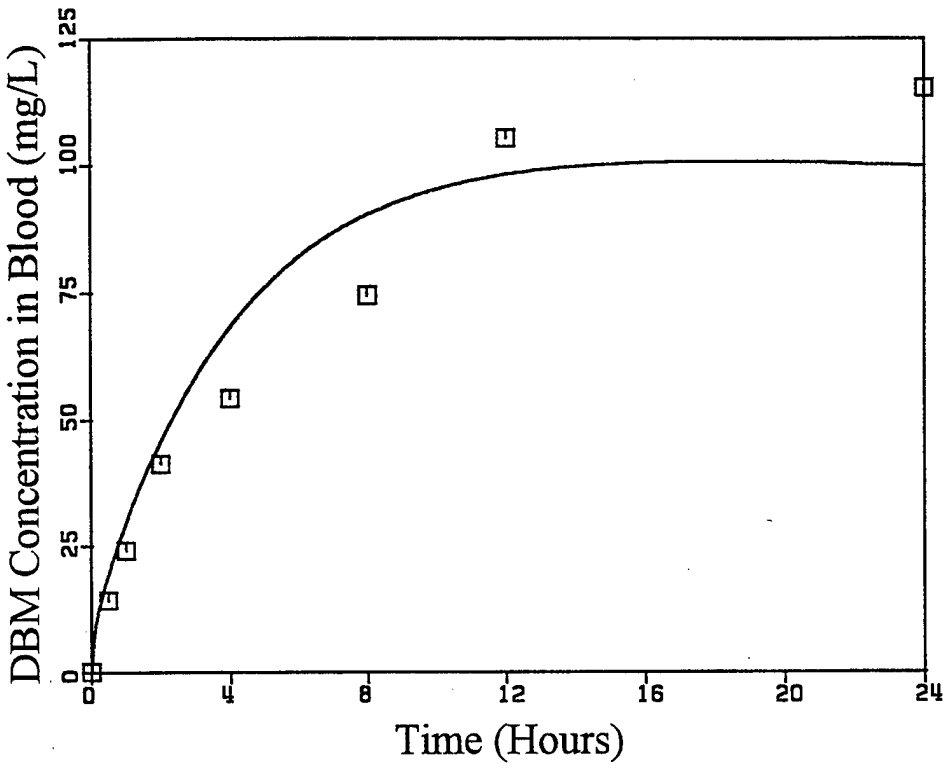

Figure 29. Simulation vs. Measured Blood Concentration of Dibromomethane (DBM) Following a Dermal Dose of 50% DBM in Mineral Oil. Mean blood concentrations are shown as squares with the simulation shown as a line. The dibromomethane concentration in mineral oil was 1239.0 mg/mL (50% solution).

The selected Kp value for the 75% dibromomethane in mineral oil exposure was statistically optimized value of 0.0025 cm/hr. The visually optimized Kp value was 0.0028 cm/hr. The computer simulation of DBM concentration in blood using the optimized Kp value is shown in Figure 30.

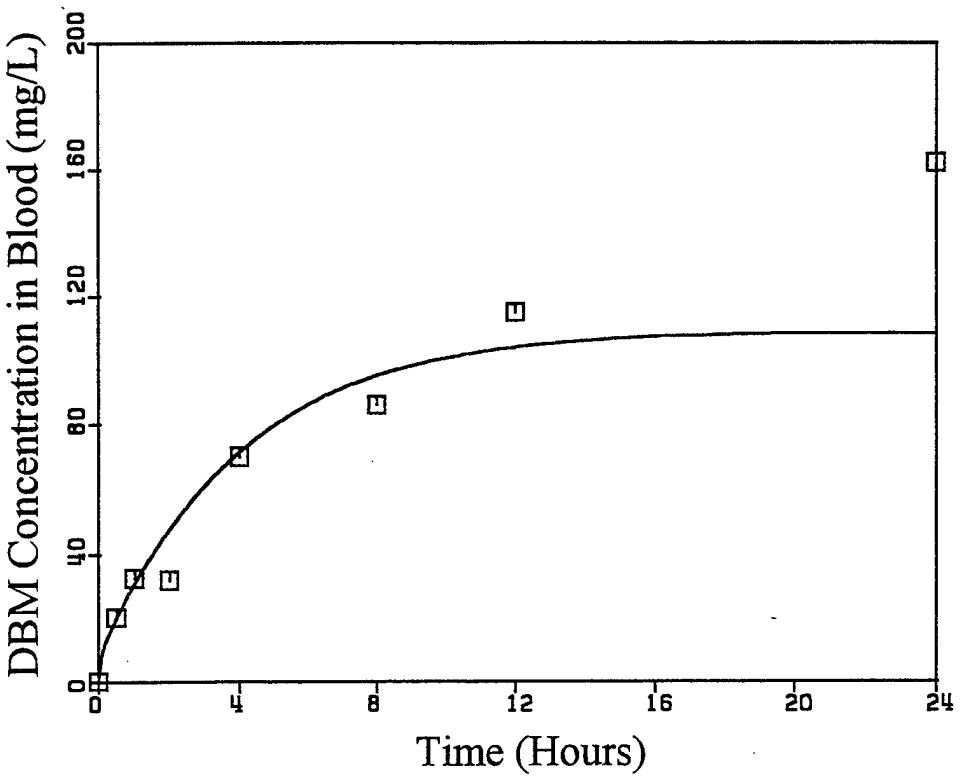

Figure 30. Simulation vs. Measured Blood Concentration of Dibromomethane (DBM) Following a Dermal Dose of 75% DBM in Mineral Oil. Mean blood concentrations are shown as squares with the simulation shown as a line. The dibromomethane concentration in mineral oil was 1858.5 mg/mL (75% solution).

The selected Kp value for the dibromomethane in water exposures was 0.2200 cm/hr. As with the bromochloromethane in water exposures, the amount of DBM dissolved in the water did not significantly affect the partition coefficient for the chemical/vehicle solution. Also as with the BCM in water exposures, the series of DBM concentrations in water were fit as a group since partition coefficient changes did not necessitate separate treatment. The computer simulation

of DBM concentration in blood using the optimized Kp value against experimentally generated data is shown in Figure 31.

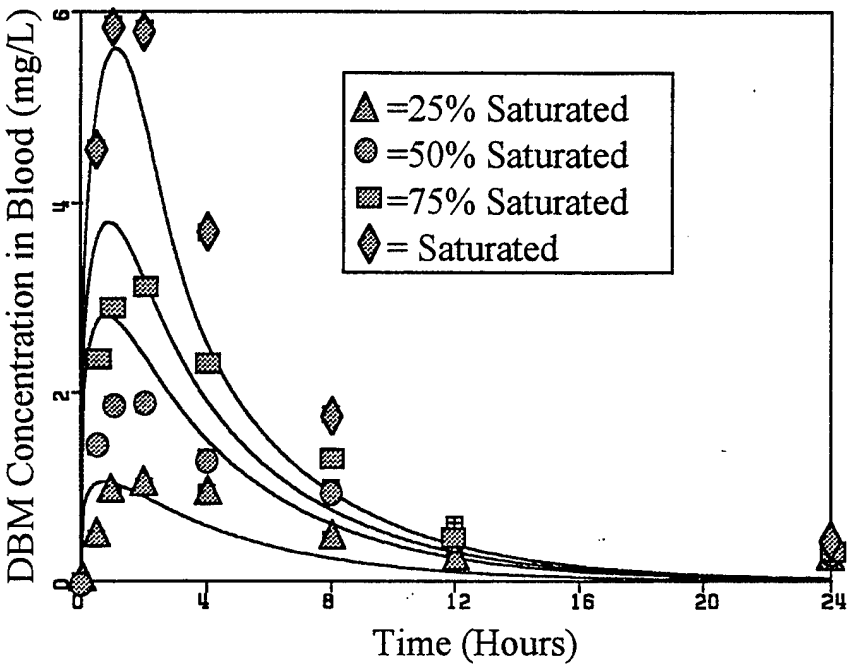

Figure 31. Simulation vs. Measured Blood Concentrations of Dibromomethane (DBM) Following Dermal Doses of DBM in Water. Mean blood concentrations are shown as squares with the simulation shown as a line. The dibromomethane concentration in water was 2.4 mg/mL, 6.1 mg/mL, 7.6 mg/mL and 9.4 mg/mL for the 25% saturated, 50% saturated, 75% saturated and saturated solutions, respectively.

PREDICTION OF Kp USING NORMALIZED PERMEABILITY

The mean normalized permeability coefficient, Kp, based on the data in Table 9, was 0.0277 with a standard deviation of 0.0062 and a coefficient of variation of 0.22.

*Table 9. Normalized Permeability Coefficients***

Chemical/Vehicle	Kp (cm/hr)	PSKV	Kp,n
DBM/Water	0.2200	8.3333	0.0264
25%DBM/75% Min Oil	0.0049	0.2473	0.0198
50%DBM/50% Min Oil	0.0036	0.1915	0.0188
75%DBM/25% Min Oil	0.0025	0.1358	0.0184
25%DBM/75% Corn Oil	0.0037	0.1078	0.0343
50%DBM/50% Corn Oil	0.0033	0.0985	0.0335
75%DBM/25% Corn Oil	0.0030	0.0893	0.0336
BCM/Water	0.1200	4.6240	0.0260
25%BCM/75% Min Oil	0.0052	0.2395	0.0217
50%BCM/50% Min Oil	0.0050	0.1930	0.0259
75%BCM/25% Min Oil	0.0038	0.1465	0.0259
25%BCM/75% Corn Oil	0.0037	0.1090	0.0340
50%BCM/50% Corn Oil	0.0033	0.1060	0.0311
75%BCM/25% Corn Oil	0.0030	0.1030	0.0291

*** Where Kp is the optimized permeability coefficient, PSKV is the skin to vehicle partition coefficient and Kp,n is the normalized permeability coefficient (Kp/PSKV).*

Using the normalized permeability coefficient and the skin to vehicle partition coefficient, permeability coefficients were estimated and used to predict the blood levels of DBM that would result from dermal exposures to 25%, 50% and 75% DBM in peanut oil. The Estimated Kp values are shown in Table 10.

Table 10. Estimated Kp Values for DBM in Peanut Oil**

Chemical/Vehicle	PSKV	Estimated Kp (Mean ± sd)
25% DBM/75% Peanut Oil	0.123	0.0034 ± 0.0008
50% DBM/50% Peanut Oil	0.109	0.0030 ± 0.0007
75% DBM/25% Peanut Oil	0.094	0.0026 ± 0.0006

***** Where PSKV is the skin to vehicle partition coefficient and Kp is the permeability coefficient (cm/hr).***

With estimated permeability coefficient values in hand, the dermal exposures using dibromomethane in peanut oil were conducted to generate DBM blood concentration data. The dibromomethane blood levels resulting from the dermal exposures are shown in Figure 32. Using the estimated Kp values, simulations of dibromomethane concentrations in blood levels were compared to laboratory generated data. Permeability coefficient values were optimized for the laboratory data and the final optimized value was compared with the predicted value. The 25% dibromomethane in peanut oil laboratory generated data and computer simulation are shown in Figure 33.

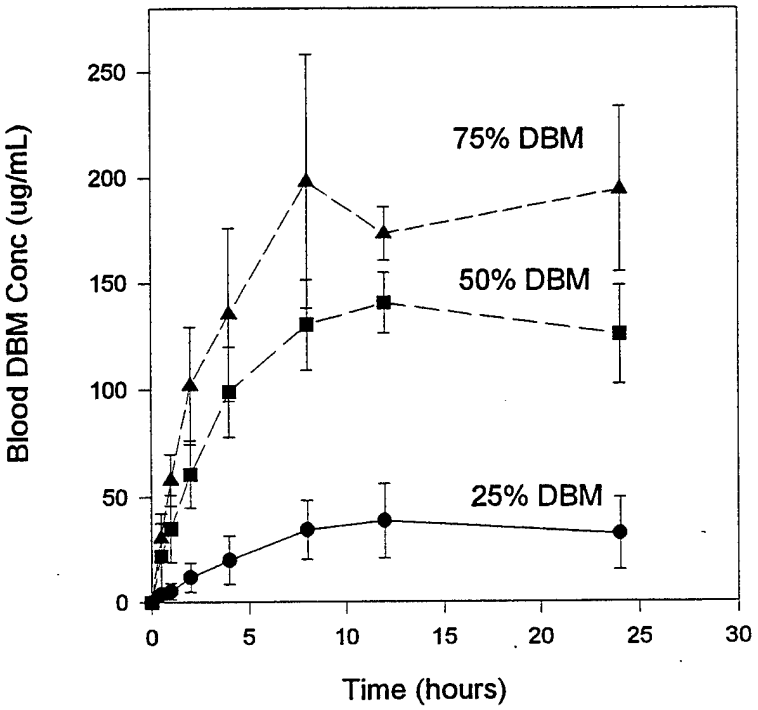

Figure 32. Dibromomethane (DBM) Concentrations in Blood Following Dermal Doses of DBM in Peanut Oil. Blood concentrations are given as the mean with error bars representing the standard deviation. Each point on the graph represents blood samples taken from 5-10 animals. Dibromomethane concentrations in peanut oil were 619.5 mg/mL, 1239.0 mg/mL and 1858.5 mg/mL for the 25%, 50% and 75% solutions, respectively.

The optimized Kp value for the 25% DBM solution was 0.0036 cm/hr which was well within the predicted Kp value of 0.0034 ± 0.0008 cm/hr.

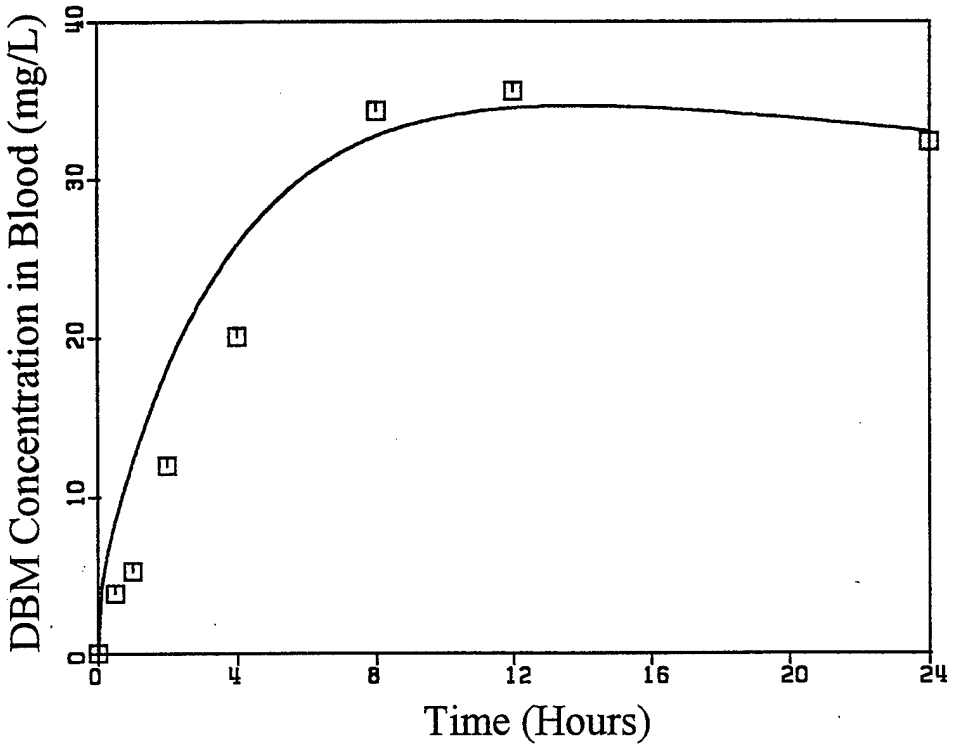

Figure 33. Simulation vs. Measured Blood Concentration of Dibromomethane (DBM) Following a Dermal Dose of 25% DBM in Peanut Oil. **Mean blood concentrations are shown as squares with the simulation shown as a line. The dibromomethane concentration in mineral oil was 619.5 mg/mL (25% solution).**

The 50% dibromomethane in peanut oil laboratory generated data and computer simulation is shown in Figure 34. The optimized Kp value for the 50% DBM solution of 0.0038 cm/hr was slightly higher (2.6%) than the 0.0037 cm/hr value representing the mean value of 0.0030 cm/hr plus the standard deviation of 0.0007 cm/hr.

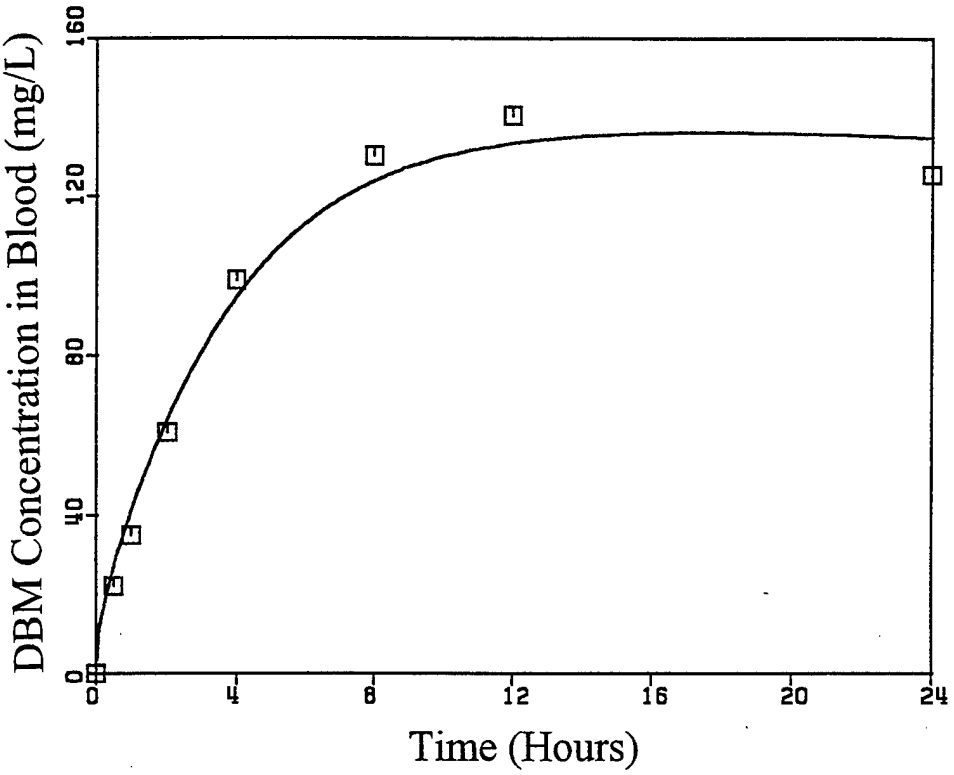

Figure 34. Simulation vs. Measured Blood Concentration of Dibromomethane (DBM) Following a Dermal Dose of 50% DBM in Peanut Oil. **Mean blood concentrations are shown as squares with the simulation shown as a line. The dibromomethane concentration in mineral oil was 1239.0 mg/mL (50% solution).**

The 75% dibromomethane in peanut oil laboratory generated data and computer simulation is shown in Figure 35. The optimized Kp value for the 75% DBM solution of 0.0032 cm/hr was within the predicted Kp value of 0.0026 ± 0.0006 cm/hr

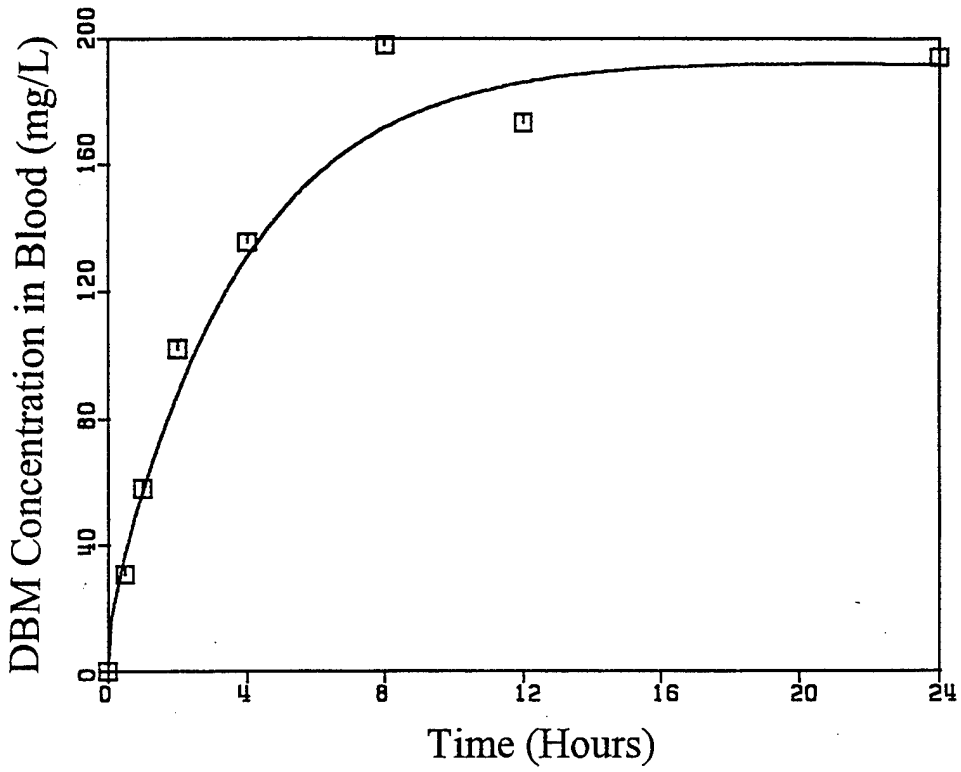

Figure 35. Simulation vs. Measured Blood Concentration of Dibromomethane (DBM) Following a Dermal Dose of 75% DBM in Peanut Oil. Mean blood concentrations are shown as squares with the simulation shown as a line. The dibromomethane concentration in mineral oil was 1858.5 mg/mL (75% solution).

A summary of the comparison between predicted (estimated as shown in Table 10) and observed permeability coefficients for DBM in peanut oil vehicle is shown in Table 11.

Table 11. Predicted versus Observed Kp Values for DBM in Peanut Oil Vehicle. **

Chemical/vehicle	Predicted Kp(cm/hr) (mean ± sd)	Observed Kp(cm/hr) Optimized
25%DBM/75% Vehicle	0.0034 ± 0.0008	0.0036
50%DBM/50% Vehicle	0.0030 ± 0.0007	0.0038
75%DBM/25% Vehicle	0.0026 ± 0.0006	0.0032

** *Where DBM is dibromomethane, Kp is the permeability coefficient and the vehicle is peanut oil.*

FINITE DOSE EXPOSURES

The description of the finite dose exposures required consideration of evaporation and changing surface area throughout the exposure. The evaporation rates determined as described in the materials and method section were 663 ± 63 mg/hr/cm^2 and 237 ± 16 mg/hr/cm^2 (mean ± sd) for bromochloromethane and dibromomethane, respectively. The time to dryness varied between the static determinations and *in vivo* exposures. In the case of the dibromomethane, the time to dryness ratio for the static versus. *in vivo* was 0.33 and for bromochloromethane the ratio was 0.55. The unpredictable movement of the animals and hair growth in the *in vivo* exposures made the static evaporation determinations gross estimates, at best. The small amount of hair on the skin increased the evaporation rate 1.43 times for dibromomethane and 1.45 times for bromochloromethane over

the rate observed when the chemicals were placed on a glass slide. Evaporation data are shown in Figure 36.

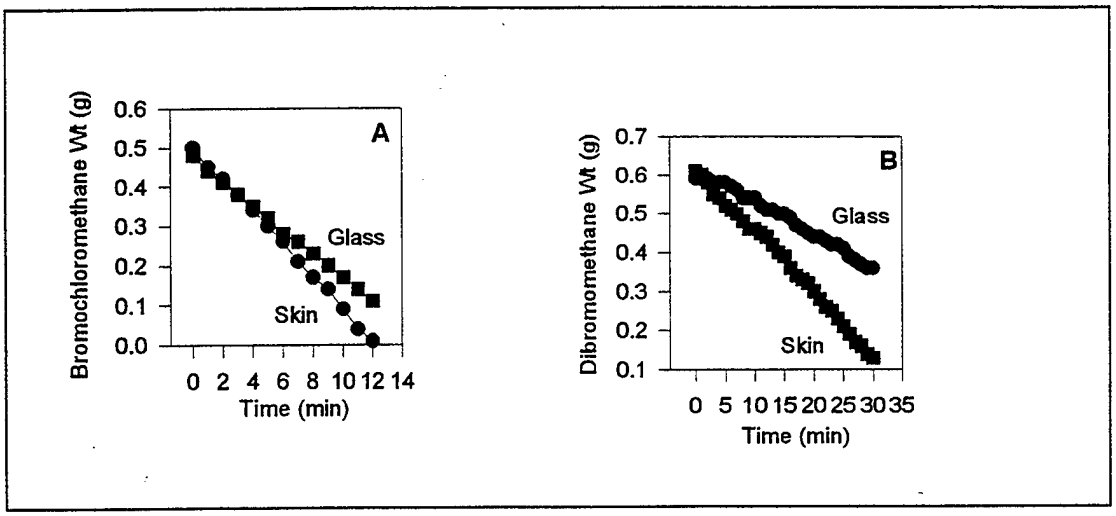

Figure 36. Evaporation Rates of Bromochloromethane (A) and Dibromomethane (B) from Glass and Skin at 32 °C. **Starting volumes were 250 µL and surface area was 3.8 cm^2.**

In order to evaluate the predictive power of the physiologically based pharmacokinetic model to estimate the blood levels resulting from a finite dose (250 µL) exposure in living, unanesthestized animals, finite dose dermal exposures were conducted. The bromochloromethane blood level resulting from finite dose dermal exposures to bromochloromethane reached a maximum of 13.67 ± 5.29 mg/L (mean ± sd) at approximately 16 minutes into the exposure. The bromochloromethane concentration in blood data is shown in Figure 37.

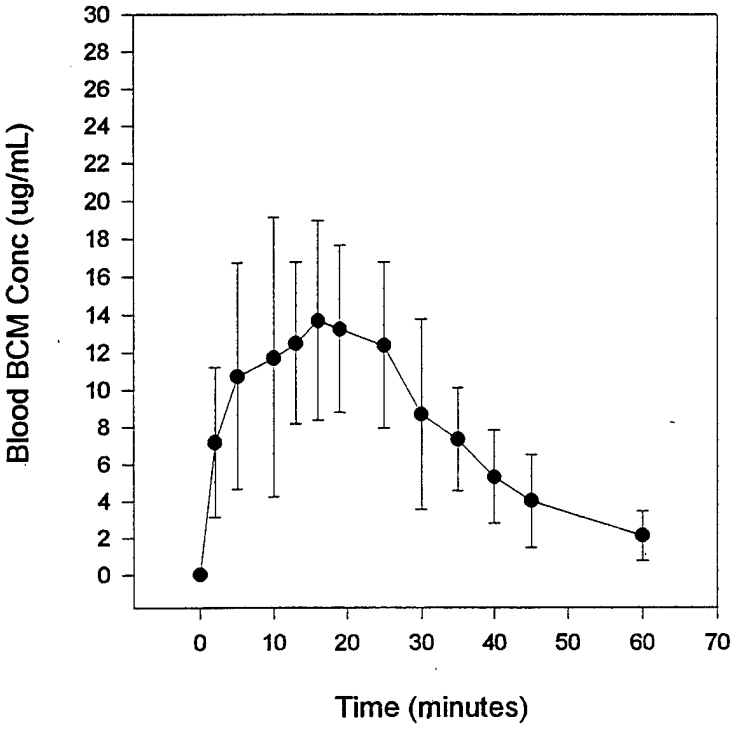

Figure 37. Bromochloromethane (BCM) Concentration in Blood Following a Finite Dermal Dose of BCM (250 µL). **Each point on the graph represents blood samples taken from 10 animals. Blood concentrations are given as the mean with error bars representing the standard deviation.**

The dibromomethane concentration in blood resulting from finite dose exposures to dibromomethane reached a maximum of 28.40 ± 5.25 mg/L (mean ± sd) at approximately 10 minutes into the exposure. The DBM concentration in blood data is shown in Figure 38.

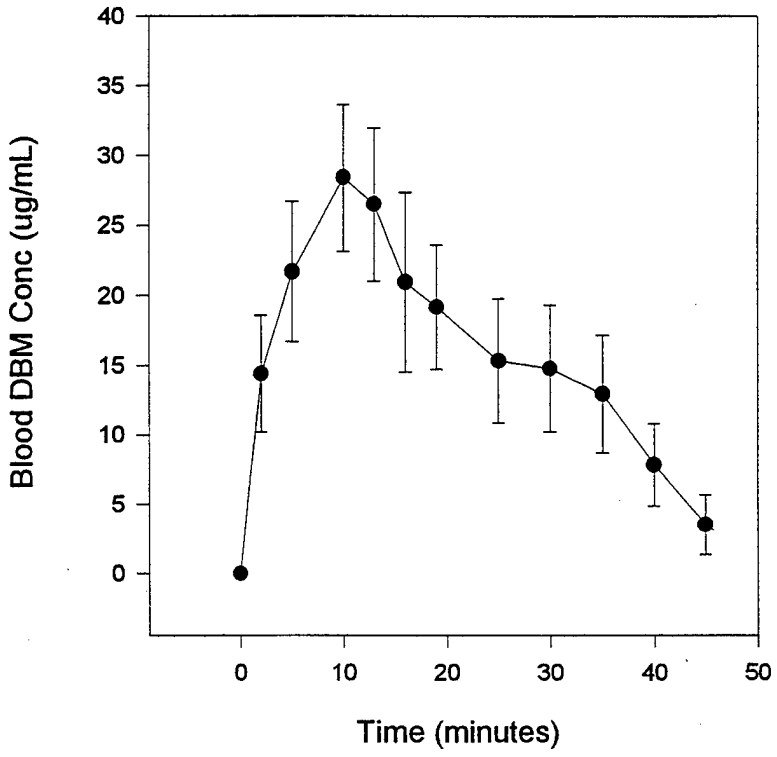

Figure 38. Dibromomethane (DBM) Concentration in Blood Following a Finite Dermal Dose of DBM (250 μL). **Each point on the graph represents blood samples taken from 10 animals. Blood concentrations are given as the mean with error bars representing the standard deviation.**

Simulation of the bromochloromethane concentration in blood following the finite dose exposure was compared to experimentally generated data. The comparison is shown in Figure 39. The simulation closely matched the experimental data through the peak concentration of 13.67 mg/L which occurred at approximately 16 minutes. The simulation

underestimated BCM blood concentration from the 25 to 60 minute time points. When the computer code was modified (Appendix A) from the constant exposure area description to reflect a loss of exposure surface area as the chemical evaporated and Kp was set to 0.002 (as compared to 0.003) cm/hr, the model simulation more closely approximated the observed chemical blood levels (Figure 40).

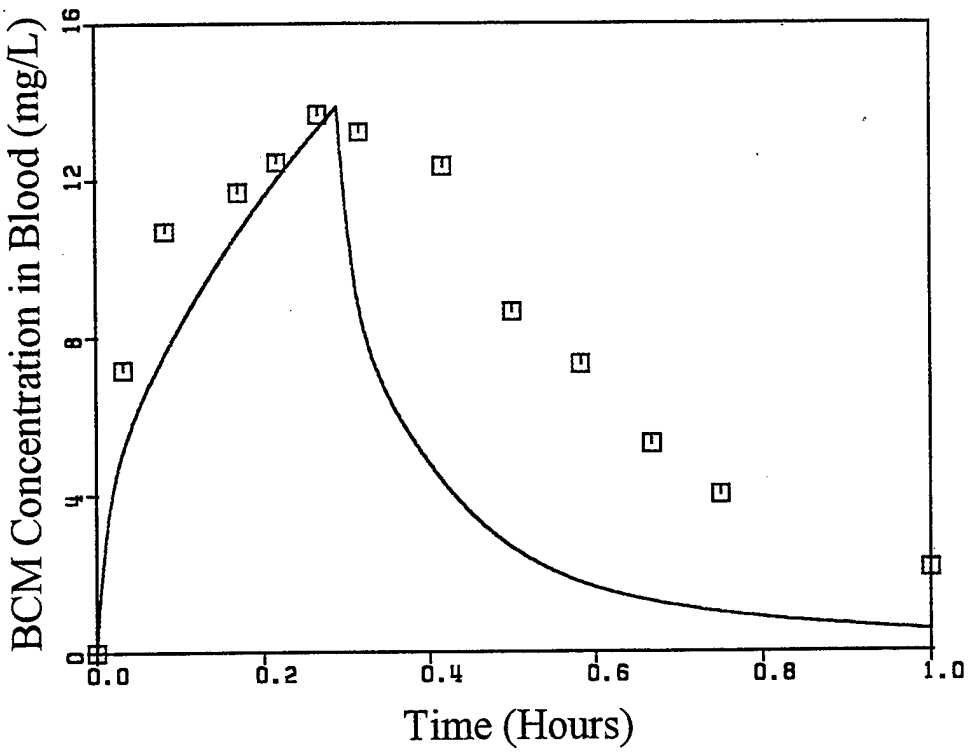

Figure 39. Simulation vs. Measured Blood Concentration of Bromochloromethane (BCM) Following a Finite Dermal Dose (250 μL) of BCM. Blood data (squares) are compared to model simulation (line) of bromochloromethane blood levels.

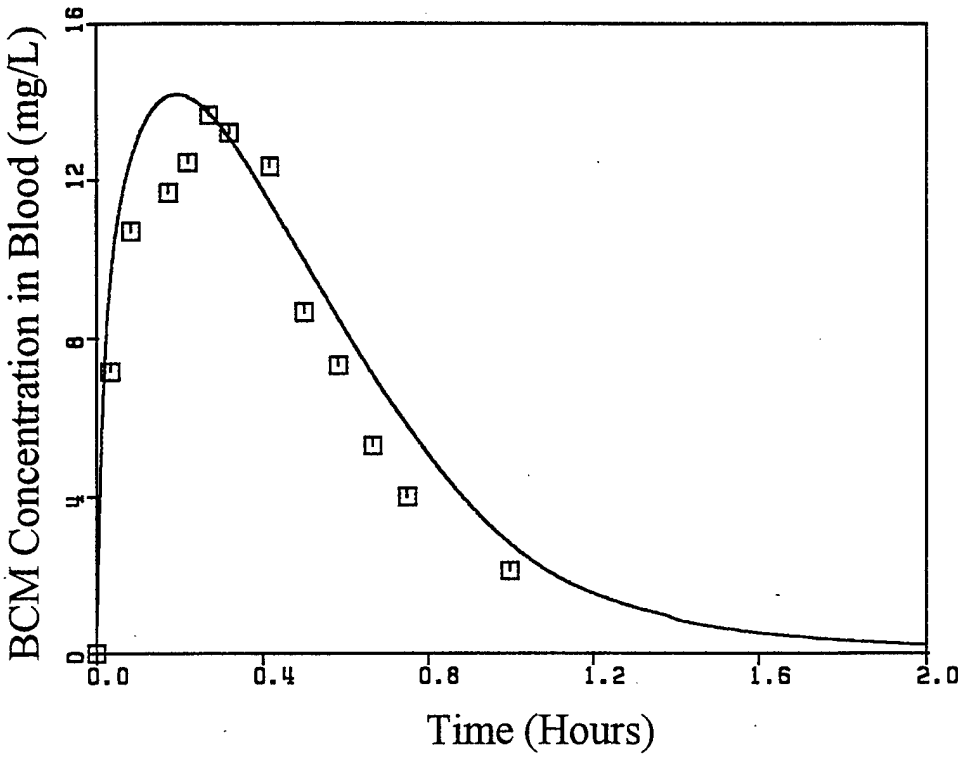

Figure 40. Dynamic Surface Area Simulation vs. Measured Blood Concentration of Bromochloromethane (BCM) Following a Finite Dermal Dose (250 µL) of BCM. **Blood data (squares) are compared to modified model simulation (line) of bromochloromethane blood levels.**

Simulation of the dibromomethane concentration in blood following a finite dose exposure was compared to experimentally generated data and is shown in Figure 41. The simulation and blood data tracked closely through the 10 minute time point. The simulation slightly over predicted the peak blood concentration and slightly under predicted the DBM blood levels from 19 to 45 minutes into the exposure. As with the bromochloromethane finite dose

simulation, the computer code was modified (Appendix A) from the constant exposure area description to reflect a loss of exposure surface area as the chemical evaporated and Kp was set to 0.004 (as compared to 0.003) cm/hr. The model simulation resulting from the modified code is shown in Figure 42.

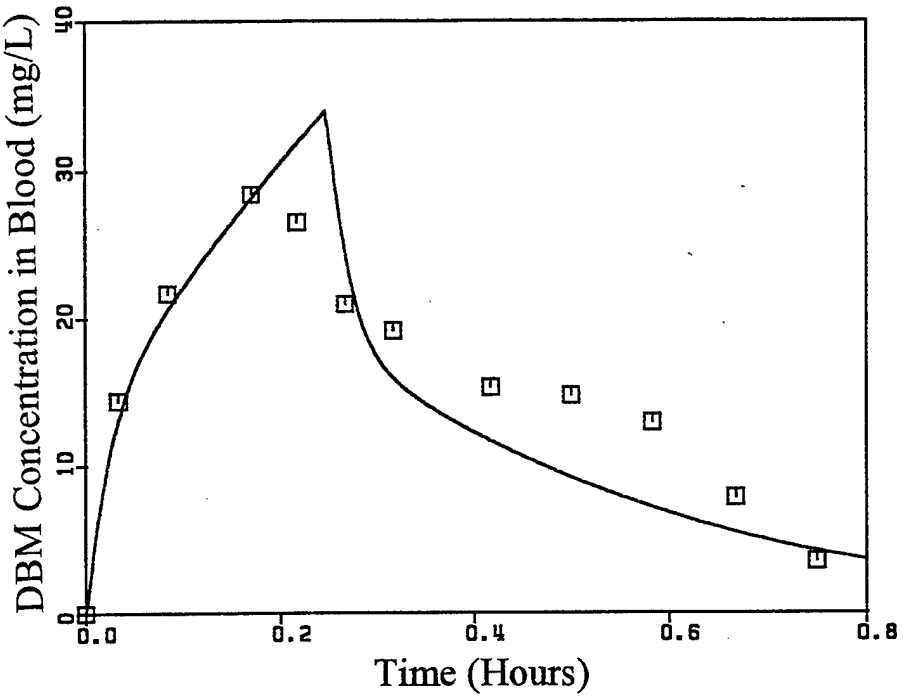

Figure 41. Simulation vs. Measured Blood Concentration of Dibromomethane (DBM) Following a Finite Dermal Dose (250 µL) of DBM. Blood data (squares) are compared to model simulation (line) of dibromomethane blood levels.

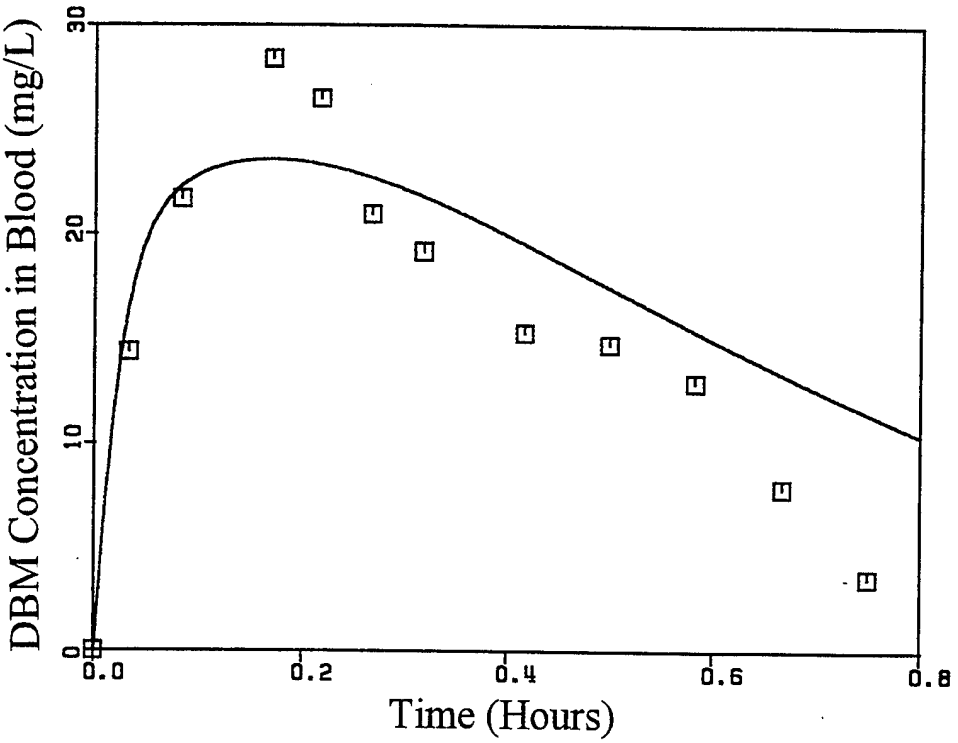

Figure 42. Dynamic Surface Area Simulation vs. Measured Blood Concentration of Dibromomethane (DBM) Following a Finite Dermal Dose (250 µL) of DBM. Blood data (squares) are compared to modified model simulation (line) of bromochloromethane blood levels.

IN VITRO ESTIMATION OF PERMEABILITY COEFFICIENTS

The diffusion coefficient of dibromomethane in dry stratum corneum as determined using thermal gravimetric analysis was $1.95 \times 10^{-9} \pm 2.12 \times 10^{-10}$ cm^2/sec (mean ± sd). The diffusion coefficient resulted from optimization of the mathematical description (Appendix C) of diffusion as

compared to experimental data and is shown in Figure 43 for dibromomethane and Figure 44 for bromochloromethane.

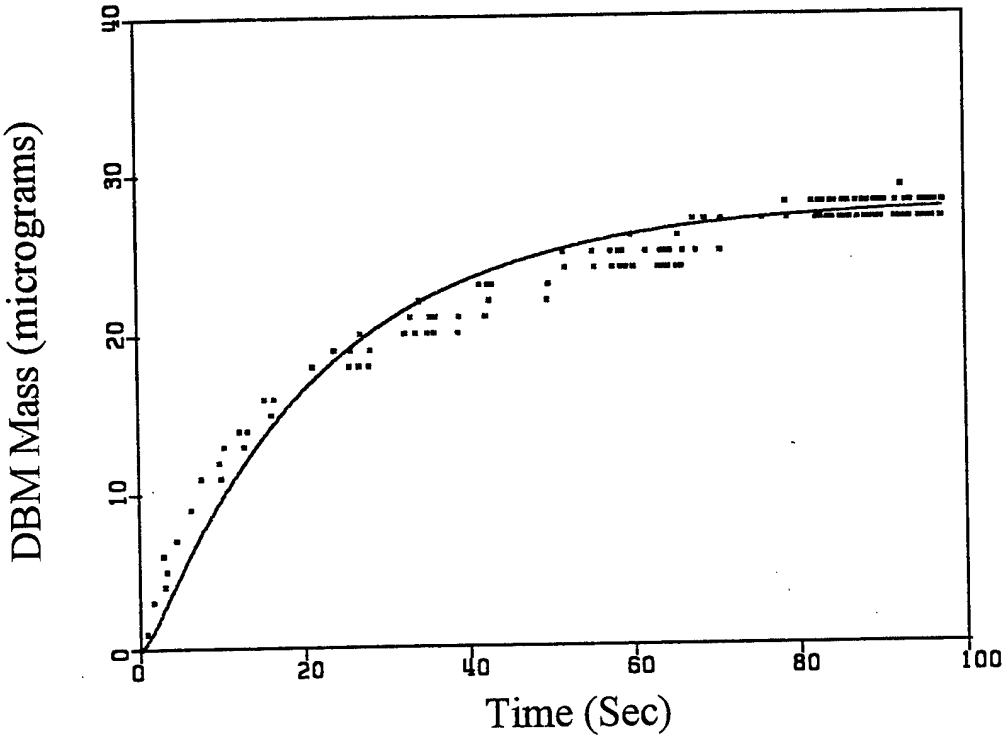

Figure 43. Dibromomethane Diffusion in Stratum Corneum. Estimation of the diffusion coefficient (cm^2/sec) by fitting the experimental mass vs. time data with a non-steady state diffusion equation. The computer generated fit to the data is shown as the line and the data is shown as small squares.

Using the diffusion coefficient, a permeability coefficient was calculated. The resulting permeability coefficient was 2.48 cm/hr compared to the reported literature value of 1.32 cm/hr for *in vivo* dermal absorption of DBM vapor in rats (McDougal, et al., 1986). The observed permeability coefficient was used to calculate a normalized

permeability coefficient for dibromomethane vapor for comparison with normalized permeability coefficients in other vehicles. The resulting value was 0.0207 cm/hr which compared favorably with the mean normalized permeability coefficient of 0.0277 for the water and oil vehicle systems.

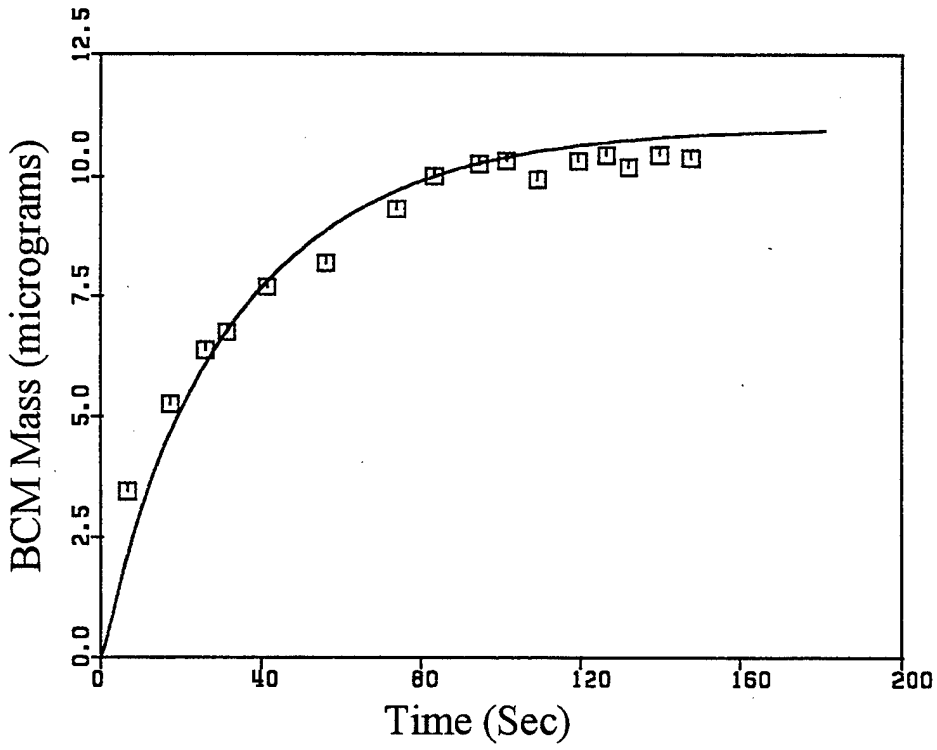

Figure 44. Bromochloromethane Diffusion in Stratum Corneum. **Estimation of the diffusion coefficient (cm^2/sec) by fitting the experimental mass vs. time data with a non-steady state diffusion equation. The computer generated fit to the data is shown as the line and the data is shown as squares.**

The permeability coefficient for bromochloromethane vapor as calculated using the thermal gravimetric analysis data was 0.23 cm/hr. This compared to a literature value of

0.79 cm/hr for bromochloromethane vapor penetration *in vivo*. Using the observed permeability coefficient value to calculate a normalized permeability coefficient the result was 0.0064 cm/hr. This value was considerably lower than the normalized permeability coefficient of 0.0277 cm/hr calculated for the water and oil vehicles.

The ability of the *in vitro* data from the thermal gravimetric analysis to produce information with predictive value for *in vivo* dermal absorption characteristics is illustrated in Table 12.

Table 12. Permeability Coefficients From In Vitro Data

Chemical/Vehicle	Predicted Kp (cm/hr)	Observed Kp
DBM/Water	0.1700	0.2200
25%DBM/75%Corn Oil	0.0022	0.0037
50%DBM/50%Corn Oil	0.0020	0.0035
75%DBM/25%Corn Oil	0.0019	0.0030
25%DBM/75%Mineral Oil	0.0051	0.0049
50%DBM/50%Mineral Oil	0.0040	0.0036
75%DBM/25%Mineral Oil	0.0028	0.0025
BCM/Water	0.0290	0.1200
25%BCM/75%Corn Oil	0.0007	0.0037
50%BCM/50%Corn Oil	0.0007	0.0033
75%BCM/25%Corn Oil	0.0007	0.0030
25%BCM/75%Mineral Oil	0.0015	0.0052
50%BCM/50%Mineral Oil	0.0012	0.0050
75%BCM/25%Mineral Oil	0.0009	0.0030

IV. DISCUSSION

DERMAL ABSORPTION OF CHEMICALS

The skin is a complex organ with a vast array of specialized features that allow the skin to perform its physiological role in mammalian systems. The structure of the skin which has evolved to perform its physiological function as a barrier to water transfer out of the body has made the skin relatively impervious to other substances as well. It is not an absolute barrier to the transfer of either water or organic chemicals across the skin, however, as was shown in this work, it is certainly true that dermal penetration occurs where chemicals with non-polar character are concerned. Such non-polar or lipid soluble chemicals are commonly present in occupational and environmental situations where ample opportunity exists for dermal exposure. In order to determine the impact of exposure to chemicals which can penetrate the skin, a quantitative approach to describe the chemical to skin interaction is useful. A functional understanding of the interaction of environmental and occupational chemicals with skin and subsequent penetration into the systemic circulation is central in meaningful health risk assessment where dermal

exposures are of concern ([a]Mattie, et al., 1994). In order to establish a functional understanding of dermal absorption of organic chemicals, the kinetic importance of the skin components should be evaluated for pertinence, something which has rarely been done. Only those compartments with kinetic uniqueness or target specificity should be explicitly included within the quantitative scheme for chemical distribution and mass balance. It is likely, however, that there will always be room for debate on the proper type and number of compartments that are appropriate for specific chemicals. Indeed, some compartments will surface as important for one chemical but not another.

The simplest possible structure of the skin for quantitative determination of dermal penetration by organic chemicals would be a single skin compartment with one surface facing the chemical source and the other surface contacting the blood. Functionally this approach treats the epidermis as a single layer with the partition coefficient and permeability coefficient assigned for the entire layer. As long as this approach allows satisfying description of available data by the model, additional complexity in the model structure is probably unwarranted. Any increase in skin compartment complexity beyond the single compartment rapidly increases the data requirements for a useful predictive physiologically based pharmacokinetic model.

This additional data requirement burden in itself is not troublesome, but, the practical aspects of acquiring appropriate data from individual epidermal layers is formidable. Additional model complexity without reliable input data moves the model away from the desired physiological description of the kinetic process and into a less desirable curve fitting mode.

The endpoints of interest in this work were the blood levels of bromochloromethane and dibromomethane that resulted upon exposing the skin of rats to these chemicals in various vehicles. While blood levels of chemical are valuable in pharmacokinetic applications, the interactions between the chemical and blood components should be considered if target specific events are of interest (Lam, et al., 1990; Monro, 1990). The chemicals of interest were dihalogenated, relatively non-polar hydrocarbons possessing a fair level of volatility. These characteristics are not uncommon in the realm of occupational chemicals used in industrial applications as well as those identified as environmental contaminants. Since the metabolism of dibromomethane and bromochloromethane have been studied in detail by other investigators, the metabolic schemes and rates are known and quantified. This provided a tremendous advantage in that focus of dermal exposure work could be on

the dermal absorption kinetics themselves and not such peripheral issues.

UTILITY OF PHYSIOLOGICALLY BASED MODELING

A physiologically based modeling approach proved useful for describing the dermal absorption kinetics of the dihalomethanes, dibromomethane and bromochloromethane. The chemical blood levels resulting from dermal exposures to these chemicals in water, corn oil and mineral oil vehicles were described with a single layer skin compartment interfaced with a physiologically based pharmacokinetic model. The physiologically based model was a central component in devising a predictive approach to dermal absorption since the model allowed the estimation of total amount of chemical absorbed during the exposure period. In turn, the total amount absorbed was used in a flux equation (Equation 31) to estimate a permeability coefficient for the chemical exposure.

$$Flux = \frac{amount\ absorbed\ (mg)}{area\ (cm^2) \times time(hours)} \qquad \textbf{Eq 31}$$

With the amount of chemical absorbed known, all of the components required to estimate a permeability coefficient (cm/hr) were available as shown in Equation 32.

$$Permeability\ Coefficient = \frac{Flux}{Chemical\ Concentration(mg/cm^3)} \qquad \textbf{Eq 32}$$

The term chemical concentration in equation 32 is commonly used in descriptions of permeability but, more correctly, it is the chemical driving force (potential) across the dermal barrier which thermodynamically moves the process. These activity adjusting elements are embodied in experimentally determined permeability coefficients. In a given phase these are related through an activity coefficient and where interfaces of two distinct phases are crossed, by partition coefficients. Based on the flux and permeability relationships described above, permeability coefficients were estimated for dibromomethane and bromochloromethane in a variety of solvent systems.

For the dibromomethane and bromochloromethane in water, corn oil and mineral exposures, a concentration series of each chemical in each vehicle was completed before the data was evaluated using the PBPK model. For example, animals were exposed to dibromomethane at concentrations of 25%, 50% and 75% in corn oil and blood concentrations versus time profiles were prepared before the data was used in the model to estimate the permeability coefficient. This process was then conducted for each of the chemical and vehicle combinations of interest.

The bromochloromethane blood levels following exposure to the 50% and 75% bromochloromethane in mineral oil dropped off after eight hours of exposure. Since there was an

inappropriate drop in the driving force, this was probably due to dermal barrier damage resulting from the long bromochloromethane contact with the live skin during the exposure. Indeed, bromochloromethane caused irritation and skin disruption to such an extent that out of concern for the animal subjects, undiluted bromochloromethane exposures were not completed. Skin damage by chemicals applied dermally can alter the behavior of the barrier function of the skin both directly and through effects on mitotic and specialization processes indirectly. Unfortunately, the permeability alterations due to skin irritation as well as the mechanisms of skin damage are complex, and to date, are undefined (Nangia, et al., 1993). However, damage in these studies and barrier alterations pertaining thereto were almost certainly direct because of the relatively short duration of the exposures. No damage or chemical alteration of the kinetic behavior was observed with any of the dibromomethane exposures or with bromochloromethane administered in corn oil.

The physiologically based model was not set up to accommodate dermal damage resulting from a chemical exposure. Given the bromochloromethane experience, a quantitative description of chemically induced dermal barrier damage and its impact on absorption kinetics may be a logical extension of this work. The blood data up to and

including the points where steady-state chemical levels in blood were achieved were used to estimate the permeability coefficient for the chemical/vehicle system. Both bromochloromethane and dibromomethane levels in blood dropped off after reaching a maximum when water was used as a vehicle. Unlike the situation with the bromochloromethane in mineral oil, the turn around resulted from depletion of chemical from the water. The chemical depletion and its influence on chemical concentrations in blood were both predicted by the physiologically based model.

The original expectation was to generate one permeability coefficient for each chemical and vehicle. For example, dibromomethane would have a permeability coefficient for water, another one for corn oil and yet another for mineral oil. Similar expectations were held for the bromochloromethane exposures. Following the original line of thought, the permeability coefficient values would then be normalized for the partition coefficient in the particular vehicle. These in turn would form a foundation for prediction of chemical blood levels following dermal exposure where the chemical was in a different vehicle or medium. The idea of producing one permeability coefficient for each of the chemicals in each of the oil vehicles was abandoned when it became clear that chemical blood levels could not be predicted over the range of chemical

concentrations using a single permeability coefficient. In effect, the addition of relatively large amounts of the dibromomethane or bromochloromethane to the oil vehicles created a chemical/vehicle system with thermodynamic properties that differed from the vehicle itself. Concentrations exceeded those for which the thermodynamic activity and concentration could be related through a common activity coefficient. Consequently and more specifically, addition of the chemicals to the oil vehicles in the high percentage strengths used altered the skin to vehicle partition coefficient for dibromomethane and bromochloromethane. Therefore, each DBM or BCM and oil vehicle combination created, from a kinetic perspective, a separate exposure and each would then require independent evaluation and permeability coefficient estimation using the PBPK model. This did not alter the concept of using normalized permeability to conduct predictive analysis, in fact, it strengthened it. However, it did dramatically increase the number of chemical/vehicle systems that needed to be evaluated and factored into the normalized permeability coefficient equation. The importance of a change in the skin to vehicle partition coefficient can be illustrated by examining its relationship to the permeability coefficient as shown in Equation 33.

$$Permeability\ Coefficient = \frac{Diffusion\ Coefficient\ (cm^2 / hr) \times Skin{:}Vehicle\ Partition\ Coefficient}{Diffusion\ Pathlength\ (cm)}$$

Eq 33

The relationship between the permeability coefficient and the skin to vehicle partition coefficient is one of proportionality. An extension of this observation is that chemical flux across the dermal barrier is a function of thermodynamic activity and prediction of permeability coefficients using concentration without regard for the medium in which the chemical resides could result in serious error. The importance of considering the thermodynamic influence of the vehicle used for chemicals that contact the skin can be readily demonstrated by using the physiologically based computer model and dermal absorption concepts described in this work. For the demonstration, the test chemical will be dibromomethane and two vehicles, one polar and one nonpolar, will be used. A realistic dibromomethane concentration of 9.4 mg of DBM per mL of vehicle can be prepared in each vehicle to yield a total volume of 3.0 mL. At this point both the polar vehicle/DBM matrix and the nonpolar vehicle/DBM matrix would contain the same total volume and same concentration of dibromomethane. If each matrix is then applied (occluded dose where no evaporation of test chemical occurs) to the same surface area (3.1 cm^2) of skin for the same exposure period of time

(24 hours), the influence of the vehicle can be quantified using the physiologically based pharmacokinetic model.

After a 24 hour exposure period the total amount of dibromomethane absorbed would be 27.95 mg from the polar vehicle/DBM matrix compared to 18.64 mg from the nonpolar vehicle/DBM matrix.

In addition to the total amount of chemical absorbed, another potentially important difference between the two exposures is the difference in peak concentration of dibromomethane in blood. In the polar vehicle/DBM matrix the peak concentration of dibromomethane achieved in the blood would be 5.62 mg/L compared to a value of only 0.96 mg/L for the nonpolar vehicle/DBM matrix. Even though the exposures in the demonstration were identical in all aspects except for the vehicle used to dissolve the dibromomethane, the amount of chemical and peak chemical concentrations in blood were vastly different. The effects of the vehicle on achieved chemical concentrations in blood and total amount of chemical absorbed are shown in Figures 45 and 46.

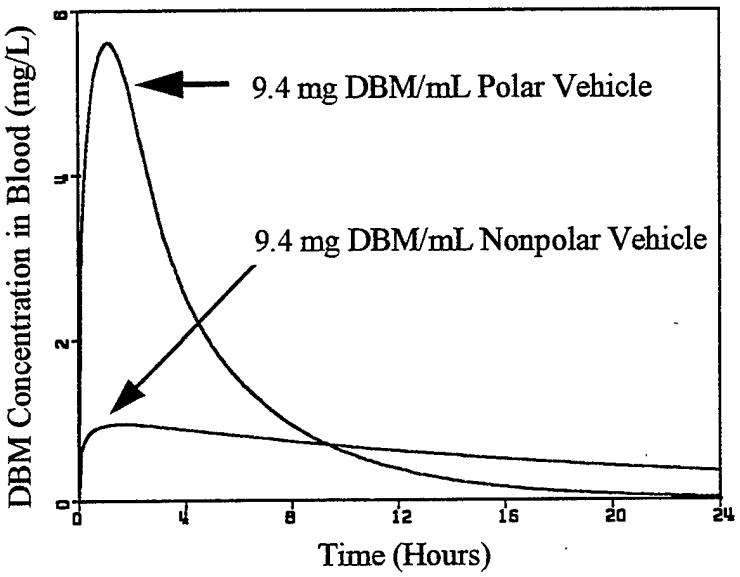

Figure 45. Effect of Vehicle on Blood Concentration. The lines represent physiologically based model simulations of dibromomethane (DBM) concentrations in blood resulting from identical exposures, except for the vehicle.

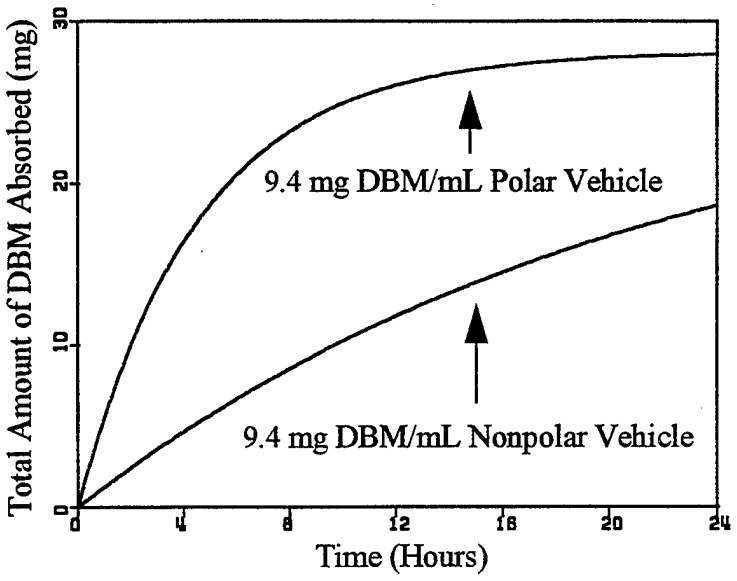

Figure 46. Effect of Vehicle on Total Amount of Chemical Absorbed During Dermal Exposure. **The lines represent physiologically based model simulations of the total amount of dibromomethane (DBM) absorbed during the exposure. The exposures were identical exposures except for the vehicle.**

Simulations can be generated and used to further evaluate the chemical levels achieved in blood for various exposure scenarios or physiological conditions using the physiologically based model. For example, the simulation in Figure 47 illustrates the impact of exposure surface area on achieved chemical concentration in blood following a dermal exposure. If in the example the surface area is 3.14 cm^2, the total amount of chemical absorbed is 281.79 mg with a peak chemical blood concentration of 65.83 mg/L. Using the same volume of application, a 10x increase in surface area would result in a total absorbed amount of 2240.54 mg and a peak chemical blood concentration of 956.21 mg/L. Since the

model keeps track of chemical mass in the entire exposure system, the surface concentration of chemical reflects the loss of chemical due to absorption. In figure 47, this exposure concentration change is also seen as a decline in chemical blood concentration following the peak achieved level. The impact of exposure area on the total amount of chemical absorbed is shown in Figure 48.

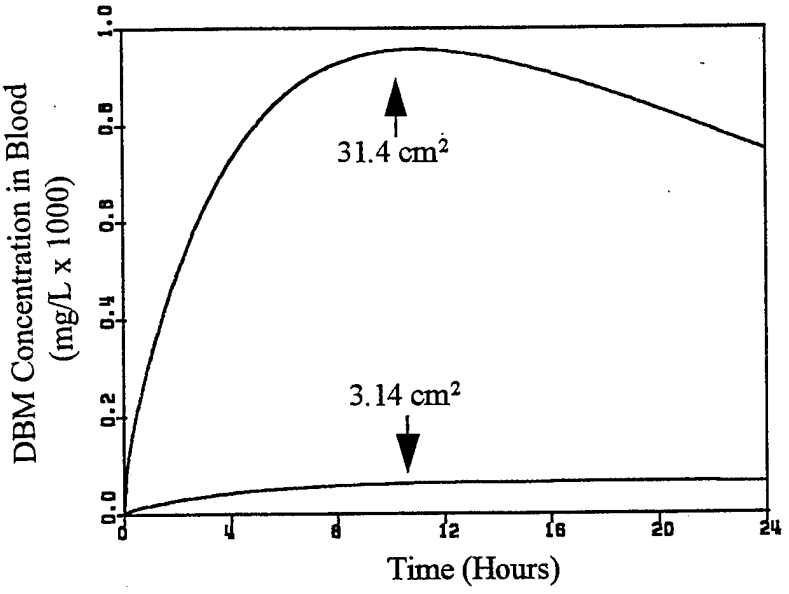

Figure 47. Effect of Exposure Area on Blood Concentration. The lines represent physiologically based model simulations of dibromomethane (DBM) concentrations in blood resulting from identical exposures, except for the dermal exposure area.

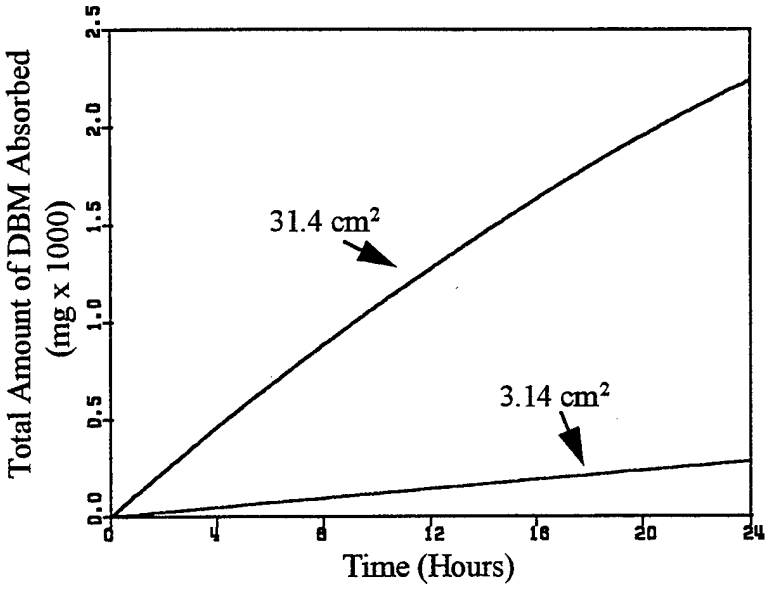

Figure 48. Effect of Exposure Area on Total Amount of Dibromomethane DBM Absorbed. **The lines represent physiologically based model simulations of the total amount of dibromomethane (DBM) absorbed during a 24 hour dermal exposure. The exposures used to generate the simulations were identical, except for the dermal exposure area.**

With the physiologically based pharmacokinetic model in place, the combination of exposure and physiological conditions that could be evaluated is enormous. However, one final use of the model will be to illustrate the impact of the dermal barrier thickness on achieved chemical blood levels. Figures 49 and 50 show the impact of skin thickness on achieved dibromomethane levels and total amount of dibromomethane absorbed during a 24 hour dermal exposure. When the skin thickness was 0.05 cm, the total amount of chemical absorbed was 281.86 mg with a peak chemical concentration in blood of 65.83 mg/L. When the skin

thickness was decreased by 10x the total amount of chemical absorbed was 281.79 mg with a peak chemical concentration in blood of 65.83. For the 24 hour steady-state exposure, the skin thickness did not significantly impact the chemical profile in blood.

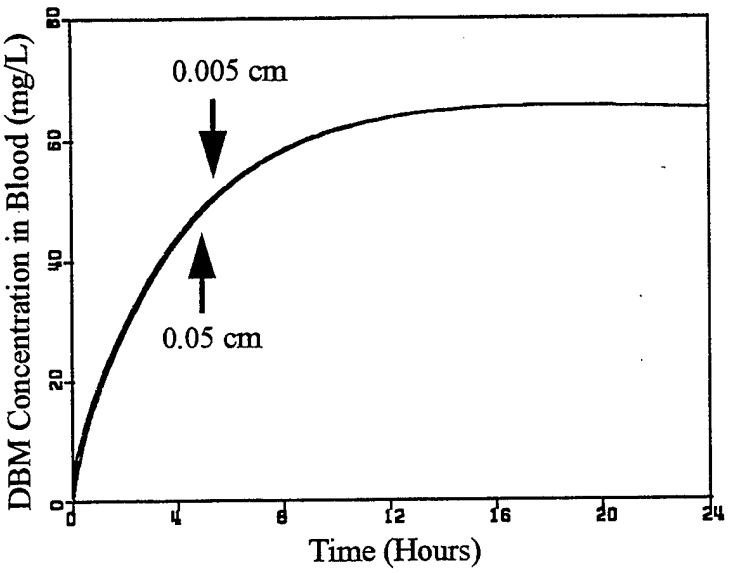

Figure 49. Effect of Skin Depth on 24 hr Blood Concentration. The lines represent physiologically based model simulations of dibromomethane (DBM) concentrations in blood resulting from identical 24 hour exposures, except for the skin depth under the exposure area.

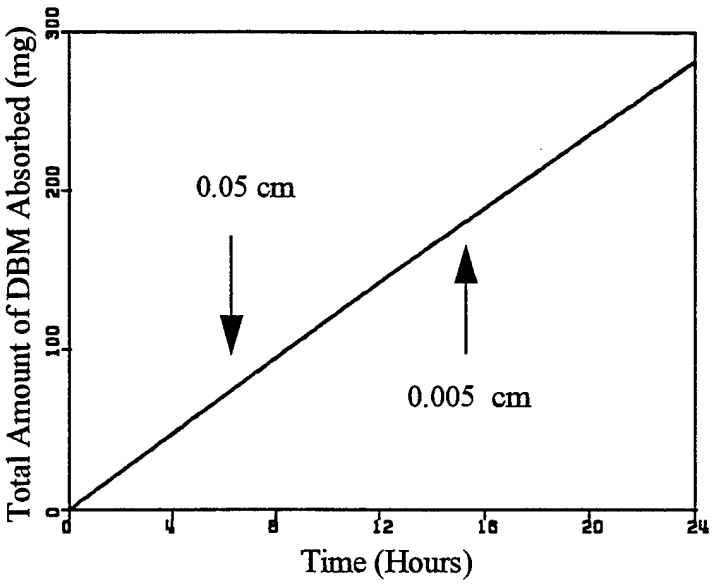

Figure 50. Effect of Skin Depth on Total Amount of Dibromomethane DBM Absorbed in 24 hr Exposure. **The lines represent physiologically based model simulations of the total amount of dibromomethane (DBM) absorbed during the exposure. The exposure conditions for the simulation were identical except for the skin depth under the exposure area.**

The data shown in Figure 49 may lead one to the conclusion that skin thickness is inconsequential in terms of influencing the achieved chemical concentrations in blood following a dermal exposure. Such a conclusion would be incorrect. The skin thickness does impact the achieved chemical concentration in blood at early, pre-steady state times. This effect is overshadowed and possibly insignificant in the long duration steady-state exposure, but, is evident in the shorter term 0.5 hour exposure shown in Figures 51 and 52. In addition to chemical levels in the blood, the influence of the dermal barrier thickness on the

amount of chemical absorbed can be seen clearly by looking at the skin compartment as shown in Figure 53.

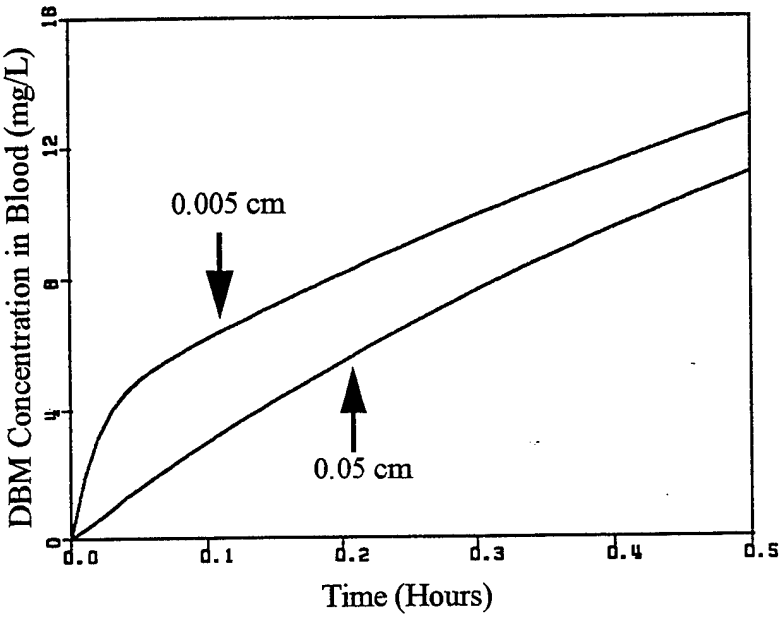

Figure 51. Effect of Skin Depth on 0.5 hr Blood Concentration. The lines represent physiologically based model simulations of dibromomethane (DBM) concentrations in blood resulting from identical 0.5 hour exposures, except for the skin depth under the exposure area.

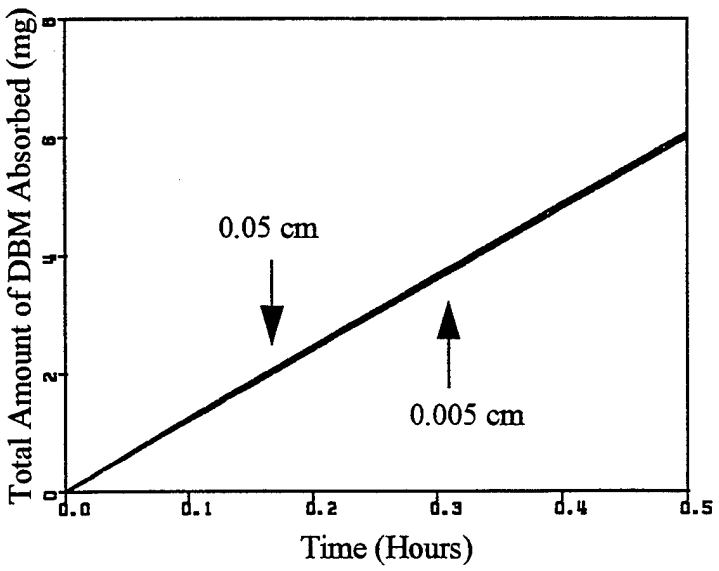

Figure 52. Effect of Skin Depth on Total Amount of Dibromomethane DBM Absorbed in a 0.5 hr Exposure. **The lines represent physiologically based model simulations of the total amount of dibromomethane (DBM) absorbed during the exposure. Exposure conditions used for the simulations were identical except for the skin depth under the exposure area.**

The value of the physiologically based pharmacokinetic model for dermal absorption of organic chemicals is not only in its predictive ability, but also, in its utility as an experimental design and analysis tool. As the dermal compartment becomes better characterized from a kinetic perspective, the physiologically based model may provide the quantitative link for interfacing laboratory work with dermal risk assessment activities.

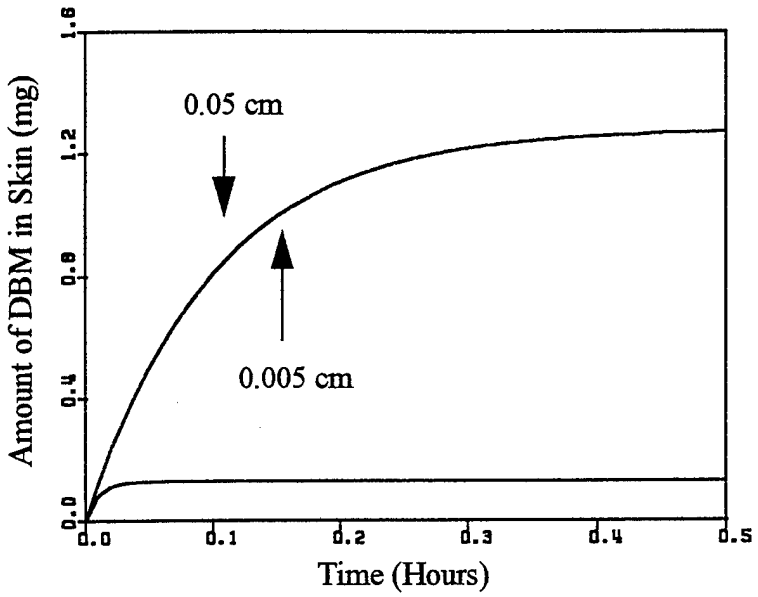

Figure 53. Effect of Skin Depth on Amount of Dibromomethane DBM Absorbed in Skin During a 0.5 hr Exposure. The lines represent physiologically based model simulations of the amount of chemical in the skin compartment during the exposure. Conditions used for the simulations were identical except for the skin depth under the exposure area.

NORMALIZED PERMEABILITY COEFFICIENTS

Even though a range of permeability coefficients were required to describe the dermal permeability of DBM in polar and non-polar vehicles, they shared a common relationship with the skin to vehicle partition coefficients. This relationship was the foundation for the use of a normalized permeability coefficient which was used to predict a permeability coefficient (K_P) for an organic chemical in a new chemical/vehicle system. The requirements for this approach are (1) a normalized permeability coefficient ($K_{p,n}$)

and (2) the skin to vehicle partition coefficient (PSKV) for the vehicle of interest, as shown in Equation 34.

$$K_p = K_{p,n} \times PSKV \qquad \textbf{Eq 34}$$

The mean normalized permeability coefficient value of 0.0277 cm/hr ± the standard deviation of 0.0062 cm/hr produced a coefficient of variation of 0.22 over the entire range of dibromomethane and bromochloromethane exposures in all of the chemical/vehicle systems. The relatively constant normalized permeability coefficient over such a large range of observed permeability constants supports the normalized permeability approach as a viable tool for prediction of permeability coefficients. Subsequently, the predicted permeability coefficient lends itself to prediction of chemical blood levels that result from dermal exposure to a chemical or chemical/vehicle system of interest.

The relatively constant normalized permeability coefficient over a wide range of exposure conditions that represented very polar to non-polar systems is probably sufficient evidence for the utility of a normalized permeability approach. However, the approach was further tested by predicting a permeability coefficient for dibromomethane in a new chemical/vehicle system. The chemical/vehicle system selected was dibromomethane/peanut oil. Dibromomethane has a peanut oil:air partition coefficient of 876 as compared to water:air partition

coefficient of 14.4 and a corn oil:air partition coefficient of 1023. The selected vehicle (peanut oil) has a vehicle:air partition coefficient intermediate between the polar vehicle (water) and the nonpolar vehicle (corn oil).

The normalized permeability coefficient was used along with the partition coefficient information for peanut oil in order to predict the observed permeability coefficient and subsequently the DBM blood levels that would result from a dermal exposure to DBM in the peanut oil vehicle. Optimized permeability coefficients were determined using a PBPK model analysis of the experimentally determined blood levels of DBM following dermal exposure to 25%, 50% and 75% DBM in peanut oil. The optimized permeability coefficients were compared to those predicted (generated before the exposure) using the normalized permeability coefficient and the PBPK model. The optimized permeability coefficients used to describe the DBM blood levels resulting from the 25% and 75% dibromomethane in peanut oil exposures were within the mean plus one standard deviation of the predicted permeability coefficient. In the case of the 50% DBM in peanut oil exposure, the optimized value was just slightly outside of the predicted mean plus one standard deviation. Specifically, the mean plus one standard deviation value was 0.0037 cm/hr and the optimized permeability coefficient was 0.0038 cm/hr (Figure 34). The results of the *in vivo*

predictions of observed permeability and resulting chemical concentrations in blood further support the concept and value of the normalized permeability method for quantitatively assessing the dermal absorption of chemicals.

Using the normalized permeability coefficient approach, the example shown in Figure 45 can be further defined. If the polar vehicle described earlier is defined as water and the nonpolar vehicle is defined as corn oil, the chemical concentrations blood can be predicted for a dermal exposure. The Kp for dibromomethane in water was assigned the value of 0.2200 cm/hr as the result of optimization of DBM in water data generated in this project. However, the Kp for the low level DBM in corn oil was calculated using the normalized permeability coefficient to be 0.0032 cm/hr. The resulting DBM concentrations in blood are dramatically different for the two exposures even though the DBM concentration is the same in both cases. The results are shown in Figure 54. In the case where the exposure was to 9.4 mg DBM/mL water, the total amount of chemical absorbed was 27.95 mg with a peak chemical concentration in blood of 5.62 mg/L. In the case where the exposure was to 9.4 mg DBM/mL corn oil, the total amount of chemical absorbed was 2.05 mg with a peak chemical concentration in blood of 0.071 mg/mL.

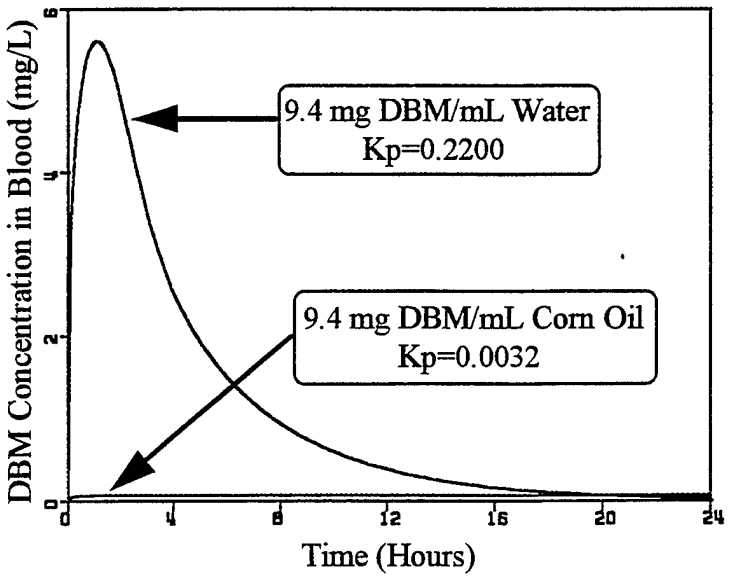

Figure 54. Vehicle and Kp Effects on Blood Concentration. The lines represent physiologically based model simulations of dibromomethane (DBM) concentrations in blood resulting from identical exposures except for the skin:vehicle partition coefficient and the Kp. The Kp was derived using the normalized permeability coefficient.

The quantitative evaluation of chemical levels in blood following dermal exposure has application to both occupational risk assessment and transdermal delivery of therapeutic agents. Clearly, the use of only chemical concentrations on the skin surface or qualitative descriptions of vehicle effects could result in large error in prediction of internal chemical doses derived from the dermal exposure.

FINITE DOSE EXPOSURES

Finite dose exposures represent a complex and dynamic system, especially with regard to the exposure scenario. In addition to all of the dermal and physiological processes described as part of the closed dermal cell exposures, the finite dose exposure involves a complicating evaporation factor.

Even though the rates of evaporation for bromochloromethane and dibromomethane were determined at 32 °C and from whole skin, just as would be expected in the *in vivo* situation, the actual evaporation rate during an *in vivo* exposure depends on air currents during the exposure and on the amount of hair present, as the latter helps establish the air boundary layer. The animals were unanesthetized and free to move around during exposures which created air movement across the exposure cell and potentially impacted the evaporation rates. The impact of using unrestrained animals for the exposures, in effect, makes any *in vitro* evaporation rate measurement a crude estimate of the actual *in vivo* evaporation rate.

The evaporation rates actually used in the physiologically based model were estimated by starting with the *in vitro* evaporation rate values and iteratively evaluating changes in the evaporation rate until the time to

peak blood level matched in the simulation and in the experimental data. No physiological parameter values were changed in the physiologically based model in order to consider the finite dose exposure scenario. The model simulation closely approximated the rise in bromochloromethane concentration in blood as well as the peak bromochloromethane blood concentration. After the peak concentration was reached the simulation underestimated the observed bromochloromethane blood concentration. The shape and magnitude of the blood versus time curve following attainment of the peak concentration was sensitive to the rapidly changing exposure concentration condition governed by evaporation and changing exposure surface area. The model as originally written did not adequately describe the exposure scenario for the finite dose dermal exposures. Similarly, the dibromomethane simulation closely approximated laboratory data for the uptake of dibromomethane into blood. The peak concentration was slightly overestimated by the model and as in the case of bromochloromethane the simulation demonstrated a more rapid drop off in dibromomethane blood concentration than was observed in the laboratory data. As an indicator of peak chemical concentration in blood and total area under the curve for systemically absorbed chemical, the model was respectable for both bromochloromethane and dibromomethane.

However, the model's ability to describe the exposure conditions as the chemical rapidly evaporated from the skin, was less than optimum. While both bromochloromethane and dibromomethane are volatile chemicals that displayed essentially a zero order evaporation rate over the measurable range of the evaporation studies, it is expected that something other than zero order conditions prevail when there is very little chemical left on the skin. Similarly, a change in exposure surface area should result from evaporation or the chemical from the skin surface which in turn affects the evaporation rate.

Another consideration is that the skin may act as somewhat of a reservoir for the chemical which then serves to release the chemical into the blood even after the surface concentration of chemical is zero. The existence of a stratum corneum reservoir has been shown for a topically applied therapeutic agents (Stoughton, 1989; Tsai et al., 1994). The existence of chemical reservoirs in the skin may be detrimental or beneficial depending on the chemical of interest and its intended application. While a dermal reservoir may occur for the dihalomethanes, it has not been proven to be a factor in the observed dermal absorption kinetics.

By incorporating mathematical code into the model which described a process for linking evaporation and exposure

area change, the simulation more appropriately represented the exposure scenario. These model changes produced no impact on the *in vivo,* closed dermal cell exposures since in those systems the chemical had no access to the atmosphere and the evaporation rate was set to zero.

IN VITRO PERMEABILITY COEFFICIENT ESTIMATION

The use of thermal gravimetric analysis for estimation of diffusion and partition coefficients shows potential as a rapid and powerful method for obtaining the information necessary for calculation of a permeability coefficient. In order to use the TGA system for organic chemicals or other rapidly diffusing chemicals, chemical delivery to the TGA system must be significantly faster than the diffusion of chemical into the sample.

The evaluation of water vapor diffusion in stratum corneum using TGA that was recently published used a system of gas washing bottles to bubble gas through liquids in order to generate water vapor atmospheres (Liron, et al., 1994). This approach worked in the relatively slowly diffusing water vapor, but, was too slow for the rapidly diffusing halogenated hydrocarbons of interest in this work. In the original thermal gravimetric analysis system design, the estimation of the diffusion coefficient was limited to an upper bound determined by the rate of chemical delivery

to the stratum corneum sample. This system was redesigned to use chemical sample bags rather than the slow gas washing bottles. Flow design and chemical vapor handling equipment were also modified to accommodate the demands of rapidly diffusion chemicals. While the chemical handling and exposure systems of the TGA were redesigned and modified, the underlying principles used to describe water vapor diffusion were still applicable to the more rapidly diffusing halogenated hydrocarbons.

As with any *in vitro* method, there is both advantage and risk associated with the investigator's control over the conditions during the exposure. On one hand, conditions may be designed as to isolate particular aspects or mechanisms of a system. This isolation potential in the *in vitro* system can provide a much more direct study of specific components of the system as compared to the complexity of the *in vivo* system. On the other hand, the manipulation and exposure control used to elucidate specific components in a system may in themselves create an environment much different than can be achieved *in vivo*. If the goal is to use *in vitro* data to describe or predict *in vivo* events, then steps taken to optimize the *in vitro* system must be scrutinized for their impact on *in vivo* behavior. The same considerations that apply to general *in vitro* to *in vivo* extrapolations discussed above were applicable to the use of

thermal gravimetric analysis to predict *in vivo* dermal permeability coefficients.

The thermal gravimetric analysis method used stratum corneum which was enzymatically separated from the underlying layers of skin. This isolation provided for kinetic study of a particular layer in the skin. If the stratum corneum is the determinant of dermal absorption rates for the chemicals of interest, then data obtained in the *in vitro* system are likely to correspond to data from the more complex *in vivo* system. Obviously such isolation is not possible in an *in vivo* system and the opportunity for detailed study of individual skin components is limited.

In the *in vitro* system the elements of water content and temperature must be controlled or maintained at some constant value, whereas in the *in vivo* system these are primarily under the control of the biological systems being studied. The impact of temperature or water content may or may not impact *in vitro* to *in vivo* extrapolation depending on their kinetic contribution to the system of study.

One other aspect of the estimation of diffusion coefficients, and subsequently the calculation of the permeability coefficients, is the diffusion pathlength. The assumption that the chemical diffusion path length is the same or even similar to the stratum corneum thickness may not be acceptable. It is likely that chemicals diffuse

primarily through the intercellular lipid matrix of the stratum corneum (Guy, and Hadcraft, 1988), which would produce a nonlinear and perhaps a much exaggerated diffusion path length. In the *in vivo* estimate of the permeability coefficient, the diffusion path length is buried in the permeability coefficient term and is not explicitly defined. The situation is different in the *in vitro*, thermal gravimetric analysis estimation of the permeability coefficient. In the TGA approach the diffusion coefficient is calculated by using the experimental kinetic data and directly uses the path length of diffusion. The diffusion coefficient is then used to estimate a permeability coefficient.

The thermal gravimetric analysis derived data was used to calculate permeability coefficients for the dibromomethane and bromochloromethane exposures in the water and oil vehicles. The TGA derived bromochloromethane permeability coefficients were approximately five times lower than the permeability coefficients determined in the course of exposure. On the other hand, the TGA derived dibromomethane permeability coefficients corresponded nearly one to one with the observed permeability coefficients. However, the behavior of the bromochloromethane in the thermal gravimetric analysis system was less than ideal as compared to the dibromomethane. The resulting

bromochloromethane data provided a much smaller linear range for analysis with the diffusion model than was observed with the dibromomethane. The bromochloromethane behavior in the TGA system may identify a situation where the TGA exposure system would perform more effectively with some modifications. Specifically, a sample chamber that could hold a larger sample volume without stacking of the sample would probably increase the linear range available for analysis. This modification would probably be useful where partition coefficients were relatively low and mass determinations where near the TGA sensitivity limit.

V. CONCLUSION

Physiologically based modeling combined with *in vivo* chemical exposures provided a solid foundation for the description of dermal absorption of organic chemicals. While successful approaches have been developed using statistical or correlation of parameters such as lipophilicity or molecular weight to predict dermal absorption of chemicals (Cleek and Bunge, 1993; Kasting, et al., 1987), the use of dermal absorption data in health risk assessment activities requires a quantitative interface with the biological system of interest (Clewell and Andersen, 1985; Conolly and Andersen, 1991; Leung, 1991). As shown here, the chemical blood levels achieved following dermal exposures are complex functions of the distribution, biotransformation and elimination of the chemicals after they have traveled through the skin and into the systemic circulation. The chemical blood levels and the chemical concentrations in target tissues where toxic events occur are not necessarily linearly related to the chemical exposure. This complex arrangement creates a demand for both a functional description of the chemical input into the system as well as a mechanism for describing the behavior of the chemical once it enters the system. The value of the physiologically based model in estimation of dermal

permeability coefficients was in its ability to maintain a chemical mass balance throughout the chemical exposure period. By summing the amount of chemical in the biological organs and tissues, the amount of chemical metabolized and the amount of unmetabolized chemical exhaled, the total amount of chemical absorbed during the dermal exposure was estimated. The total amount of chemical absorbed was in turn used to calculate a dermal permeability coefficient which is a functional quantitative descriptor of a chemical's movement through the skin and into the systemic circulation. The dermal compartment as included in the model was represented as a single homogenous, well-stirred layer which was in contact with chemical on one side and blood on the other. While such a description of the skin compartment may not apply to all chemicals in all exposure scenarios, it may be adequate for most of the chemicals in the occupationally and environmentally relevant group of volatile, halogenated hydrocarbons.

By applying a normalized permeability coefficient approach, the physiologically based model was demonstrated to be predictive as well as descriptive for chemical concentrations in blood during dermal exposures to halogenated hydrocarbons in vehicles ranging from air to water to oil. In addition to using physiological modeling and *in vivo* exposures to generate permeability coefficients,

an *in vitro* thermal gravimetric analysis approach was described. The motivation for the thermal gravimetric analysis approach was to develop a rapid method for estimation of permeability coefficients for volatile chemicals without the use of large numbers of experimental animals. The success of the thermal gravimetric analysis approach in terms of predicting permeability coefficients for liquid DBM or BCM in water and oil vehicles was mixed. The TGA permeability coefficient predictions for dibromomethane were much better than those for bromochloromethane. However, even the worst case bromochloromethane predictions were about 2-fold better than the order of magnitude error commonly accepted in dermal risk assessment applications. The thermal gravimetric analysis method demonstrated merit in description of diffusion and partition coefficients and could be a valuable tool for evaluation of individual components of the skin or to study the impact of humidity or temperature on dermal absorption kinetics.

REFERENCES

Andersen ME 1981. A Physiologically Based Toxicokinetic Description of the Metabolism of Inhaled Gases and Vapors: Analysis at Steady State. Toxicology and Applied Pharmacology 60:509-526.

Anderson YA, Jackson JA and Birnbaum LS. 1993. Maturational Changes in Dermal Absorption of 2,3,7,8-Tetrachlorodibenzo-p-dioxin (TCDD) in Fischer 344 Rats. Toxicology and Applied Pharmacology 119:214-220.

Banks YB, Brewster DW and Birnbaum LS. 1990. Age-Related Changes in Dermal Absorption of 2,3,7,8-Tetrachlorodibenzo-p-dioxin and 2,3,4,7,8-Pentachlorodibenzofuran. Fundamental and Applied Toxicology 15:163-173.

Black JG and Kamat VB 1988. PERCUTANEOUS ABSORPTION OF OCTOPIROX. Fd. Chem. Toxic. 26(1):53-58.

Bronaugh RL and Congdon ER. 1984. Percutaneous Absorption of Hair Dyes: Correlation with Partition Coefficients. The Journal of Investigative Dermatology 83:124-127.

Bronaugh RL. 1990. Metabolism in Skin. In Principles of Route-to-Route Extrapolation for Risk Assessment. Gerrity TR and Henry CJ, eds. Elsevier Science Publishing Co., Inc., pp 185-190.

Bucks DAW, Marty JPL and Maibach HI. 1985. Percutaneous Absorption of Malathion in the Guinea-Pig: Effect of Repeated Topical Application. Fd Chem. Toxic. 23(10):919-922.

Chang SK and Riviere JE. 1991. Percutaneous Absorption of Parathion In Vitro in Porcine Skin: Effects of Dose, Temperature, Humidity, and Perfusate Composition on Absorptive Flux. Fundamental And Applied Toxicology 17:494-504.

Chien YW, XU H Chiang CC and Huang YC. 1988. Transdermal Controlled Administration of Indomethacin. I. Enhancement of Skin Permeability. Pharmaceutical Research. 5(2):103-106.

Cleek RL and Bunge AL. 1993. A New Method for Estimating Dermal Absorption from Chemical Exposure. 1. General Approach. Pharmaceutical Research 10(4):497-506.

Clewell HJ III and Andersen ME. 1985. Risk Assessment Extrapolations and Physiological Modeling. Toxicology and Industrial Health 1(4):111-131.

Conolly RB and Andersen ME. 1991. Biologically Based Pharmacodynamic Models: Tools for Toxicological Research and Risk Assessment. Annu. Rev. Pharmacol. Toxicol. 31:503-523.

Cooper ER and Berner B. 1985. Finite Dose Pharmacokinetics of Skin Penetration. Journal of Pharmaceutical Sciences 74(10):1100-1102.

Curatolo W. 1987. The Lipoidal Permeability Barriers of the Skin and Alimentary Tract. Pharmaceutical Research, Vol. 4, No. 4:274-276.

Crank J. 1975. The Mathematics of Diffusion: Second Edition. Oxford University Press, New York. p 48.

Emmett EA. 1986. Toxic Responses of the Skin. In Toxicology: The Basic Science of Poisons. Klaassen CD., Amdur MO. and Doull J., eds. Macmillan Publishing Co., New York, pp 413-417.

Fiserova-Bergerova V. 1993. Relevance of Occupational Skin Exposure. Annals of Occupational Hygiene 37(6):673-685.

Fisher HL, Shah PV, Sumler MP and Hall LL. 1989. In Vivo and In Vitro Dermal Penetration of 2.4,5,2',4',5'-Hexachlorobiphenyl in Young and Adult Rats. Environmental Research 50:120-139.

Flynn G. 1990. Physicochemical Determinants of Skin Absorption. In Principles of Route-to-Route Extrapolation for Risk Assessment. Gerrity TR and Henry CJ, eds. Elsevier Science Publishing Co., Inc., pp 93-127.

Frederick CB and Chang-Mateu M. 1990. Contact Site Carcinogenicity: Estimation of an Upper Limit for Risk of Dermal Dosing Site Tumors Based on Oral Dosing Site Carcinogenicity. In Principles of Route-to-Route Extrapolation for Risk Assessment. Gerrity TR and Henry CJ, eds. Elsevier Science Publishing Co., Inc., pp 237-269.

Gallo JM, Lam FC and Perrier DG. 1987. Pharmacometrics: Area Method for the Estimation of Partition Coefficients for Physiological Pharmacokinetic Models. Journal of Pharmacokinetics and Biopharmaceutics 15(3):271-280.

Gargas ML and Andersen ME. 1982. Metabolism of Inhaled Brominated Hydrocarbons: Validation of Gas Uptake Results by Determination of a Stable Metabolite. Toxicology and Applied Pharmacology 66:55-68.

Gargas ML, Clewell HJ and Andersen ME. 1986. Metabolism of Inhaled Dihalomethanes In Vivo: Differentiation of Kinetic Constants for Two Independent Pathways. Toxicology and Applied Pharmacology 82:211-223.

Gargas ML, Burgess RJ, Voisard DE, Cason GH and Andersen ME. 1989. Partition Coefficients of Low-Molecular-Weight Volatile Chemicals in Various Liquids and Tissues. Toxicology and Applied Pharmacology 98:87-99.

Genderen JV, Mol MAE and Wolthuis OL. 1985. On the Development of Skin Models for Toxicity Testing. Fundamental and Applied Toxicology 5:S98-S111.

Groning R. 1987. Electrophoretically Controlled Dermal or Transdermal Application Systems with Electronic Indicators. International Journal of Pharmaceutics 36:37-40.

Guy RH and Hadgraft J. 1988. Physiochemical Aspects of Percutaneous Penetration and its Enhancement. Pharmaceutical Research 5(12):753-758.

Jacob SW. 1978. Structure and Function in Man. W.B. Saunders Co., Philadelphia, pp 75-82.

Kasting GB, Smith RL and Cooper ER. 1987. Effect of Lipid Solubility and Molecular Size on Percutaneous Absorption. Pharmacol. Skin 1:138-153.

Kemppainen BW, Riley RT, Pace JG, Hoerr FJ and Joyave J. 1986. Evaluation of Monkey Skin as a Model for In Vitro Percutaneous Penetration and Metabolism of [^{3}H]T-2 Toxin in Human Skin. Fundamental and Applied Toxicology 7:367-375.

Lam CW, Galen TJ, Boyd JF and Pierson DL. 1990. Mechanism of Transport and Distribution of Organic Solvents in Blood. Toxicology and Applied Pharmacology 104:117-129.

Lam CW, Weir FW, Cavender KW, Tan MN, Galen TJ and Pierson DL. 1993. Toxicokinetics of Inhaled Bromotrifluoromethane (Halon 1301) in Human Subjects. Fundamental and Applied Toxicology 20:231-239.

Leung HW. 1991. Development and Utilization of Physiologically Based Pharmacokinetic Models For Toxicological Applications. Journal of Toxicology and Environmental Health 32:247-267.

Leung HW and Paustenbach DJ. 1994. Techniques for Estimating the Percutaneous Absorption of Chemicals Due to Occupational and Environmental Exposure. Appl. Occup. Environ. Hyg. 9(3):187-197.

Lin JH, Sugiyama Y, Awazu S and Hanano M. 1982. In Vitro and In Vivo Evaluation of the Tissue-to-Blood Partition Coefficient for Physiological Pharmacokinetic Models. Journal of Pharmacokinetics and Biopharmaceutics 10(6):637-646.

Liron Z, Clewell HJ and McDougal JN. 1994. Kinetics of Water Vapor Sorption in Porcine Stratum Corneum. Journal Pharmaceutical Sciences 83(5):692-698.

Loth H. 1989. Skin Permeability. Meth and Find Exp Clin Pharmacol 11(3):155-164.

[a]Mattie DR, Grabau JH and McDougal JN. 1994. Significance of the Dermal Route of Exposure to Risk Assessment. Risk Analysis 14(3):277-284.

[b]Mattie DR, Bates GD, Jepson GW, Fisher JW and McDougal JN. 1994. Determination of Skin:Air Partition Coefficients for Volatile Chemicals: Experimental Method and Applications. Fundamental and Applied Toxicology 22:51-57.

McDougal JN, Jepson GW, Clewell HJ, MacNaughton MG and Andersen ME. 1986. Toxicology and Applied Pharmacology 85:286-294.

McDougal JN and Clewell HJ. 1990. Dermal to Inhalation Extrapolation for Organic Chemicals. In Principles of Route-to-Route Extrapolation for Risk Assessment. Gerrity

TR and Henry CJ, eds. Elsevier Science Publishing Co., Inc., pp 313-317.

Monro AM. 1990. Interspecies Comparisons in Toxicology: The Utility and Futility of Plasma Concentration of the Test Substance. Regulatory Toxicology and Pharmacology 12:137-160.

Nangia A, Camel E, Berner B and Maibach H. 1993. Influence of Skin Irritants on Percutaneous Absorption. Pharmaceutical Research 10(12):1756-1759.

Paterson S and Mackay D. 1989. Correlation of Tissue, Blood and Air Partition Coefficients of Volatile Organic Chemicals. British Journal of Industrial Medicine 46:321-328.

Quinn, D. 1994. Professor of Mathematics, Air Force Institute of Technology, WPAFB, OH. Personal Communication.

Ramsey JC and Andersen ME. 1984. A Physiologically Based Description of the Inhalation Pharmacokinetics of Styrene in Rats and Humans. Toxicology and Applied Pharmacology 73:159-175.

Ritschel WA. and Hussain AS. 1988. The Principles of Permeation of Substances Across the Skin. Meth and Find Exptl Clin Pharmacol 10(1):39-56.

Sato A and Nakajima T. 1979. A Vial-Equilibrium Method to Evaluate the Drug-Metabolizing Enzyme Activity for Volatile Hydrocarbons. Toxicology and Applied Pharmacology 47:41-46.

Scheuplein RJ and Blank IH. 1971. Permeability of the Skin. Physiological Reviews 51(4):702-747.

Shu H, Teitelbaum P, Webb AS, Brunck MB, Rossi DD, Murray FJ and Paustenbach D. 1988. Bioavailability of Soil-Bound TCDD: Dermal Bioavailability in the Rat. Fundamental and Applied Toxicology 10:335-343.

Storm JE, Collier SW, Stewart RF and Bronaugh RL. 1990. Metabolism of Xenobiotics During Percutaneous Penetration: Role of Absorption Rate and Cutaneous Enzyme Activity. Fundamental and Applied Pharmacology 15:132-141.

Stoughton RB. 1989. Percutaneous Absorption of Drugs. Annu. Rev. Pharmacol. Toxicol. 29:55-69.

Sultatos LG, Kim B and Woods L. 1990. Evaluation of Estimations In Vitro of Tissue/Blood Distribution Coefficients for Organophosphate Insecticides. Toxicology and Applied Pharmacology 103:52-55.

Surber C, Wilhelm KP, Maibach HI, Hall LL and Guy RH. 1990. Partitioning of Chemicals into Human Stratum Corneum: Implications for Risk Assessment Following Dermal Exposure. Fundamental and Applied Toxicology 15:99-107.

Tsai JC, Flynn GL, Weiner N and Ferry JJ. 1994. Influence of Application Time and Formulation Reapplication on the Delivery of Minoxidil Through Hairless Mouse Skin As Measured in Franz Diffusion Cells. Skin Pharmacology 7(5)270-277.

Weast RC (editor). 1987. CRC Handbook of Chemistry and Physics, 67th Edition. CRC Press, Inc., Boca Raton, FL., pp C348-C349.

Wester RC, Maibach HI, Bucks DAW, McMaster J and Mobayen M. 1990. Percutaneous Absorption and Skin Decontamination of PCBs: In Vitro Studies with Human Skin and In Vivo Studies in the Rhesus Monkey. Journal of Toxicology and Environmental Health 31:345-246.

Willsteed EM, Bhogal BS, Das A, Bekir SS, Wojnarowska F, Black MM and Mckee PH. 1991. An Ultrastructural Comparison of Dermo-epidermal Separation Techniques. J Cutan Pathol 18:8-12.

Woollen BH, Hall MG Craig R and Steel GT. 1985. Dinitrotoluene: An assessment of occupational absorption during the manufacture of blasting explosives. Int Arch Occup Environ Health 55:319-330.

THIS PAGE INTENTIONALLY LEFT BLANK

APPENDIX A

APPENDIX A

SOURCE CODE FOR SIMUSOLV PROGRAM

```
PROGRAM: DERMAL LIQUID SKIN MODEL(DERM.CSL)
' MODEL IS SET UP TO SIMULATE BOTH FINITE AND INFINITE'
' DERMAL EXPOSURES'

INITIAL

'RAT PHYSIOLOGICAL VALUES'

CONSTANT  QPC = 15.       $'PULMONARY VENTIL (L/KG/HR)'
CONSTANT  QCC = 15.       $'CARDIAC FLOW (L/KG/HR)'
CONSTANT  QLC = .25       $'FRACTION OF FLOW TO LIVER'
CONSTANT  QFC = .07       $'FRACTION OF FLOW TO FAT'
CONSTANT  QSKC = .05      $'FRACTION OF FLOW TO SKIN'
CONSTANT  BW = .22        $'BODY WT (KG)'
CONSTANT  VSKC = .10      $'PERCENT SKIN'
CONSTANT  VFC = .07       $'PERCENT FAT'
CONSTANT  VLC = .04       $'PERCENT LIVER'
CONSTANT  DEPTH = .005    $'SKIN THICKNESS (cm)'

'CHEMICAL SPECIFIC VALUES'

CONSTANT  D = 1.          $'DENSITY (MG/ML)'
CONSTANT  MOLWT = 1       $'MOL WT'
CONSTANT  PL = 1.         $'LIVER/BLOOD PART COEF'
CONSTANT  PF = 1.         $'FAT/BLOOD PART COEF'
CONSTANT  PS = 1.         $'MUSCLE/BLOOD PART COEF'
CONSTANT  PR = 1.         $'LIVER/BLOOD PART COEF'
CONSTANT  PB = 1.         $'BLOOD/AIR PART COEF'
CONSTANT  PSK = 1.        $'SKIN/AIR PART COEF'
CONSTANT  VMAXC = 1.      $'MAX REACTION RATE (MG/KG/HR)'
CONSTANT  KM = 1.         $'MICHAELIS-MENTEN (MG/ML)'
CONSTANT  KFC = 1.        $'FIRST ORDER CONST (HR-1/KG)'
CONSTANT  P = 1.          $'PERMEABILITY CONST (CM/HR)'
CONSTANT  VP = 1          $'VAPOR PRESSURE AT 25 DEG'
CONSTANT  PV = 1.         $'VEHICLE/AIR PART COEF'
```

```
CONSTANT    MPSKLQ =1.          $'MEAS SK/LIQ PC (NEAT)'
```

'DOSE VALUES FOR CHEMICAL'

```
CONSTANT    DOSE = 1.           $'INITIAL AMT ON SKIN SFC (MG)'
CONSTANT    VSFC = 1.           $'INITIAL VOLUME ON SFC (ML)'
CONSTANT    A = 1.              $'AREA EXPOSED (CM2)'
CONSTANT    ESWTCH = 0.         $'EVAPORATION RATE TURNED OFF'
CONSTANT    FSWTCH = 1.         $'OFF WHEN USING MPSKLQ'
CONSTANT    ASWTCH = 1.         $'OFF FOR NEAT FINITE DOSE'
CONSTANT     ZERO = 1.          $'TURN OFF SURFACE CONC (0)'
CONSTANT    VVEH = 1.           $'VOLUME OF VEHICLE (ML)'
CONSTANT    EVAP = 1.           $'EVAP RATE (MG/HR/CM2)'
CONSTANT    PPMCI = 0.          $'CONC IN AIR, PPM'
CONSTANT    TEVAP = 1.          $'TIME CHEM EVAPORATED, HR'
CONSTANT    TVAPOR = 1.         $'TIME VAPOR IS ZERO, HR'
CONSTANT....SFCL= 0.            $'SURFACE CONC CUTOFF, MG/ML'
```

'TIMING COMMANDS'

```
CONSTANT  TSTOP = 1.            $'TIME EXPOSURE STOPS, HR'
CONSTANT  CINT  = 1.            $'COMMUNICATION INTERVAL'
```

'SCALED PARAMETERS'

```
TA = (9.1*((BW*1000.)**.667))   $'SURFACE AREA OF SKIN, CM2'
QC = QCC * BW**0.74             $'SCALED CARDIAC BLOOD FLOW , L/HR'
QP = QPC * BW**0.74             $'SCALED VENTILATION RATE, L/HR'
QL = QLC * QC                   $'LIVER BLOOD FLOW, L/HR'
QF = QFC * QC                   $'FAT BLOOD FLOW, L/HR'
QR = 0.76 * QC - QL             $'RAPIDLY PERFUSED BLOOD FLOW, L/HR'
QSK = QSKC * QC * 1000.* (A/TA)$'EXPOSED SKIN BLOOD FLOW, ML/HR'
QS = 0.24 * QC - QF - QSK/1000  $'SLOWLY PERFUSED BLOOD FLOW, L/HR'
VL = VLC * BW                   $'LIVER VOLUME, L'
VF = VFC * BW                   $'FAT VOLUME, L'
VSK = A * DEPTH                 $'EXPOSED SKIN VOLUME, CM2'
VS = 0.82 * BW - VF - VSK/1000  $'SLOWLY PERFUSED VOLUME, L'
VR = 0.09 * BW - VL                   $'RAPIDLY PERFUSED VOLUME, L'
VMAX = VMAXC * BW**0.7          $'SCALED MAXIMUM SATURABLE'
                                      'METABOLISM VELOCITY, MG/HR'
KF = KFC / BW**0.3              $'SCALED FIRST ORDER METABOLISM'
                                      'RATE'
PSKB = PSK/PB                   $'SKIN:BLOOD PARTITION COEFF'
PSKLQ = (((PSK/PV) * FSWTCH) + MPSKLQ)  $'SKIN:VEHICLE'
                                        'PARTITION COEFFICIENT'
```

```
AVF = DOSE/A                    $'WEIGHT/SURFACE AREA'
                                    'FACTOR, MG/CM2'
CI= PPMCI*(MOLWT/24450.)        $'CONC IN AIR, MG/L'

                END             $'END OF INITIAL'

                                DYNAMIC

ALGORITHM IALG = 2                  $'GEAR STIFF METHOD'

TERMT(T.GE.TSTOP)               $'TERMINATION STATEMENT'

PROCEDURAL
IF(ASFC.LE.SFCL) EVAP=0.        $'SETS EVAP=0 WHEN ASFC=0'
IF(ASFC.LE.SFCL) ZERO=0.        $'SETS ZERO=0 WHEN AFSC =SFCL'
IF(MPSKLQ.GT.0.) FSWTCH=0.      $'SETS FSWTCH TO ZERO IF MPSKLQ IS >0'
                                    'FSWTCH=0 FOR NEAT CHEMICAL'
                                    'AND 1 FOR DILUTED CHEMICAL'
IF(FSWTCH.EQ.1.) MPSKLQ=0.      $'SETS MPSKLQ=0 IF FSWTCH=1'
END
```

DERIVATIVE

DEFINITIONS SHOWN IN THE BOLD PRINT FOLLOWING EACH COMPARTMENT DESCRIPTION ARE PROVIDED FOR CLARITY. THIS ADDED TEXT DID NOT APPEAR IN MODEL CODE RUN ON THE VAX

```
'ASFC = AMOUNT OF CHEMICAL ON SKIN SURFACE (MG)'
      RASFC =  P*DAR*(CSK/PSKLQ-CSFC) - RAEVAP
      DASFC = INTEG(RASFC,DOSE)
      ASFC =   AMAX1(DASFC,1.E-30)
      CSFC = (ASFC/(VLSFC + VVEH))*ZERO
      VLSFC = ASFC/D
      RAEVAP = EVAP*DAR*ESWTCH
      AEVAP = INTEG(RAEVAP,0.)
      RAC = EVAP*DAR/AVF
      AC = INTEG(RAC,0.)
      DAR = (A-AC)+ ASWTCH*AC
```

ASFC= RATE OF CHANGE OF CHEMICAL ON SKIN SURFACE
DASFC=AREA UNDER THE RATE CURVE, RASFC
AFSC= AMOUNT OF CHEMICAL ON THE SKIN SURFACE, SET TO GREATER

```
        OF DASFC OF 1E-30.
CSFC= CONCENTRATION OF CHEMICAL ON THE SKIN SURFACE
VLSFC= VOLUME OF CHEMICAL ON THE SKIN SURFACE
RAEVAP= RATE OF CHEMICAL EVAPORATION FROM SKIN SURFACE
RAC= RATE OF CHANGE OF EXPOSURE AREA DUE TO EVAPORATION
AC= SKIN SURFACE AREA LOSS TO EVAPORATION
DAR= REMAINING SKIN SURFACE AREA FOR EXPOSURE

'ASK = AMOUNT IN SKIN (MG)'
      RASK = P*DAR*(CSFC-(CSK/PSKLQ)) + QSK*((CA/1000.) - CVSK)
      ASK = INTEG(RASK,0.)
      CVSK = ASK/(VSK*PSKB)
      CSK = ASK/VSK

RASK= RATE OF CHANGE OF CHEMICAL ON SKIN
ASK= AMOUNT OF CHEMICAL ON THE SKIN SURFACE
CVSK=CONCENTRATION OF CHEMICAL LEAVING SKIN IN VENOUS BLOOD
CSK= CONCENTRATION OF CHEMICAL IN SKIN

'CA = ART BLOOD CONC (MG/L)'
      CA = (QC*CV + QP*CI)/(QP/PB+QC)
      AUCB = INTEG(CA,0.)
      CX = CA/PB

AUCB= AREA UNDER THE ARTERIAL BLOOD CONCENTRATION CURVE
CX= CONCENTRATION OF CHEMICAL IN EXHALED AIR

'AX = AMOUNT EXHALED (MG)'
      RAX = QP * CX
      AX = INTEG(RAX,0.)

RAX= RATE OF CHEMICAL EXHALATION
AX= AMOUNT OF CHEMICAL EXHALED

'AI= AMOUNT INHALED (MG)'
      RAI = QP*CI
      AI = INTEG(RAI,0.)

RAI= RATE OF CHEMICAL INHALATION
AI= AMOUNT OF CHEMICAL INHALED

'AF = AMOUNT IN FAT (MG)'
      RAF = QF * (CA - CVF)
      AF = INTEG(RAF,0.)
      CVF = AF / (VF * PF)
      CF = AF / VF
```

```
RAF= RATE OF CHANGE OF CHEMICAL IN FAT
AF= AMOUNT OF CHEMICAL IN THE FAT
CVF=CONCENTRATION OF CHEMICAL LEAVING FAT IN VENOUS BLOOD
CF= CONCENTRATION OF CHEMICAL IN FAT

'AL = AMOUNT IN LIVER (MG)'
      RAL = QL * (CA - CVL) - RAM
      AL = INTEG(RAL,0.)
      CVL = AL / (VL * PL)
      CL = AL / VL

RAL= RATE OF CHANGE OF CHEMICAL IN LIVER
AL= AMOUNT OF CHEMICAL IN THE LIVER
CVL=CONCENTRATION OF CHEMICAL LEAVING LIVER IN VENOUS BLOOD
CL= CONCENTRATION OF CHEMICAL IN LIVER
RAM= RATE OF METABOLISM

'AS = AMOUNT IN SLOWLY PERF (MG)'
      RAS = QS * (CA - CVS)
      AS = INTEG(RAS,0.)
      CVS = AS / (VS * PS)
      CS = AS / VS

RAS RATE OF CHANGE OF CHEMICAL IN SLOWLY PERFUSED
AS= AMOUNT OF CHEMICAL IN SLOWLY PERFUSED
CVS=CONCENTRATION OF CHEMICAL LEAVING SLOWLY PERFUSED IN
VENOUS BLOOD
CS= CONCENTRATION OF CHEMICAL IN SLOWLY PERFUSED

'AR = AMOUNT IN RAPIDLY PERF (MG)'
      RAR = QR * (CA - CVR)
      AR = INTEG(RAR,0.)
      CVR = AR / (VR * PR)
      CR = AR / VR

RAR RATE OF CHANGE OF CHEMICAL IN RAPIDLY PERFUSED
AR= AMOUNT OF CHEMICAL IN RAPIDLY PERFUSED
CVR=CONCENTRATION OF CHEMICAL LEAVING RAPIDLY PERFUSED IN
VENOUS BLOOD
CR= CONCENTRATION OF CHEMICAL IN RAPIDLY PERFUSED

'AM1 = AMT METABOLIZED-SATURABLE (MG)'
      RAM1 = (VMAX * CVL) / (KM + CVL)
      AM1 = INTEG(RAM1,0.)
```

```
RAMI=RATE OF SATURABLE METABOLISM
AMI=AMOUNT OF CHEMICAL METABOLISED VIA SATURABLE

'AM2 = AMT METABOLIZED-1ST ORDER (MG)'
      RAM2= KF*CVL*VL
      AM2 = INTEG(RAM2,0.)

RAM2= RATE OF FIRST ORDER METABOLISM
AM2= ANOUNT OF CHEMICAL METABOLISED VIA FIRST ORDER

'TOTAL METABOLISM'
      RAM = RAM1 + RAM2
      AMT = AM1 + AM2

'CV = MIXED VENOUS CONC (MG/L)'
      CV = (QF*CVF + QL*CVL + QS*CVS + QR*CVR + QSK*CVSK)/QC

'TMASS = MASS BALANCE'
      TABS = AF + AL + AS + AR + AMT + AX + ASK
      TMASS = TABS+ ASFC + AEVAP - AI
      MBAL = DOSE-TMASS

            END         $'OF DERIVATIVE'
            END         $'OF DYNAMIC'
            END         $'OF PROGRAM'
```

THIS PAGE INTENTIONALLY LEFT BLANK

APPENDIX B

APPENDIX B

DATA FILE FOR SIMUSOLV PROGRAM

```
'ALSO CONTAINS RUN-TIME EXECUTIVE FOR SIMUSOLV PROGRAM'

'DERM.DAT'

PREPAR T,'ALL'

SET NRWITG=.F.,FTSPLT=.T.,HVDPRN=.T.,NCIPRN=10
SET WESITG=.F.,DPSITG=.T.,GRDCPL=.F.

                    'VEHICLE PARTITION COEFFICIENTS'

' FOR DBM:  CORN OIL:AIR=1023, MIN OIL:AIR=396, PEANUT OIL;AIR=876'
        'WATER:AIR=14.4'
' FOR BCM:  CORN OIL:AIR=358, MIN OIL:AIR=140, PEANUT OIL:AIR=322'
        'WATER:AIR=8.65'

PROCED SETDBM  $'SETS DBM SPECIFIC VALUES'
SET D=2478.,MOLWT=173.85,PL=.918,PF=10.8,PS=.546,PR=.9
SET PSK=120.,VMAXC=12.5,KM=.36,KFC=.557,P=.0
SET CINT=.1,PB=74.1,VP=45.26
END

PROCED DBMFIN $'VALUES FOR DBM FINITE DOSE'
SETDBM
SET DOSE=619.5,MPSKLQ=.08,P=.0040,ESWTCH=1.,A=3.8
SET BW=.241, DPSITG=.T., FSWTCH=0.,ASWTCH=0.
SET EVAP=658.4, ZERO=1.,TEVAP=.17,TVAPOR=.21
SET VVEH=0.,TSTOP=2.,CINT=.001,DEPTH=.005
DATA
T       CV
0.      0.
.033    14.40
.083    21.69
.170    28.40
.217    26.49
.267    20.95
```

```
.317    19.17
.417    15.32
.500    14.76
.583    12.94
.667    7.85
.75     3.53
END
END

PROCED CDBM25
SETDBM
SET DOSE=1858.5,VVEH=2.25,BW=.304,PV=1110.31
SET FSWTCH=1.,MPSKLQ=0.,ZERO=1.,ESWTCH=0.,
SET ASWTCH=1.,EVAP=0.,A=3.14,PPMCI=0.,TSTOP=24.
SET P=.0037
DATA
T       CV
0.0     0.0
.5      2.28
1.      2.21
2.      3.92
4.      8.83
8.      18.13
12.     12.67
24.     15.74
END
END

PROCED CDBM50
SETDBM
SET DOSE=3717.,VVEH=1.5,BW=.310,PV=1215.14
SET FSWTCH=1.,MPSKLQ=0.,ZERO=1.,ESWTCH=0.
SET ASWTCH=1.,EVAP=0.,A=3.14,PPMCI=0.,TSTOP=24.
SET P=.0033
DATA
T       CV
0.0     0.0
.5      10.46
1.      20.93
2.      32.91
4.      49.03
8.      54.97
12.     63.96
24.     60.82
END
```

```
END

PROCED CDBM75
SETDBM
SET DOSE=5575.5,VVEH=.75,BW=.302,PV=1340.32
SET FSWTCH=1.,MPSKLQ=0.,ZERO=1.,ESWTCH=0.
SET ASWTCH=1.,EVAP=0.,A=3.14,PPMCI=0.,TSTOP=24.
SET P=.0030
DATA
T       CV
0.0     0.0
.5      19.71
1.      39.04
2.      44.50
4.      66.96
8.      111.71
12.     112.08
24.     128.77
END
END

PROCED MDBM25
SETDBM
SET DOSE=1858.5,VVEH=2.25,BW=.264,PV=485.19
SET FSWTCH=1.,MPSKLQ=0.,ZERO=1.,ESWTCH=0.
SET ASWTCH=1.,EVAP=0.,A=3.14,PPMCI=0.,TSTOP=24.
SET P=.0051
DATA
T       CV
0.0     0.0
.5      8.4
1.      14.2
2.      24.5
4.      39.5
8.      48.5
12.     46.9
24.     35.6
END
END

PROCED MDBM50
SETDBM
SET FSWTCH=1.,MPSKLQ=0.,ZERO=1.,ESWTCH=0.
SET ASWTCH=1.,EVAP=0.,A=3.14,PPMCI=0.,TSTOP=24.
SET DOSE=3717.0,VVEH=1.5,BW=.257,PV=626.57
```

```
SET P=.0036
DATA
T       CV
0.0     0.0
.5      14.2
1.      24.2
2.      41.4
4.      54.3
8.      74.4
12.     105.3
24.     115.3
END
END

PROCED MDBM75
SETDBM
SET DOSE=5575.5,VVEH=.75,BW=.262,PV=883.56
SET FSWTCH=1.,MPSKLQ=0.,ZERO=1.,ESWTCH=0.
SET ASWTCH=1.,EVAP=0.,A=3.14,PPMCI=0.,TSTOP=24.
SET P=.0028
DATA
T       CV
0.0     0.0
.5      20.4
1.      32.6
2.      32.0
4.      70.0
8.      85.9
12.     114.9
24.     162.4
END
END

PROCED WDBM25
SETDBM
SET FSWTCH=1.,MPSKLQ=0.,ZERO=1.,ESWTCH=0.
SET ASWTCH=1.,EVAP=0.,A=3.14,PPMCI=0.,TSTOP=24.
SET DOSE=7.3,VVEH=2.997,BW=.235,PV=14.4
SET P=.22
DATA
T       CV
0.0     0.0
.5      .450
1.      .916
2.      1.00
```

```
4.      .930
8.      .440
12.     .287
24.     .213
END
END

PROCED WDBM50
SETDBM
SET FSWTCH=1.,MPSKLQ=0.,ZERO=1.,ESWTCH=0.
SET ASWTCH=1.,EVAP=0.,A=3.14,PPMCI=0.,TSTOP=24.
SET DOSE=18.4,VVEH=2.992,BW=.243,PV=14.4
SET P=.22
DATA
T       CV
0.0     0.0
.5      1.43
1.      1.87
2.      1.88
4.      1.31
8.      .985
12.     .378
24.     .244
END
END

PROCED WDBM75
SETDBM
SET FSWTCH=1.,MPSKLQ=0.,ZERO=1.,ESWTCH=0.
SET ASWTCH=1.,EVAP=0.,A=3.14,PPMCI=0.,TSTOP=24.
SET DOSE=22.7,VVEH=2.991,BW=.241,PV=14.4
SET P=.22
DATA
T       CV
0.0     0.0
.5      2.36
1.      2.91
2.      3.13
4.      2.32
8.      1.32
12.     .536
24.     .280
END
END
```

```
PROCED WDBMSA
SETDBM
SET FSWTCH=1.,MPSKLQ=0.,ZERO=1.,ESWTCH=0.
SET ASWTCH=1.,EVAP=0.,A=3.14,PPMCI=0.,TSTOP=24.
SET DOSE=28.1,VVEH=2.989,BW=.241,PV=14.4
SET P=.22
DATA
T       CV
0.0     0.0
.5      4.57
1.      5.87
2.      5.82
4.      3.69
8.      1.77
12.     .596
24.     .245
END
END

PROCED DBM
SETDBM
SET FSWTCH=1.,MPSKLQ=0.,ZERO=1.,ESWTCH=0.
SET ASWTCH=1.,EVAP=0.,A=3.14,PPMCI=0.,TSTOP=24.
SET DOSE=7434.,VVEH=0.,BW=.250,PV=1496.14
SET P=.003
DATA
T       CV
0.0     0.0
.5      45.17
1.      68.6
2.      108.4
4.      141.53
8.      176.5
12.     200.4
24.     176.7
END
END


PROCED DBMW
SETDBM
SET FSWTCH=1.,MPSKLQ=0.,ZERO=1.,ESWTCH=0.
SET ASWTCH=1.,EVAP=0.,A=3.14,PPMCI=0.,TSTOP=24.
SET P=.22
DATA
```

```
T       CV      DOSE BW     PV      VVEH
0.0     0.0     7.3     .235    14.4    2.997   INITIAL
.5      .450    .       .       .       .
1.      .916    .       .       .       .
2.      1.00    .       .       .       .
4.      .930    .       .       .       .
8.      .440    .       .       .       .
12.     .287    .       .       .       .
24.     .213    .       .       .       .
0.0     0.0     18.4    .243    14.4    2.992   INITIAL
.5      1.43    .       .       .       .
1.      1.87    .       .       .       .
2.      1.88    .       .       .       .
4.      1.31    .       .       .       .
8.      .985    .       .       .       .
12.     .378    .       .       .       .
24.     .244    .       .       .       .

0.      0.      22.7    .241    14.4    2.991   INITIAL
.5      2.36    .       .       .       .
1.      2.91    .       .       .       .
2.      3.13    .       .       .       .
4.      2.32    .       .       .       .
8.      1.32    .       .       .       .
12.     .536    .       .       .       .
24.     .280    .       .       .       .
0.0     0.0     28.1    .241    14.4    2.989   INITIAL
.5      4.57    .       .       .       .
1.      5.87    .       .       .       .
2.      5.82    .       .       .       .
4.      3.69    .       .       .       .
8.      1.77    .       .       .       .
12.     .596    .       .       .       .
24.     .245    .       .       .       .
END
END

PROCED PDBM25
SETDBM
SET FSWTCH=1.,MPSKLQ=0.,ZERO=1.,ESWTCH=0.
SET ASWTCH=1.,EVAP=0.,A=3.14,PPMCI=0.,TSTOP=24.
SET DOSE=1858.5,BW=.200,PV=975.71,VVEH=2.25
SET P=.004
DATA
T       CV
```

```
0.0     0.0
.5      3.84
1.      5.24
2.      11.96
4.      20.07
8.      34.33
12.     35.58
24.     32.35
END
END

PROCED PDBM50
SETDBM
SET FSWTCH=1.,MPSKLQ=0.,ZERO=1.,ESWTCH=0.
SET ASWTCH=1.,EVAP=0.,A=3.14,PPMCI=0.,TSTOP=24.
SET DOSE=3717.,BW=.200,PV=1106.1,VVEH=1.5
SET P=.0037
DATA
T       CV
0.0     0.0
.5      22.27
1.      35.10
2.      60.74
4.      98.96
8.      130.22
12.     140.42
24.     125.44
END
END

PROCED PDBM75
SETDBM
SET FSWTCH=1.,MPSKLQ=0.,ZERO=1.,ESWTCH=0.
SET ASWTCH=1.,EVAP=0.,A=3.14,PPMCI=0.,TSTOP=24.
SET DOSE=5575.,BW=.200,PV=1272.67,VVEH=.75
SET P=.0031
DATA
T       CV
0.      0.
.5      30.69
1.      58.01
2.      102.02
4.      135.30
8.      198.02
12.     173.20
```

```
24.     194.18
END
END

PROCED SETBCM
SET MOLWT=129.39,PL=.704,PF=7.8,PS=.268,PR=.704
SET PB=41.5,PSK=36.4,VMAXC=7.,KM=.4,KFC=.7
SET P=.00,VP=45.26,A=3.14,TEVAP=100.,TVAPOR=100.
SET CINT=.1,D=1991.
END

PROCED BCMFIN $'VALUES FOR FINITE DOSE'
SETBCM
SET DOSE=497.75,MPSKLQ=.104,P=.0011,ESWTCH=1.,A=3.8
SET BW=.218,DPSITG=.T.,FSWTCH=0.,ASWTCH=0.
SET EVAP=450.,ZERO=1.,TEVAP=.092,TVAPOR=.134
SET VVEH=0.,TSTOP=2.,CINT=.001,depth=.005
SET P=.0011
DATA
T       CV
0.0     0.0
.033    7.16
.083    10.69
.170    11.68
.217    12.45
.267    13.67
.317    13.22
.417    12.34
.500    8.65
.583    7.31
.667    5.29
.750    4.00
1.000   2.10
END
END

PROCED CBCM25
SETBCM
SET FSWTCH=1.,MPSKLQ=0.,ZERO=1.,ESWTCH=0.
SET ASWTCH=1.,EVAP=0.,A=3.14,PPMCI=0.,TSTOP=24.
SET DOSE=1493.3,VVEH=2.25,BW=.230,PV=367.85
SET P=.004
DATA
T       CV
0.0     0.0
```

```
.5      2.3
1.      7.4
2.      16.8
4.      23.7
8.      28.0
12.     25.9
24.     21.0
END
END

PROCED CBCM50
SETBCM
SET DOSE=2986.5,VVEH=1.5,BW=.238,PV=378.26
SET FSWTCH=1.,MPSKLQ=0.,ZERO=1.,ESWTCH=0.
SET ASWTCH=1.,EVAP=0.,A=3.14,PPMCI=0.,TSTOP=24.
SET P=.0032
DATA
T       CV
0.0     0.0
.5      19.2
1.      29.3
2.      44.1
4.      47.4
8.      52.2
12.     45.3
24.     46.4
END
END

PROCED CBCM75
SETBCM
SET FSWTCH=1.,MPSKLQ=0.,ZERO=1.,ESWTCH=0.
SET ASWTCH=1.,EVAP=0.,A=3.14,PPMCI=0.,TSTOP=24.
SET DOSE=4479.8,VVEH=.75,BW=.222,PV=389.28
SET P=.0030
DATA
T       CV
0.0     0.0
.5      34.1
1.      62.8
2.      72.5
4.      80.4
8.      71.9
12.     78.3
24.     87.7
```

```
END
END

PROCED MBCM25
SETBCM
SET FSWTCH=1.,MPSKLQ=0.,ZERO=1.,ESWTCH=0.
SET ASWTCH=1.,EVAP=0.,A=3.14,PPMCI=0.,TSTOP=24.
SET P=.0052
SET DOSE=1493.3,VVEH=2.25,BW=.209,PV=167.18
DATA
T       CV
0.0     0.0
.5      8.1
1.      26.7
2.      34.2
4.      45.5
8.      42.0
12.     31.3
24.     25.9
END
END

PROCED MBCM50
SETBCM
SET FSWTCH=1.,MPSKLQ=0.,ZERO=1.,ESWTCH=0.
SET ASWTCH=1.,EVAP=0.,A=3.14,PPMCI=0.,TSTOP=24.
SET P=.0050
SET DOSE=2986.5,VVEH=1.5,BW=.209,PV=207.46
DATA
T       CV
0.0     0.0
.5      35.3
1.      62.7
2.      76.6
4.      93.2
8.      112.5
12.     78.10
24.     81.22
END
END

PROCED MBCM75
SETBCM
SET FSWTCH=1.,MPSKLQ=0.,ZERO=1.,ESWTCH=0.
SET ASWTCH=1.,EVAP=0.,A=3.14,PPMCI=0.,TSTOP=24.
```

```
SET P=.0038
SET DOSE=4479.8,VVEH=.75,BW=.210,PV=273.3
DATA
T       CV
0.0     0.0
.5      34.6
1.      63.8
2.      88.6
4.      93.6
8.      130.8
12.     111.4
24.     90.35
END
END

PROCED WBCM25
SETBCM
SET FSWTCH=1.,MPSKLQ=0.,ZERO=1.,ESWTCH=0.
SET ASWTCH=1.,EVAP=0.,A=3.14,PPMCI=0.,TSTOP=24.
SET P=.12
SET DOSE=10.8,VVEH=2.995,BW=.248,PV=8.65
DATA
T       CV
0.0     0.0
.5      .426
1.      .822
2.      .715
4.      .754
8.      .469
12.     .155
24.     .000
END
END

PROCED WBCM50
SETBCM
SET FSWTCH=1.,MPSKLQ=0.,ZERO=1.,ESWTCH=0.
SET ASWTCH=1.,EVAP=0.,A=3.14,PPMCI=0.,TSTOP=24.
SET P=.12
SET DOSE=19.8,VVEH=2.990,BW=.238,PV=8.65
DATA
T       CV
0.0     0.0
.5      1.69
1.      1.99
```

```
2.      2.25
4.      1.65
8.      .910
12.     .382
24.     .000
END
END

PROCED WBCM75
SETBCM
SET FSWTCH=1.,MPSKLQ=0.,ZERO=1.,ESWTCH=0.
SET ASWTCH=1.,EVAP=0.,A=3.14,PPMCI=0.,TSTOP=24.
SET P=.12
SET DOSE=27.9,VVEH=2.986,BW=.248,PV=8.65
DATA
T       CV
0.0     0.0
.5      2.68
1.      2.95
2.      3.51
4.      2.21
8.      1.26
12.     .571
24.     .043
END
END

PROCED WBCMSA
SETBCM
SET FSWTCH=1.,MPSKLQ=0.,ZERO=1.,ESWTCH=0.
SET ASWTCH=1.,EVAP=0.,A=3.14,PPMCI=0.,TSTOP=24.
SET P=.12
SET DOSE=38.3,VVEH=2.981,BW=.250,PV=8.65
DATA
T       CV
0.0     0.0
.5      7.93
1.      8.94
2.      7.56
4.      4.50
8.      1.53
12.     .733
24.     .120
END
END
```

```
PROCED BCMW
SETBCM
SET FSWTCH=1.,MPSKLQ=0.,ZERO=1.,ESWTCH=0.
SET ASWTCH=1.,EVAP=0.,A=3.14,PPMCI=0.,TSTOP=24.
SET P=.12
DATA
T       CV      DOSE BW      PV      VVEH
0.0     0.0     10.8 .248    8.65    2.995   INITIAL
.5      .426    .    .       .       .
1.      .822    .    .       .       .
2.      .715    .    .       .       .
4.      .754    .    .       .       .
8.      .469    .    .       .       .
12.     .155    .    .       .       .
24.     .001    .    .       .       .
0.0     0.0     19.8 .238    8.65    2.990   INITIAL
.5      1.69    .    .       .       .
1.      1.99    .    .       .       .
2.      2.25    .    .       .       .
4.      1.65    .    .       .       .
8.      .910    .    .       .       .
12.     .382    .    .       .       .
24.     .001    .    .       .       .
0.0     0.0     27.9 .248    8.65    2.986   INITIAL
.5      2.68    .    .       .       .
1.      2.95    .    .       .       .
2.      3.51    .    .       .       .
4.      2.21    .    .       .       .
8.      1.26    .    .       .       .
12.     .571    .    .       .       .
24.     .043    .    .       .       .
0.0     0.0     38.3 .250    8.65    2.981   INITIAL
.5      7.93    .    .       .       .
1.      8.94    .    .       .       .
2.      7.56    .    .       .       .
4.      4.50    .    .       .       .
8.      1.53    .    .       .       .
12.     .733    .    .       .       .
24.     .120    .    .       .       .
END
END
```

THIS PAGE INTENTIONALLY LEFT BLANK

APPENDIX C

APPENDIX C

MODEL CODE FOR DIFFUSION COEFFICIENT ESTIMATION

```
PROGRAM IN-VITRO SKIN
 INITIAL
  INTEGER I,NMAX
  CONSTANT CI = 0.05                    $'INITIAL SKIN CONCENTRATION
(G/CM)'
  CONSTANT D = 1.24E-10          $ 'DIFFUSIVITY (CM**2/SEC)'
  CONSTANT L = 3.4E-4            $ 'THICKNESS (CM)'
  CONSTANT BETA = 0.0017         $ 'LAG CONSTANT'
  CONSTANT PI = 3.1416
  CONSTANT MINF = 0.340          $ 'MASS AT INFINITE TIME (MG)'
  CONSTANT NMAX = 250            $ 'NUMBER OF TERMS IN MASS EQN.'
  CONSTANT TSTOP = 18.           $ 'DURATION (HRS)'
  CE = MINF/2./L
  CONSTANT CINT=60.
  MAXT = 1.
  TMAX = TSTOP*60.*60.
 END $ 'OF INITIAL'
 DYNAMIC
  ALGORITHM IALG = 4
  DERIVATIVE
   TMIN = T/60.
   THRS = TMIN/60.
   PROCEDURAL (MASS = T,D)
   CURV= 1.-EXP(-BETA*T)
  ' CURV = (CI+(CE-CI)*(1.-EXP(-BETA*T)))/CE'
F=(16./(PI*PI))
G=(2.*L*L*BETA)/((D*PI*PI)-(4.*BETA*L*L))
C=(BETA*T)
H=(D*PI*PI*T)/(4.*L*L)
SUM = F*G*(EXP(-C)-EXP(-H))
DO 100 I=1,NMAX
N=REAL(I)
 A=(16./((2.*N+1.)*(2.*N+1.)*PI*PI))
 B=(2.*L*L*BETA)/((D*(2.*N+1.)*(2.*N+1.)*PI*PI)-(4.*BETA*L*L))
C=(BETA*T)
E=(D*(2.*N+1.)*(2.*N+1.)*PI*PI*T)/(4.*L*L)
      SUM =SUM +(A*B*(EXP(-C)-EXP(-E)))
       100..CONTINUE
```

```
      MASS = (CURV - SUM)*MINF
    END $ 'OF PROCEDURE'
    TERMT(T.GT.TMAX)
  END $ 'OF DERIVATIVE'
END $ 'OF DYNAMIC'
END $ 'OF PROGRAM'
```